MEASUREMENTS OF NITROUS ACID, NITRATE RADICALS, FORMALDEHYDE AND NITROGEN DIOXIDE FOR THE SOUTHERN CALIFORNIA AIR QUALITY STUDY BY DIFFERENTIAL OPTICAL ABSORPTION SPECTROSCOPY

Final Report

CONTRACT NUMBER A6-146-32

CALIFORNIA AIR RESOURCES BOARD

December 1989

Principal Investigator

Arthur M. Winer

Co-Investigator

Heinz W. Biermann

Contributing Researchers

Travis M. Dinoff
Li Li N. Parker
Minn P. Poe

STATEWIDE AIR POLLUTION RESEARCH CENTER
UNIVERSITY OF CALIFORNIA
RIVERSIDE, CALIFORNIA 92521

ARB-90:scaqsfinal

Abstract

Two differential optical absorption spectrometer (DOAS) systems were operated during the 1987 Southern California Air Quality Study (SCAQS) for the primary purpose of measuring atmospheric concentrations of nitrous acid (HONO) and the nitrate (NO_3) radical, as well as ambient levels of nitrogen dioxide (NO_2) and formaldehyde (HCHO). Measurements were conducted at the "Type A" sites at Long Beach and Claremont, California, during the summer phase of the program and at Long Beach during the fall episodes. In both DOAS systems, rapid scanning spectrometers (~3000 spectra per min) were interfaced to 25 m basepath open, multiple reflection systems operated at total optical paths of 800 m. An extensive set of time-resolved (i.e., 15 min) measurements of HONO, NO_2 and HCHO concentrations, as well as NO_3 radical concentrations, were obtained during the SCAQS program by the DOAS technique under a wide range of pollutant and meteorological conditions.

Pronounced diurnal profiles in the atmospheric concentrations of NO_2, HONO, HCHO and NO_3 radicals were observed for most of the episodes studied, with clear evidence for the influence of mobile emission sources on ambient levels of NO_2 and HCHO at both Claremont and Long Beach.

During several of the fall episodes at Long Beach, levels of gaseous HONO were the highest observed to date by the DOAS technique (>15 ppb). Although ~50%, to as much as 100%, of the measured nighttime HONO could be accounted for by heterogeneous formation pathways involving NO_2 and water vapor, HONO concentrations correlated well with primary pollutants such as CO and NO, suggesting that elevated nighttime HONO concentrations in the western end of the basin may be influenced by emissions of HONO from combustion sources. This has significant implications for models which assume HONO arises only from secondary formation, rather than a combination of direct emissions and atmospheric reactions.

Calculations showed that OH radical production at Long Beach from photolysis of elevated HONO concentrations after sunrise produced a large pulse of OH radicals at a time when there was little or no contribution from photolysis of HCHO and O_3. For the fall episodes, the total OH radical production from HONO photolysis under these conditions was comparable to total OH radical production from HCHO photolysis through the rest of the day.

As expected, elevated NO_3 concentrations (~50-175 ppt) were observed in the summer at Claremont only under conditions involving the co-occurrence of significant O_3 and NO_2 concentrations and the absence of NO. Levels of HONO observed at Claremont during the summer episodes fell in the range ~1-7 ppb, characteristic of HONO concentrations previously observed in downwind receptor areas of California's South Coast Air Basin.

With further analysis and correlation with other SCAQS data, the DOAS results for HCHO should be useful in exploring the partitioning of ambient concentrations of HCHO between direct emissions and formations from secondary reactions in the atmosphere.

TABLE OF CONTENTS

TABLE OF CONTENTS
(continued)

ACKNOWLEDGMENTS

The contributions of many individuals made this research project possible. We especially thank Ernesto C. Tuazon and Roger Atkinson for providing assistance with the spectroscopic measurements and for valuable discussions concerning this study. Ervin Mateer, Michael Kienitz and Chris Berglund helped in assembling the DOAS systems. Fran Tepper and Bret McMillan spent many hours entering the reduced data into the computer for further analysis. We also thank James N. Pitts, Jr., for making available equipment obtained in earlier studies, and the physical plant staff at Long Beach City College for their cooperation in siting the DOAS system.

Eric Fujita, ARB Project Officer for this study, provided effective support and understanding throughout this entire project and Douglas Lawson and Susanne Hering worked tirelessly and effectively during SCAQS to solve problems related to siting and operating the DOAS systems. We appreciated valuable discussions with these three individuals, as well as with John Holmes, Bruce Appel and Gervase Mackay concerning the scientific aspects of the SCAQS program. Pleasant conversations with Yosh Tokiwa and Victor Povard of the Air and Industrial Hygiene Laboratory (AIHL) helped pass the long nights at Long Beach during the fall episodes, and their willingness to periodically monitor the DOAS instrument even permitted a few hours of sleep on occasion.

Our participation in this study would not have been possible without the support of the SAPRC fiscal and administrative staff, including Diane Skaggs, Anne Greene and Mae Minnich. We wish to thank Christy LaClaire and Barbara Crocker for typing and assembling this report.

We thank Gervase Mackay and Harold Schiff of Unisearch, George Wolff of General Motors Research Laboratory and Bruce Appel of the AIHL for permission to use, prior to their publication, HCHO, NO_2 and HONO SCAQS data, respectively. The support of the ARB Research Division of this research (Contract No. A6-146-32) is gratefully acknowledged.

This report was submitted in fulfillment of Contract No. A4-081-32 by the Statewide Air Pollution Research Center, University of California, Riverside, under the partial sponsorship of the California Air Resources Board. Research for this project was completed as of December 1989.

DISCLAIMER

The statements and conclusions in this paper are those of the authors and not necessarily those of the California Air Resources Board. The mention of commercial products, their sources, or use in connection with material reported herein is not to be construed as either an actual or implied endorsement of such products.

LIST OF FIGURES

LIST OF FIGURES
(continued)

LIST OF FIGURES
(continued)

LIST OF FIGURES
(continued)

LIST OF FIGURES
(continued)

LIST OF FIGURES
(continued)

LIST OF FIGURES
(continued)

LIST OF FIGURES
(continued)

LIST OF TABLES

LIST OF TABLES
(continued)

GLOSSARY OF TERMS, ABBREVIATIONS AND SYMBOLS

AIHL	Air Industrial Hygiene Laboratory, Berkeley
ARB	(California) Air Resources Board
°C	Degrees Centigrade
cm	Centimeter
CO	Carbon monoxide
DOAS	Differential optical absorption spectroscopy
ENSR	Acronym for environmental consulting company which was formerly ERT, Inc.
EPA	Environmental Protection Agency
ft	Feet
FT-IR	Fourier transform infrared spectroscopy
gm	Gram
HCHO	Formaldehyde
HONO	Nitrous acid
hr	Hour
I	Light intensity
in	Inch
I_o	Initial light intensity
K	Degrees Kelvin
km	Kilometer
m	Meter
m^3	Cubic meter
min	Minute
mℓ	Milliliter
mm	Millimeter
nm	Nanometer (10^{-9} meter)

GLOSSARY
(continued)

NO	Nitric oxide
NO_2	Nitrogen dioxide
NO_3	Nitrate radical
NO_x	Oxides of nitrogen ($NO + NO_2$)
N_2O_4	Dinitrogen tetraoxide
N_2O_5	Dinitrogen pentoxide
O.D.	Optical density
OH	Hydroxyl radical
O_3	Ozone
oz	Ounce
PST	Pacific standard time
ppb	Part per billion
ppt	Part per trillion
SAPRC	Statewide Air Pollution Research Center
SCAQMD	South Coast Air Quality Management District
SCFM	Standard cubic feet per minute
SoCAB	South Coast Air Basin
TDLS	Tunable diode laser spectrometer
UCR	University of California, Riverside
µg	Microgram (10^{-6} gram)
µℓ	Microliter (10^{-6} liter)
µm	Micrometer (10^{-6} meter)
uv/vis	Ultraviolet/visible
W	Watt

I. PROJECT SUMMARY

A. Introduction and Statement of the Problem

The SCAQS program provided a unique opportunity to characterize the geographical and temporal distribution of gaseous and particulate pollutants in the South Coast Air Basin (SoCAB) under well documented meteorological conditions, yielding a data base essential to the development and testing of the next generation of urban airshed models. Among the many inputs required for such models are the atmospheric concentrations of the nitrate (NO_3) radical, which plays an important role in nighttime atmospheric chemistry, and nitrous acid (HONO), which by its photolysis initiates photochemical smog formation at sunrise. Knowledge of the corresponding atmospheric concentrations of nitrogen dioxide (NO_2) and formaldehyde (HCHO), including their partitioning between primary and secondary sources, is also important in view of their essential role in photochemical smog formation.

Despite substantial progress over the past decade in the development of analytical methods for most atmospheric pollutants, the reliable measurement of many of these remains challenging. This is especially true for those labile species which are present at part per billion (ppb) or even part per trillion (ppt) mixing ratios, and there continues to be a need for measurements involving instruments with high specificity, adequate sensitivity, and in-situ measurement properties. Since its development a decade ago, the differential optical absorption spectroscopy (DOAS) technique, by employing long optical paths through the atmosphere and rapid data acquisition, has afforded these characteristics for the measurement of HONO, NO_3 radicals, NO_2 and HCHO.

The SCAQS program provided an opportunity to extend previous DOAS studies of these species in the SoCAB, particularly at the less well-studied western end of the basin which is characterized by strong emission sources, especially oxides of nitrogen (NO_x) sources. Moreover, the presence of other complementary instrumental or wet chemical techniques for related or redundant pollutant species, further multiplied the value of the data collected by DOAS measurements.

B. Objectives

The specific objectives of this project were the following:

- To obtain continuous, time-resolved, in situ measurements of HONO, NO_2 and HCHO at both the source (Long Beach) and receptor (Claremont) type A SCAQS sites during the summer.
- To measure NO_3 radical concentrations at Claremont during the summer SCAQS episodes.
- To monitor HONO, HCHO and NO_2 ambient concentrations at the Long Beach type A site during the fall SCAQS episodes.

C. Methods of Approach

To meet these objectives, two DOAS systems were operated during the SCAQS program. In both systems, rapid scanning spectrometers (~3000 spectra min^{-1}) were interfaced to 25 m basepath open, multiple reflection systems operated routinely at total optical paths of 800 m. The system at Long Beach was assembled with a 0.3 m McPherson spectrograph and operated during both the summer and fall measurement periods, while the DOAS system at Claremont was based on a SPEX 0.5 m spectrograph operated only during the summer.

In each case white light from a 75 W high-pressure Xenon arc lamp was transmitted through an optical system of the three-mirror White design whose mirrors were fabricated from 30 cm diameter, 6 cm thick Pyrex blanks and coated with custom 37 layer dielectric coatings for optimum reflectivity. At both sites, the optical systems were located approximately 10 m to the west of the platforms containing the other measurement systems employed during the SCAQS program, and were completely open to the air. To elevate the DOAS systems to the required height of 1.9 m, the spectrometers, mirror systems and their housings were set on massive concrete blocks.

A new instrument capability added for the SCAQS program was the use of vertical- and horizontal-adjustment micrometer motors on one of the out-of-focus mirrors. To further automate the DOAS, these motors were operated by a computer driven servo system. Light from a HeNe laser, aligned coaxially with the white light source and passing through the multiple reflection optical system was focused onto a photodiode-based, position-sensing device whose output was fed to the computer. Movements

of the laser reference image from a pre-selected position on the photodiode resulted in a computer command to one or both of the micrometer motors, correcting mirror movement due to the diurnal variation in temperature.

After passing through the multiple reflection system, white light from the Xenon arc was focused onto the entrance slit of the spectrographs and the resulting intensity monitored by a photomultiplier (EMI 9659Q) whose output was acquired by a DEC MINC 11/23 minicomputer. During each 15-min measurement period, approximately 50,000-70,000 scans were added in the computer memory, providing a signal-to-noise ratio sufficiently high that optical densities as low as 3×10^{-4} (base 10) could be determined.

Based on the appropriate absorption cross sections, an 800 m absorption pathlength, and the actual noise levels in the spectra, we calculated detection limits of 4, 0.8, and 5 ppb for NO_2, HONO, and HCHO, respectively, and approximately 30 ppt for NO_3. Accounting for noise levels, baseline drift, and data-processing effects, the error limits for NO_2 data were estimated at ±10% while for the HONO and HCHO data the corresponding errors were ±30% due to the more complex deconvolution. For NO_3 radical concentrations, the error was estimated to be ±15%.

D. Summary of Results and Conclusions

An extensive set of measurements of HONO, NO_2 and HCHO concentrations, as well as NO_3 radical concentrations, were obtained during the SCAQS program by the DOAS technique under a wide range of pollutant and meteorological conditions, thereby achieving the specific objectives of this project. In addition, the principal findings from the DOAS measurements were the following:

- Pronounced diurnal profiles in the atmospheric concentrations of NO_2, HONO, HCHO and NO_3 radicals were observed for most of the episodes studied, with clear evidence for the influence of mobile emission sources on ambient levels of NO_2 and HCHO at both Claremont and Long Beach.
- Maximum HONO levels observed at Long Beach during the fall episodes were approximately 50% to a factor of two higher than maximum DOAS HONO concentrations previously reported anywhere.
- Calculations showed that OH radical production from photolysis of these elevated HONO concentrations after sunrise produced a large pulse of

OH radicals at a time when there was little or no contribution from photolysis of HCHO and O_3. For the fall episodes at Long Beach, the total OH radical production from HONO photolysis under these conditions was comparable to total OH radical production from HCHO photolysis through the rest of the day and, as expected, approximately an order of magnitude greater than radical production from O_3 photolysis.

- Although as much as half, to all, of the ambient nighttime levels of HONO observed at Long Beach could result from heterogeneous atmospheric formation pathways involving NO_2, factor analyses for the SCAQS data (and data obtained in the winter of 1986 at Torrance, California), as well as partitioning calculations, suggest that HONO levels in the western end of the SoCAB during the fall/winter period may contain a significant contribution from HONO emissions from combustion sources.

- Under conditions prevailing at Claremont during the summer SCAQS episodes, only limited periods of elevated NO_3 concentrations occurred. This was due to both declining NO_2 and O_3 precursor concentrations and to increasing NO levels in the early evening hours of most episode days.

- With further analysis and correlation with other SCAQS data, the DOAS results for HCHO should be useful in exploring the partitioning of ambient concentrations of HCHO between direct emissions and formations from secondary reactions in the atmosphere.

E. Recommendations for Future Research

The present DOAS study provided a set of data which, along with the entire SCAQS data base, will be useful over at least the next five years in the development and testing of chemical mechanisms and air shed models. However, several suggestions for future research employing the DOAS technique resulted from the experience of the SCAQS program.

- For future ambient air studies, a third generation DOAS instrument should be developed based on the availability of commercial photodiode array detectors and the dramatic advances in microcomputer capabilities since the present DOAS instruments were initially developed a decade ago.

- Additional atmospheric measurements should be conducted of HONO concentrations occurring at the western edge of the SoCAB during fall and winter periods. In each of the previous two DOAS studies (at Torrance and Long Beach) conducted under these conditions, assumptions concerning the

maximum HONO concentrations occurring in the SoCAB were shown to underestimate the actual measured HONO levels. With respect to both accurately modeling HONO's role in the formation of photochemical air pollution, and establishing a data base for health effects researchers, it is important to better characterize the maximum levels of HONO which may occur along the coastal region of the SoCAB, from West Los Angeles to Orange County.

- The DOAS technique should be used to investigate further the production of HONO from a range of combustion sources, including stationary, as well as mobile, sources.

II. INTRODUCTION

A. Background to SCAQS Program

The 1987 Southern California Air Quality Study (SCAQS) was conceived by the California Air Resources Board (ARB) as the first comprehensive study of air pollution in California's South Coast Air Basin (SoCAB) since the Aerosol Characterization Experiment study which was held nearly 15 years earlier. The SCAQS program was proposed in recognition of the substantial changes in the kinds and geographical distributions of air pollutant sources in the SoCAB which took place during that period, and the many difficult regulatory issues which will confront the ARB, South Coast Air Quality Management District (SCAQMD), and Environmental Protection Agency (EPA) during the 1990's. It was also recognized that knowledge of atmospheric chemistry had increased dramatically over the past two decades as well, and that more comprehensive field measurements of the species participating in these reactions were required.

The overall goal of this program of measurement, data analysis and modeling was to provide the understanding of source-receptor relationships necessary to develop the next generation of cost-effective emission control strategies. The specific major objectives of the SCAQS project were the following (Blumenthal et al. 1987):

- To develop a comprehensive and properly archived air quality and meteorological data base for the SoCAB which can be used to test and improve air quality simulation models for oxidants, NO_2, PM-10, and acidity.

- To evaluate measurement methods for PM-10, acidic species, and important nitrogen and carbon species.

- To elucidate relationships between precursor emissions and the spatial and temporal distributions of secondary air pollutants.

In order to achieve these objectives, an international team of atmospheric scientists was assembled to operate a wide range of state-of-the-

art gaseous and particulate pollutant samplers and meteorological instruments. Many of these techniques had been employed and evaluated in the Nitrogen Species Methods Comparison Study (NSMCS) and the Carbonaceous Species Methods Comparison Study (CSMCS) conducted in the SoCAB in 1985 and 1986, respectively, under ARB sponsorship.

B. Role of DOAS Measurements

The SCAQS project offered a unique opportunity to characterize the geographical and temporal distribution of gaseous and particulate pollutants in the SoCAB under well documented meteorological conditions. As noted above, the resulting data base will be essential in the development and testing of the next generation of urban airshed models. Among the many inputs required for such models are the atmospheric concentrations of the nitrate (NO_3) radical, which plays an important role in nighttime atmospheric chemistry, and nitrous acid (HONO), which by its photolysis initiates photochemical smog formation at sunrise (Finlayson-Pitts and Pitts 1986; Seinfeld 1989). Knowledge of the corresponding atmospheric concentrations of nitrogen dioxide (NO_2) and formaldehyde (HCHO), including their partitioning between primary and secondary sources, is also important in view of their essential role in photochemical smog formation.

Despite substantial progress over the past decade in the development of analytical methods for most atmospheric pollutants, the reliable measurement of many of these remains challenging. This is especially true for those labile species which are present at part per billion (ppb) or even part per trillion (ppt) mixing ratios, and there continues to be a need for measurements involving instruments with high specificity, adequate sensitivity and in-situ measurement properties. Since its development a decade ago (Perner and Platt 1979), the differential optical absorption spectroscopy (DOAS) technique, by employing long optical paths through the atmosphere and rapid data acquisition, has afforded these characteristics for the measurement of HONO, NO_3 radicals, NO_2 and HCHO (Platt et al. 1980a,b; Harris et al. 1982; Biermann et al. 1988a; Winer et al. 1987).

The SCAQS program provided an opportunity to extend previous DOAS studies of these species in the SoCAB, particularly at the less well-

studied western end of the basin which is characterized by strong emission sources, especially of oxides of nitrogen (NO_x) sources. Moreover, the presence of other complementary instrumental or wet chemical techniques for related or redundant pollutant species, afforded a unique opportunity to enhance the value of the data collected by DOAS measurements.

C. Importance of Gaseous Species Measured by DOAS Technique

An essential requirement in urban airshed computer modeling studies is to have reliable atmospheric concentrations of key species as initial inputs to the models and for purposes of comparison between model results and measured ambient air concentrations. The free radicals of greatest importance in this regard are OH, NO_3 and HO_2, while two of the most important precursors for OH radicals are nitrous acid and formaldehyde.

1. Nitrous Acid

Nitrous acid is a key precursor to OH radicals since, under atmospheric and sunlight conditions typically prevalent in the SoCAB, any HONO present in predawn hours rapidly photolyzes after sunrise:

$$HONO + h\nu \rightarrow OH + NO \qquad (1)$$

providing an early morning source of OH radicals. Studies prior to the SCAQS program in both the Los Angeles basin (Platt et al. 1980b; Harris et al. 1982; Pitts et al. 1984a; Biermann et al. 1988a) and Germany (Perner and Platt 1979; Platt and Perner 1980) measured HONO in nighttime atmospheres with concentrations typically increasing through the night to a pre-dawn maximum. In particular, HONO was observed in the Los Angeles basin at concentrations up to ~8 ppb (Biermann and Winer 1986) and it was evident from these data that in the predawn hours HONO concentrations are typically ~3-5% of those of NO_x.

While, prior to the SCAQS program, HONO was known to be emitted from vehicle exhaust (Pitts et al. 1984c) and to be formed from the heterogeneous hydrolysis of NO_2 (Sakamaki et al. 1983; Pitts et al. 1984b) in laboratory systems and indoor environments, the source of atmospheric HONO during nighttime hours was still not well understood (Stockwell and Calvert 1983; Pitts et al. 1984a; Killus and Whitten 1985). However it was clear that nighttime HONO levels are highly important, since the

enhanced early morning OH radical levels due to photolysis of HONO lead to a more rapid initiation of photochemical air pollution processes (Harris et al. 1982), as shown in Figure II-1.

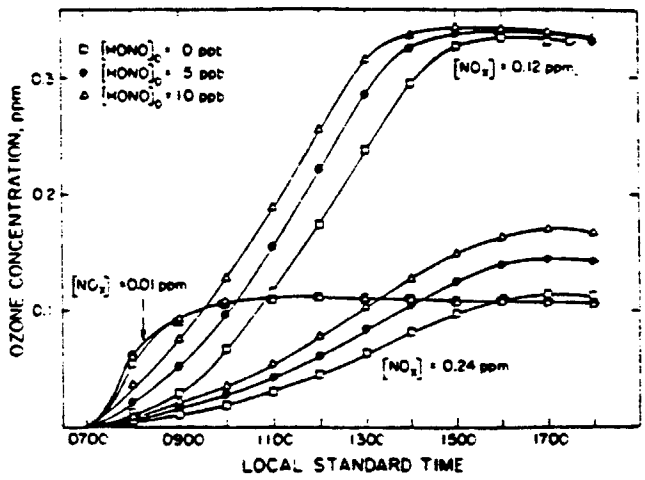

Figure II-1. Calculated ozone profiles for low (0.01 ppb), medium (0.12 ppm), and high (0.24 ppm) NO_x concentration including 0, 5, and 10 ppb of HONO. See Harris et al. (1982) for details.

Clearly, accurate measurements of nitrous acid were needed for several reasons. First, determinations of early morning concentrations of HONO, particularly at an emission "source" site in the western end of the Basin could, via appropriate computer kinetic models, be correlated with calculations of ambient OH radical concentrations at that site. Second, measurements of HONO at an emission "source" site, during both the summer and winter study periods, could provide essential information concerning the rate of nighttime formation of nitrous acid. Finally, characterization of HONO concentrations at a "receptor" site would contribute to determination of an overall nitrogen-species mass balance.

In summary, it would be difficult to overestimate the importance of accurately measured HONO concentrations as inputs to airshed models which are to be used to reliably establish source-receptor relationships and develop emission control strategies. Historically, models have differed

greatly in their assumptions concerning the concentrations of HONO assumed to be present at the start of their simulations, ranging from complete exclusion of HONO from starting conditions (U.S. EPA 1977, 1978, 1980) up to maximum values determined by the $NO-NO_2-H_2O$ equilibrium (Chan et al. 1976). As noted above, however, and illustrated in Figure II-1, Harris et al. (1982) showed that increasing initial HONO levels cause distinct enhancements in both the rates of ozone formation under simulated atmospheric conditions and (in the case of high NO_x levels) the final ozone concentrations achieved. This effect was shown to have direct implications for the degree of control of reactive organic gases required to achieve a given reduction in peak ozone concentrations. Clearly, experimentally determined, accurate HONO concentrations as a function of time, with emphasis on the predawn hours at a source site, was a critical requirement for reliable airshed model development and application under the SCAQS program.

2. Nitrate Radicals

In contrast to HONO, the role of the NO_3 radical is more important in receptor areas of the South Coast Air Basin. This is due in part to the rapid reaction between nitric oxide (NO) emitted from mobile and stationary sources and NO_3 radicals, which will usually suppress the concentration of NO_3 radicals in source regions to unimportant levels. In receptor areas, however, we have previously shown that NO_3 radical concentrations can increase after sunset, reaching maxima on a given night of more than 400 parts per trillion (Winer et al. 1987). These maxima in NO_3 radical concentrations generally have been observed between early evening (~2000) and midnight, with the exact time of the maximum depending presumably upon the relative strength of source and sink processes.

Based on these and other DOAS measurements, it has been recognized over the past decade that the NO_3 radical is an important constituent of nighttime atmospheres (Winer et al. 1984; Atkinson et al. 1986; Finlayson-Pitts and Pitts 1986). Nitrate radicals are formed from the reaction of nitrogen dioxide with ozone

$$NO_2 + O_3 \rightarrow NO_3 + O_2 \qquad (2)$$

and exist in equilibrium (with this equilibrium being attained in <1 min. at 298 K and 760 torr total pressure) with N_2O_5

$$NO_3 + NO_2 \rightleftarrows N_2O_5 \qquad (3,-3)$$

Since NO_3 radicals photolyze rapidly, with a lifetime of ~5 sec at solar noon,

$$NO_3 + h\nu \rightarrow NO + O_2 \qquad (4a)$$

$$\rightarrow NO_2 + O(^3P) \qquad (4b)$$

elevated NO_3 radical concentrations can only exist at night.

As summarized in Table II-1, NO_3 radicals have been shown to react rapidly with the more reactive alkenes (including monoterpenes), hydroxy substituted aromatics, reduced organosulfur compounds and nitrogen heterocycles. Indeed, we have shown that these reactions can be a nighttime sink for these organics and/or NO_3 radicals (and hence NO_x), depending on their emission/formation rates (Winer et al. 1984). Additionally, N_2O_5 can, via its heterogeneous hydrolysis, be a precursor to acid deposition via formation of HNO_3

$$N_2O_5 + H_2O \xrightarrow{\text{heterogeneous}} HNO_3 \qquad (5)$$

Based on previous NO_3 measurements in ambient air, it was believed important to characterize the NO_3 radical concentrations at a SCAQS "receptor" site during the summer monitoring period: (a) in order to contribute to the goal of obtaining a complete NO_x mass balance across the basin; (b) because NO_3 radicals have been shown to be important sinks for certain classes of organic compounds (Winer et al. 1984); and (c) because NO_3 radical concentrations can, along with measured NO_2 concentrations, be used to estimate ambient N_2O_5 levels (Atkinson et al. 1986). With regard to the latter, it is now believed (Platt et al. 1980b; Stockwell and Calvert 1983; Richards 1983; Tuazon et al. 1983; Platt et al. 1984; Russell et al. 1985) that hydrolysis of N_2O_5 may provide a significant nighttime pathway to the formation of nitric acid (HNO_3).

Table II-1. Rate Constants and Lifetimes for a Series of Monoterpenes, Phenol, Cresols and Naturally Emitted Organo-sulfur Organics Due to Reaction with O_3 and with OH and NO_3 Radicals at Room Temperature

Organic Compound	Rate Constant (cm^3 $molecule^{-1}$ sec^{-1})			Lifetime[a]		
	O_3[b]	OH[c]	NO_3[d]	O_3	OH (daytime)	NO_3 (nighttime)
α-Pinene	8.4×10^{-17}	5.5×10^{-11}	5.8×10^{-12}	4.6 hr	5.1 hr	11 min
β-Pinene	2.1×10^{-17}	8.0×10^{-11}	2.4×10^{-12}	18 hr	3.5 hr	28 min
Δ^3-Carene	1.2×10^{-16}	8.7×10^{-11}	1.0×10^{-11}	3.2 hr	3.2 hr	6.3 min
d-Limonene	6.4×10^{-16}	1.7×10^{-10}	1.3×10^{-11}	36 min	1.6 hr	5.0 min
Myrcene	1.2×10^{-15}	2.6×10^{-10}	1.1×10^{-11}	19 min	1.3 hr	6.3 min
Phenol	-	2.8×10^{-11}	3.6×10^{-12}	-	9.9 hr	18 min
o-Cresol	2.6×10^{-19}	4.2×10^{-11}	2.2×10^{-11}	6.2 day	6.9 hr	3.2 min
CH_3SH	-	3.3×10^{-11}	1.0×10^{-12}	-	8.4 hr	1.2 hr
C_2H_5SH	-	4.7×10^{-11}	1.2×10^{-12}	-	5.9 hr	1.0 hr
CH_3SCH_3	$<8.3 \times 10^{-19}$	6.3×10^{-12}	9.9×10^{-13}	>19 day	3.7 day	1.2 hr

[a]Calculated for clean tropospheric concentrations of 7.2×10^{11} molecule cm^{-3} of O_3, 1×10^6 molecule cm^{-3} of OH radicals (during daytime hours) and 2.4×10^8 molecule cm^{-3} of NO_3 radicals (during nighttime hours).
[b]From Atkinson and Carter (1984).
[c]From Atkinson (1989).
[d]From Atkinson et al. (1988).

3. Formaldehyde

The importance of reliably characterizing HCHO time-concentration profiles at a SCAQS "source" site, both under winter and summer episode conditions, and at a SCAQS "receptor" site, during the summer intensive monitoring period, arise from the role of HCHO as a precursor to HO_2 radicals, and hence OH radicals.

$$HCHO + h\nu \rightarrow H_2 + CO \quad (6a)$$

$$\rightarrow H + HCO \quad (6b)$$

$$HCO + O_2 \rightarrow HO_2 + CO \quad (7)$$

$$HO_2 + NO \rightarrow OH + NO_2 \quad (8)$$

In addition, the reaction between HO_2 radicals and formaldehyde leads to the formation of formic acid in ambient air

$$HO_2 + HCHO \rightarrow \rightarrow HCOOH + OH \quad (9)$$

An additional important aspect of formaldehyde's occurrence in ambient air is that it is both emitted directly in automotive exhaust as well as being formed in the atmosphere from the photooxidation of hydrocarbons, but prior to the SCAQS program reliable partitioning of ambient HCHO between primary and secondary formation pathways had not been established. The DOAS spectrometer can provide time-concentration data for HCHO on an absolute, in situ basis providing baseline measurement against which data obtained from other methods can be compared. The capability of the DOAS technique for high time resolution also permits identification of short-term variations of pollutant concentrations which can in turn provide information on the partitioning of primary and secondary contributions to ambient HCHO concentrations.

Finally, accumulation of a robust data base concerning ambient concentrations of HCHO was important in order to establish baseline data, prior to potential widespread introduction of methanol-fueled vehicles which might enhance atmospheric levels of HCHO.

4. Nitrogen Dioxide

Although NO_2 concentrations can be readily measured by continuous chemiluminescence gas analyzers, it is useful to obtain NO_2 data from the in situ DOAS technique for intercomparison purposes, to provide backup data when instrumental problems occur for the chemiluminescence measurements, and to test for possible interference contributions to NO_2 concentrations determined by the chemiluminescence method (Winer et al. 1974). Since NO_2 concentrations must be determined in the course of DOAS data reduction, prior to obtaining HONO, NO_3 radical, or HCHO concentrations, NO_2 data were to be provided as a matter of course from DOAS participation in the SCAQS program.

III. MEASUREMENT SITES AND PROTOCOLS

A. Measurement Sites

After extensive evaluation, a total of nine monitoring stations were selected by SCAQS planners to supplement the network of existing routine monitoring stations (type "C" sites) in the SoCAB. The nine monitoring sites, designated as "B" sites, were located along characteristic air trajectories from west to east in the basin and were designated for aerosol and gas measurements of a well-defined nature. These nine sites were generally co-located with C sites.

One B site in the source area, located at Long Beach City College, and one B site in a receptor area of the SoCAB, Claremont College, was also designated as a type "A" site, at which the "research grade" instrumental and analytical methods assembled by principal investigators from California, the U.S. and Europe were operated. The specific location of the two type A sites, at which DOAS measurements were made, are shown in Figure III-1, along with the location of an earlier DOAS-based field study conducted in 1985-86 at El Camino Community College in Torrance, California (Winer et al. 1987).

The Long Beach City College type A site was located ~1 mile north of the Interstate 405 freeway and ~3 miles west of the Interstate 605 freeway. An overview of this A site is given in Figure III-2, which shows the proximity of the sampling area to the Douglas Aircraft hangers to the south and the athletic fields of Long Beach City College (LBCC) to the north. The principal location for the measurement methods employed at LBCC was a rectangular, paved area measuring approximately 75 ft by 130 ft. The DOAS spectrometer was located at the extreme western end of the sampling area, with the multiple reflection optics aligned in a NW/SE direction in an attempt to minimize stray light effects due to sunlight entering the multiple reflection cell at sunrise and sunset. A more detailed indication of the orientation and distance of the DOAS spectrometer with respect to the sampling platform and other measurement groups utilizing mobile laboratories or vans during the fall measurement period is given in Figure III-3.

The siting of SCAQS-related measurement facilities on the campus of the Claremont College, the type A receptor site, is shown in Figure III-4.

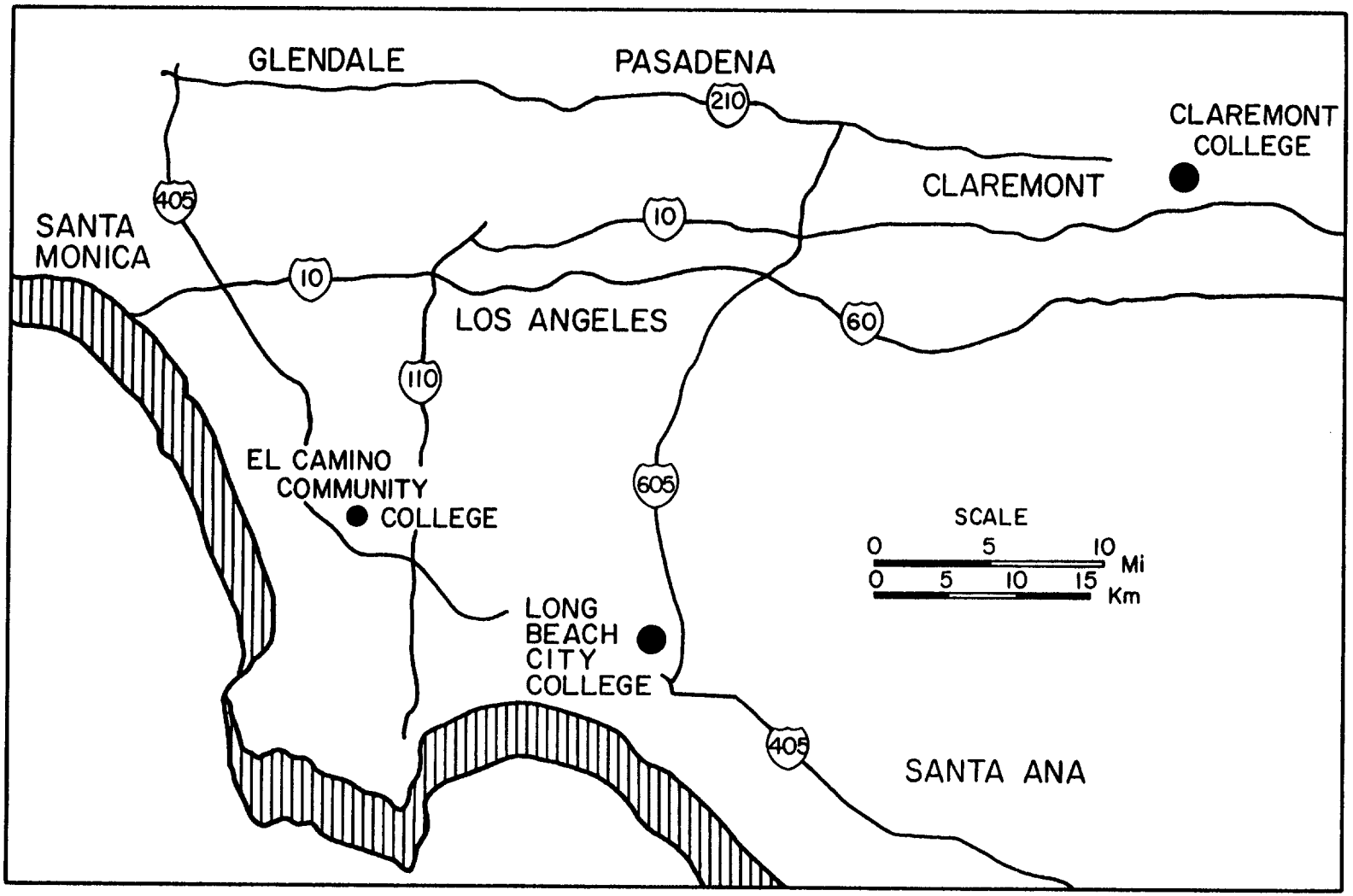

Figure III-1. Locations of Long Beach and Claremont type A sites and site of 1986 DOAS study El Camino Community College.

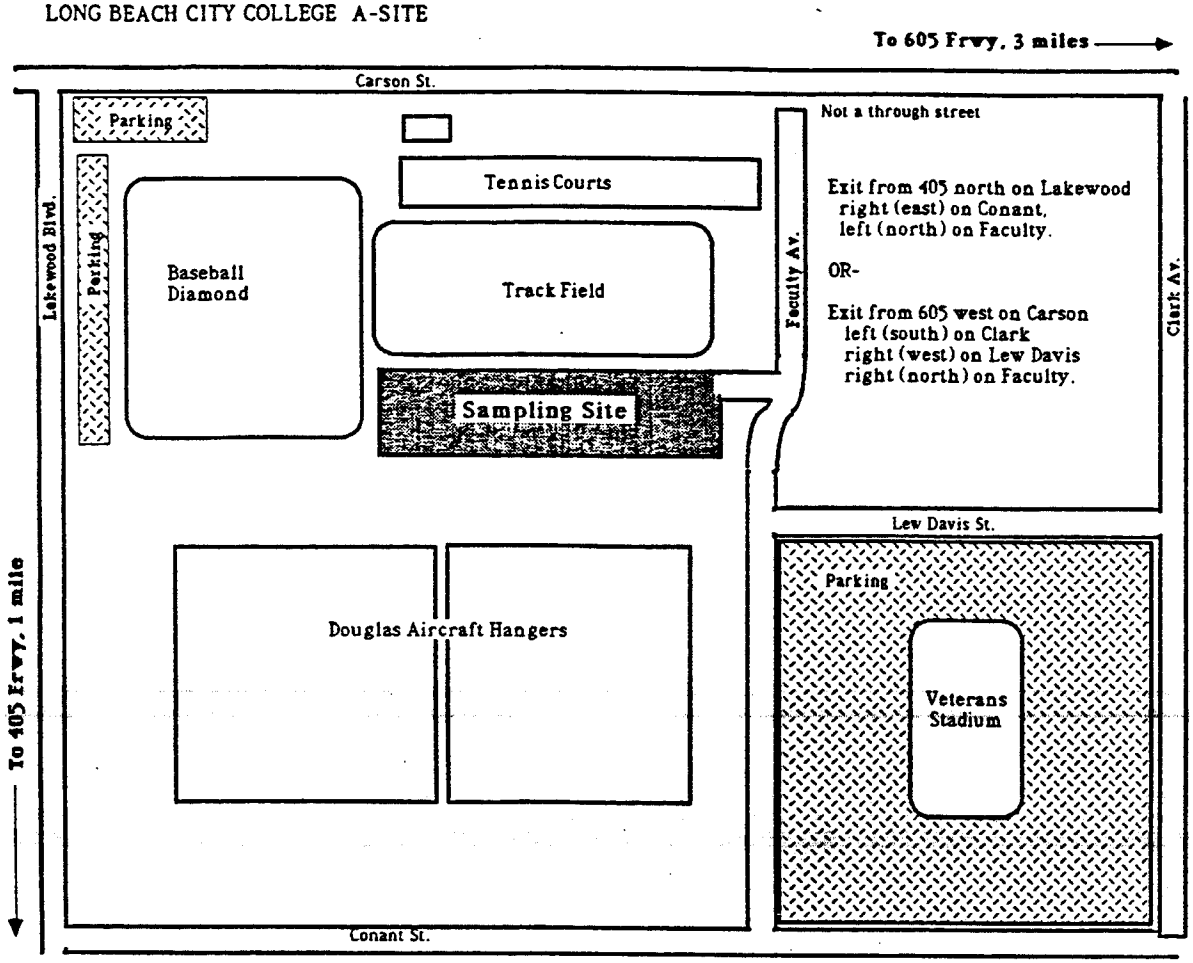

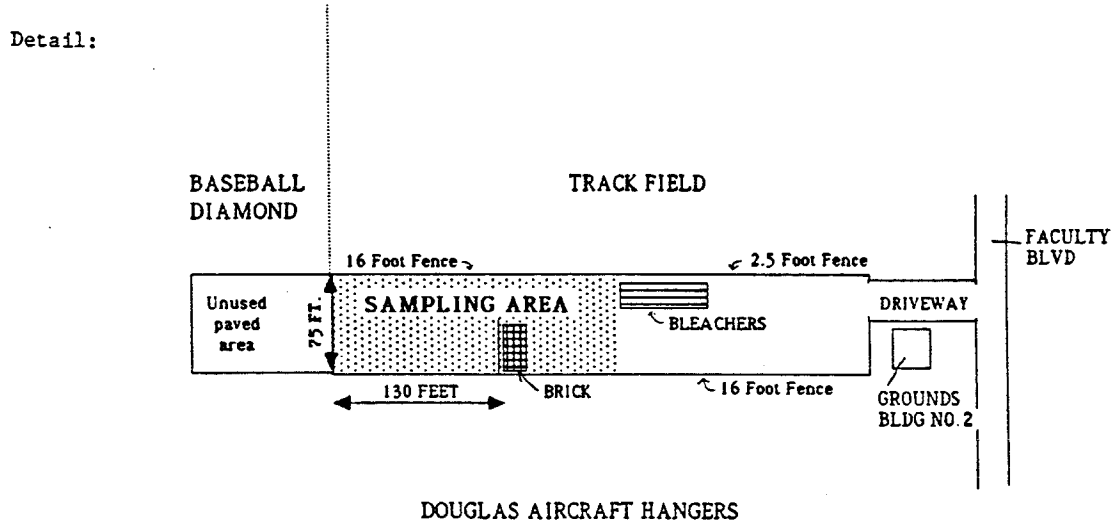

Figure III-2. Location of sampling area at Long Beach City College type A site.

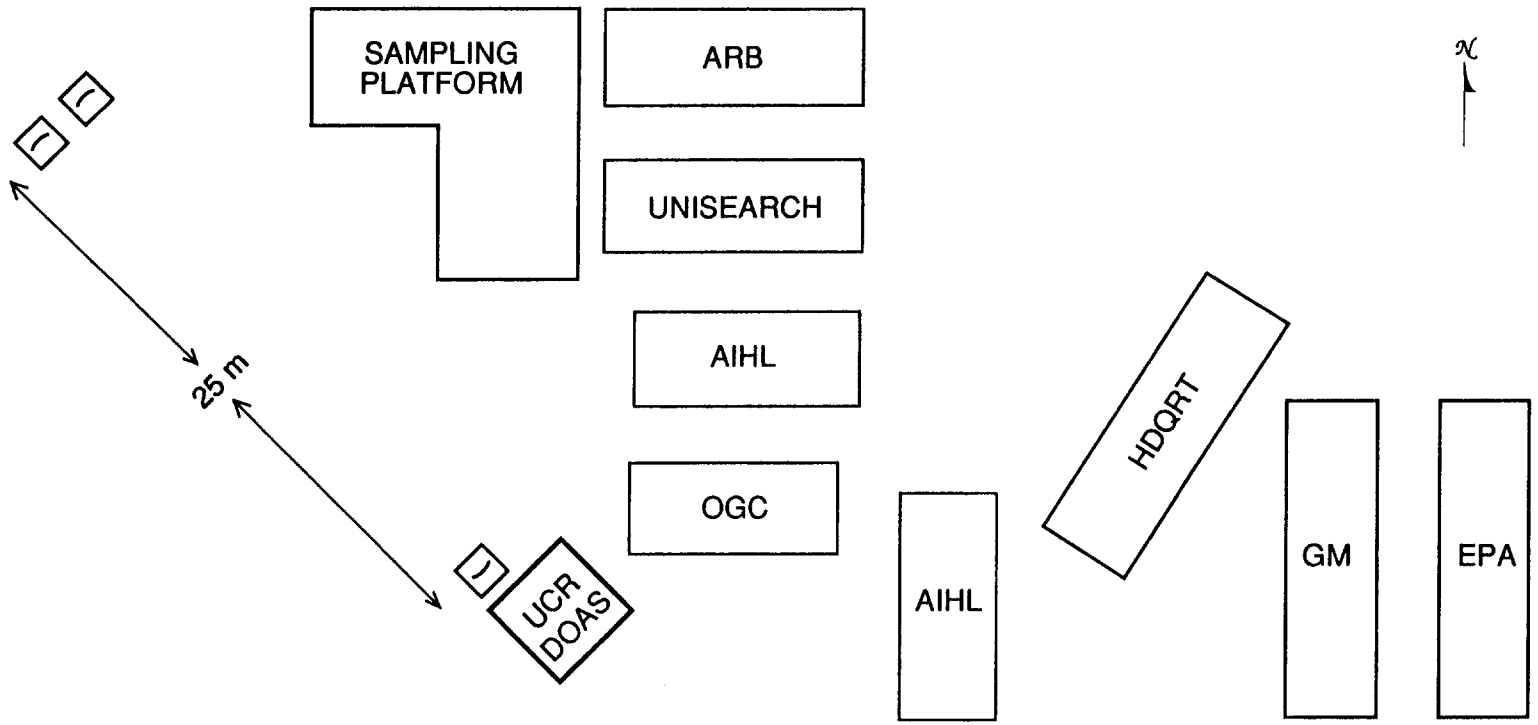

Figure III-3. Arrangement of research groups at Long Beach City College SCAQS site (Fall 1987).

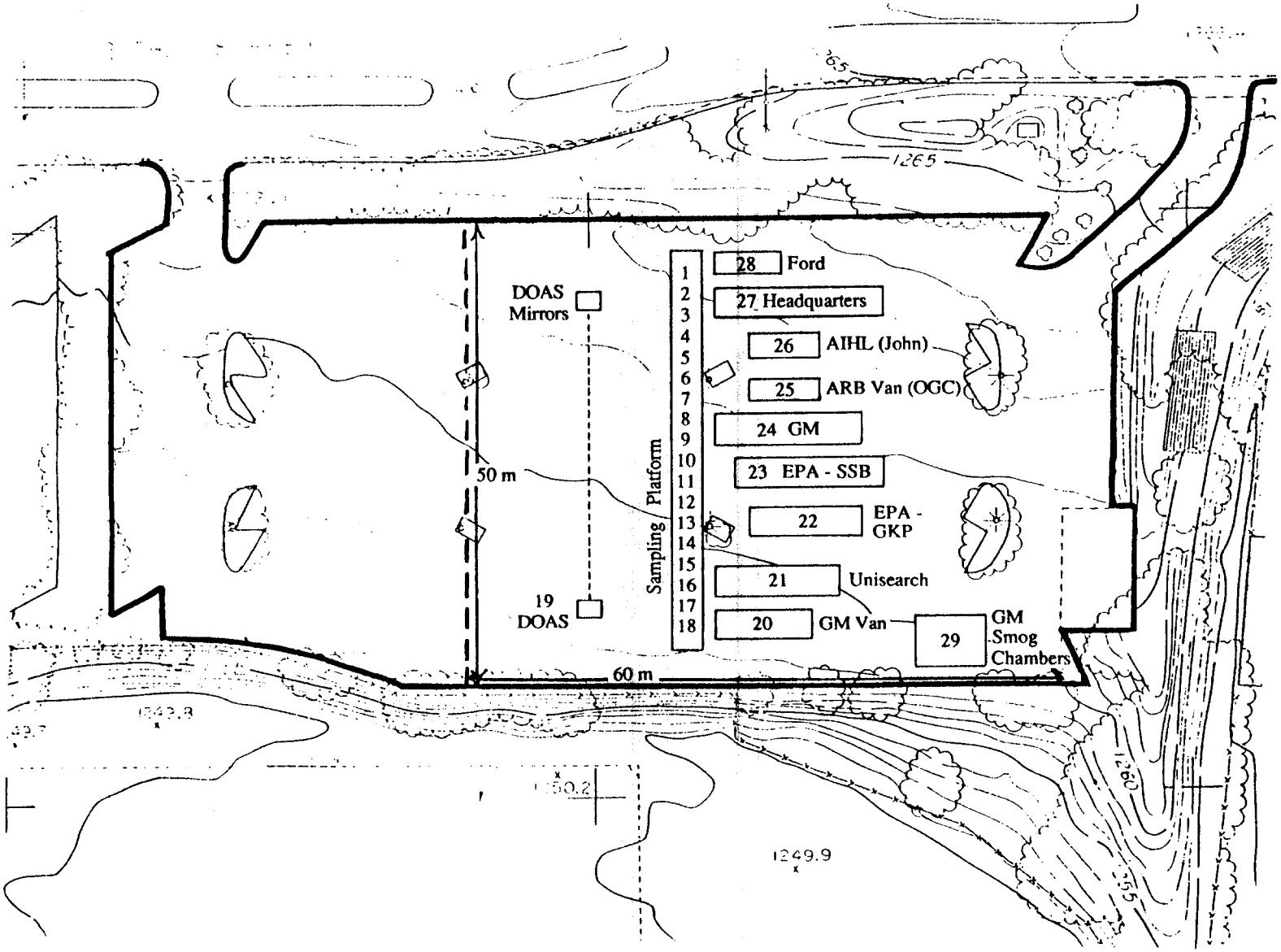

Figure III-4. Claremont site for summer 1987 episodes.

This site was a vacated parking lot of the campus, which was located ~1.5 miles north of the Interstate 10 freeway and ~0.5 miles south of Foothill Blvd. Buildings bordered the parking lot to the north with an open field to the south. A more detailed representation of the orientation and distance of the DOAS system with respect to the instrument sampling platform and the mobile laboratories of other research groups is shown in Figure III-5. Given the greater space available at Claremont, we were able to orient the multiple reflection cell in a north-south alignment to minimize interference from sunlight during periods near sunrise and sunset.

B. Measurement Protocols

Based on analysis of historical meteorological records and previous air monitoring programs, SCAQS program planners selected the early to mid-summer and fall periods for intensive monitoring. Unfortunately, the occurrence of low pollution periods in the early and mid-summer periods of 1987 forced postponement of approximately half of the summer episodes until late August and early September, following monitoring sessions on June 19, 24 and 25 and July 13-15.

With the exception of June 19 in the summer and December 3 in the fall, all monitoring periods consisted of at least two and as many as three consecutive days. Episodes were "called" between 12 and 24 hours prior to the start of monitoring, at 0100 PDT in the summer and midnight (PST) during the fall. Typically the DOAS spectrometer was brought to operating status 2-6 hours before the start of an episode and allowed to run continuously until the morning or afternoon following the midnight or 0100 ending time of a given multi-day episode. Ambient air spectra were recorded at all times, except during collection of pollutant reference spectra (generally after sunrise or around sunset), periods of fog, power failures at the site, or computer malfunctions.

Spectral records were recorded over approximately fifteen minute averaging times and saved to floppy disks as described in Section IV. Approximately 48 hr of data could be stored on one floppy disk. The specific dates of the SCAQS episodes and the corresponding episode designations are listed in Tables III-1 to III-3, for Claremont, Long

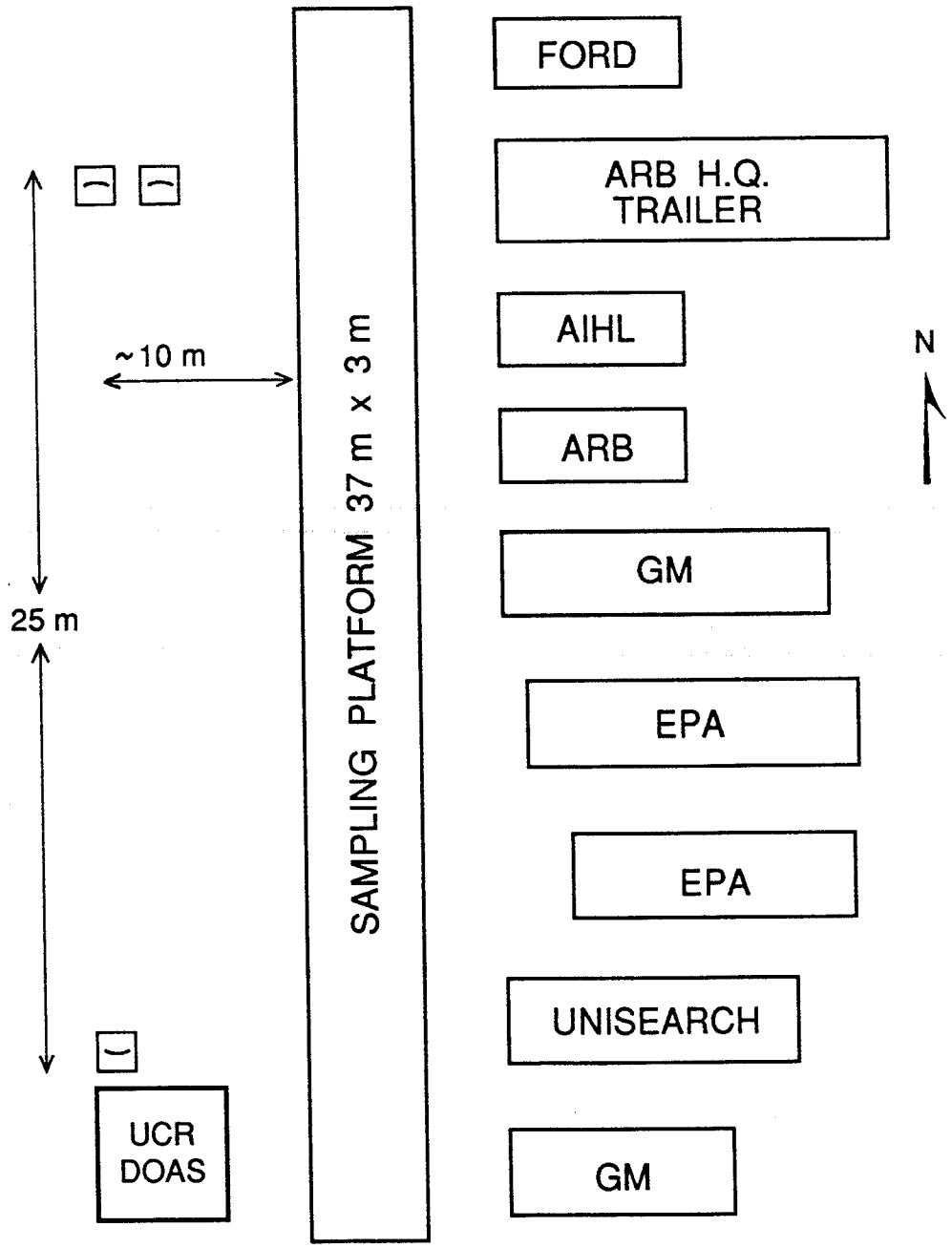

Figure III-5. Arrangement of research groups at Claremont College SCAQS site (summer 1987).

Table III-1. Organization of DOAS Data Files From Summer Phase of SCAQS Program: Long Beach Site

Episode	Date	Data Diskette Number	Inclusive Dates	Inclusive Times (PDT)	Inclusive File Numbers	Reference Spectra File Numbers			Back-up Diskette Number
						NO_2	HONO	HCHO	
S-1	6/19	1530	June 18 - June 20 JD169 - JD171[a]	19:33-08:35	15191-15334	15331 15332			1537
S-2	6/24	1531	June 23 - June 25 JD174 - JD176	21:27-22:34	15335-15493	15467 15468			1538
S-3	6/25								
S-4	7/13	1532	July 12 - July 14 JD193 - JD195	21:00-19:30	15494-15668	15542 15667		15543 15668	1555
S-5	7/14								
S-6	7/15	1533	July 14 - July 16 JD195 - JD197	19:30-09:53	15669-15817	15811 15812	15815 15816 15817	15813 15814	1556
S-7	8/27	1534	Aug. 26 - Aug. 28 JD238 - JD240	20:35-23:59	15825-16018	15898 15899		15900 15901	1561
S-8	8/28								
S-9	8/29	1535	Aug. 29 - Aug. 30 JD241 - JD242	00:00-13:37	16019-16166	16161 16162	16164 16165 16166	16163	1562
S-10	9/2	1536	Sept. 1 - Sept. 4 JD244 - JD247	22:00-10:30	16167-16395	16333 16336	16337 16338 16395	16334 16335	1563
S-11	9/3								

[a]Julian days.

Table III-2. Organization of DOAS Data Files From Summer Phase of SCAQS Program: Claremont Site

Episode	Date	Data Diskette Number	Inclusive Dates	Inclusive Times (PDT)	Inclusive File Numbers	Reference Spectra File Numbers			Back-up Diskette Number
						NO_2	HONO	HCHO	
S-1	6/19	1501	June 18 - June 20 JD169 - JD171[a]	18:30-11:25	10195-10360	10196 10360 10359			1570
S-2	6/24	1503	June 23 - June 25 JD174 - JD176	17:50-18:47	10433-10601	10435 10605		10434	1571
S-3	6/25	1504[b]							
S-4	7/13	1505	July 12 - July 14 JD193 - JD195	20:30-19:00	10705-10890	10706 10791		10705 10790	1558
S-5	7/14								
S-6	7/15	1506	July 14 - July 17 JD195 - JD197	19:15-09:00	10891-11098	10891 10987		10892 10988	1559
S-7	8/27	1507	Aug. 26 - Aug. 28 JD240 - JD242	19:15-18:25	11099-11286	11099 11190		11100 11191	1560
S-8	8/28								
S-9	8/29	1508	Aug. 28 - Aug. 30 JD240 - JS242	18:25-20:15	11287-11481	11287 11384		11288 11385	1567
S-10	9/2	1509	Sept. 1 - Sept. 3 JD244 - JD246	20:35-18:30	11482-11643	11482 11519 11548		11483 11518 11547	1568
S-11	9/3	1510	Sept. 3 - Sept. 4 JD246 - JD247	18:30-16:45	11644-11737	11644 11729 11739	11735 11736 11737	11645 11728 11732 11730	1565
		1566[b]	Sept. 8	NO_3 reference spectra:	11740,11742				1572

[a]Julian days.
[b]Only reference spectra on this diskette.

Table III-3. Organization of DOAS Data Files From Fall Phase of SCAQS Program: Long Beach Site

Episode	Date	Data Diskette Number	Inclusive Dates	Inclusive Times (PDT)	Inclusive File Numbers	Reference Spectra File Numbers			Back-up Diskette Number
						NO_2	HONO	HCHO	
F-1	11/11	1540	Nov 10 - Nov 12 JD314 - JD316[a]	14:00-20:00	16500-16710	16570 16666		16571 16667 16668	1580
F-2	11/12								
F-3	11/13	1541	Nov 12 - Nov 14 JD316 - JD318	20:00-13:20	16711-16871	16760 16761 16866 16867	16870 16871	16762 16763 16769 16868	1581
F-4	12/3	1542[b]	Dec 2 - Dec 4 JD336 - JD338	13:00-14:30	16872-17066	17059 17062	17065 17066	16963 16964 16965 17060 17061	1582 (1547)
F-5	12/10	1543	Dec 9 - Dec 12 JD343 - JD346	13:40-12:00	17068-17298	17145 17146 17240 17243	17351	17147 17148 17149 17150 17241 17242	1583
F-6	12/11	1544	Dec 12 JD346	00:01-13:30	17299-17350	17344 17345	17349 17350	17346 17347 17348	1584

[a]Julian days.
[b]Clean air background spectra: 17058, 17063

Beach summer and Long Beach fall, respectively. These tables also show the numbers of the primary and back-up data diskettes, the inclusive dates, times and file numbers for the data on each diskette, and the reference spectra file numbers for each episode.

Additional information concerning measurement protocols and DOAS operating procedures are given in Section IV.

IV. EXPERIMENTAL METHODS

A. Introduction and Background

As a result of collaboration with researchers from Julich, West Germany, the SAPRC developed its own capability in the early 1980's for conducting DOAS measurements of key atmospheric constituents such as NO_3 radicals and HONO. These earlier measurements at sites throughout California, including Death Valley, Pt. Reyes and Edwards Air Force Base, utilized a single-pass configuration in which a white light source was imaged through the atmosphere over distances up to 17 km and then analyzed with the rapid-scanning DOAS spectrometer. Although results from these studies led to important insights into the critical role played in the atmosphere by HONO and NO_3 radicals (Pitts et al. 1984a, Platt et al. 1984), the long, single-pass optical path yielded data integrated over a large air mass, and hence not suitable for direct correlation with other measurements made for discrete air parcels by more conventional instruments.

To address this concern prior to a series of ARB sponsored inter-comparison studies, we designed and constructed (under ARB Agreement A4-081-32, A. M. Winer, P.I.) a new folded optical path DOAS system based on a 25 m basepath, open multiple reflection cell capable of total optical paths approaching 2 km. This system was applied in several studies prior to the SCAQS program, including at El Camino Community College in early 1986, with continual refinements and improvements leading up to the summer of 1987 and the commencement of the SCAQS episodes.

In this section, we describe in detail the design, assembly and operation of two 25 m basepath DOAS systems, and the application of these systems to the measurement of ambient levels of NO_3 radicals, HONO, HCHO and NO_2 at the two type A sites described in the preceding section.

B. Design and Operation of 25 m Basepath DOAS Systems

1. DOAS System Design

A schematic diagram of the DOAS systems employed in the SCAQS program is shown in Figure IV-1. The two spectrometers differed primarily in that at Long Beach a McPherson 0.3 m spectrograph was employed while at Claremont a SPEX 0.5 m spectrograph was used. In each case, white light

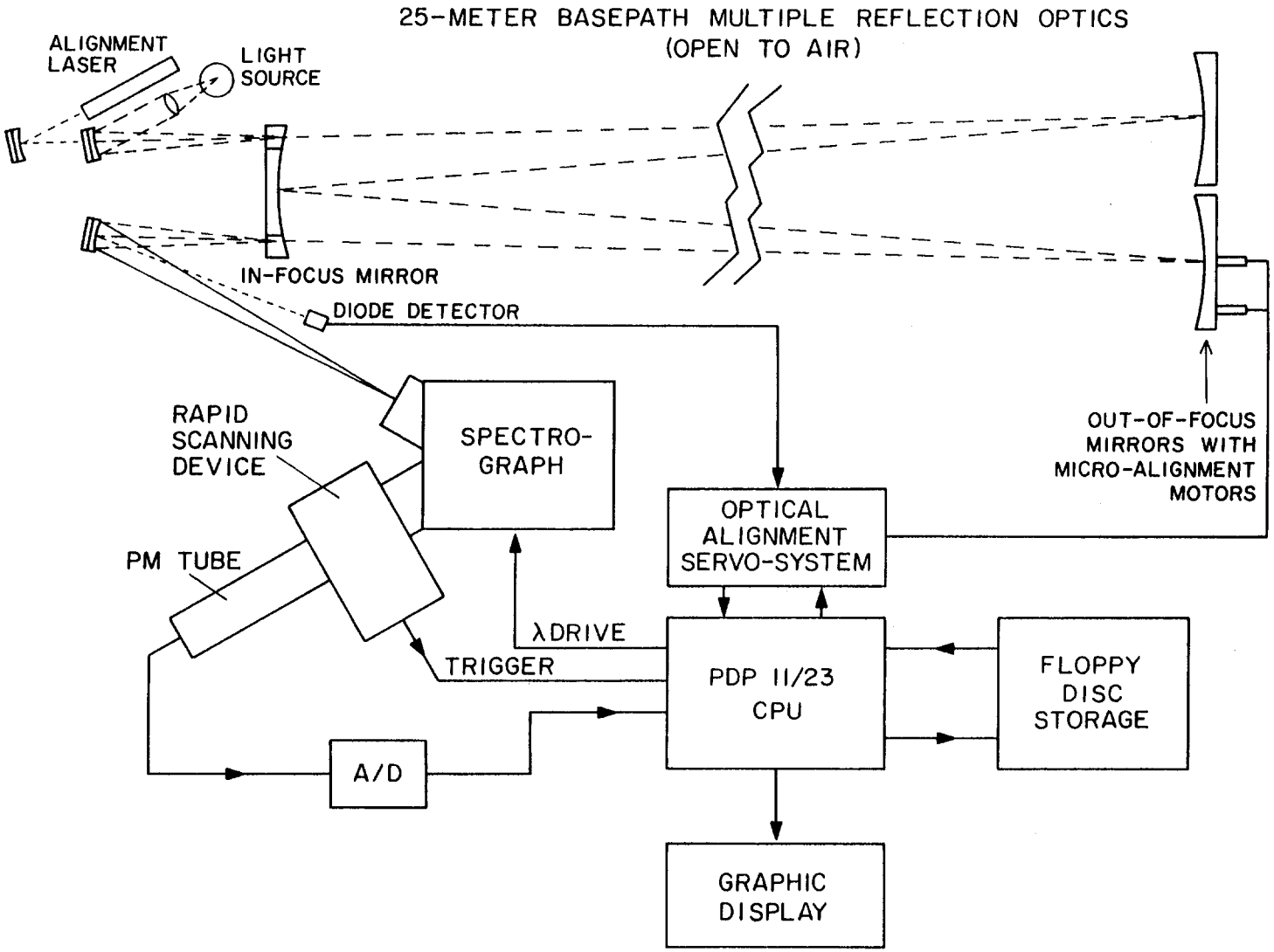

Figure IV-1. Schematic diagram of differential optical absorption spectrometer (DOAS) systems employed during SCAQS program.

from a 75 W high-pressure Xenon arc lamp was transmitted through a 25 m base path optical system of the three-mirror White design (White 1942). The mirrors were fabricated from 30 cm diameter, 6 cm thick Pyrex blanks and coated with custom 37 layer dielectric coatings supplied by Newport Thin Film Corporation (see below).

At both sites, the optical systems were located approximately 10 m to the west of the platforms containing the other measurement systems employed during the SCAQS program. At Claremont the optical path was oriented in a north-south alignment while at Long Beach, due to the constraints of the site, the alignment was closer to a west-east orientation. Both optical systems were completely open to the air.

An important requirement for the study was that all analytical techniques sample at a common height of 1.9 m (6 ft) above the ground in order to minimize influences of dry deposition of nitric acid and other nitrogenous species on the measurement data. This requirement necessitated elevating the DOAS spectrometer and optical system. In order to augment the 1.2 m (4 ft) height initially designed into the optical axes of the long pathlength mirror assemblies, while at the same time preventing extraneous vibrations, the spectrometers, mirror systems and their housings were set on massive concrete blocks.

Six 4 ft x 4 ft x 10 ft concrete structures were obtained from the Pyramid Precast Company, which provided the necessary machinery to position the blocks on premarked areas at the study site. Three of these blocks constituted the support platform for the DOAS spectrometer and one supported the out-of-focus mirrors at the other end of the optical path.

A new instrument capability added for the SCAQS program was the use of vertical- and horizontal-adjustment micrometer motors (Newport Research) on one of the out-of-focus mirrors. To further automate the DOAS, these motors were operated by a computer driven servo system. Light from a HeNe laser, aligned coaxially with the white light source and passing through the multiple reflection optical system was focused onto a photodiode-based, position-sensing device whose output was fed to the computer. Movements of the laser image from a pre-selected position on the photodiode resulted in a computer command to one or both of the micrometer motors, correcting mirror movement due to the diurnal variation in temperature. The arrangement of the DOAS and laser transfer optics is shown in Figure IV-2.

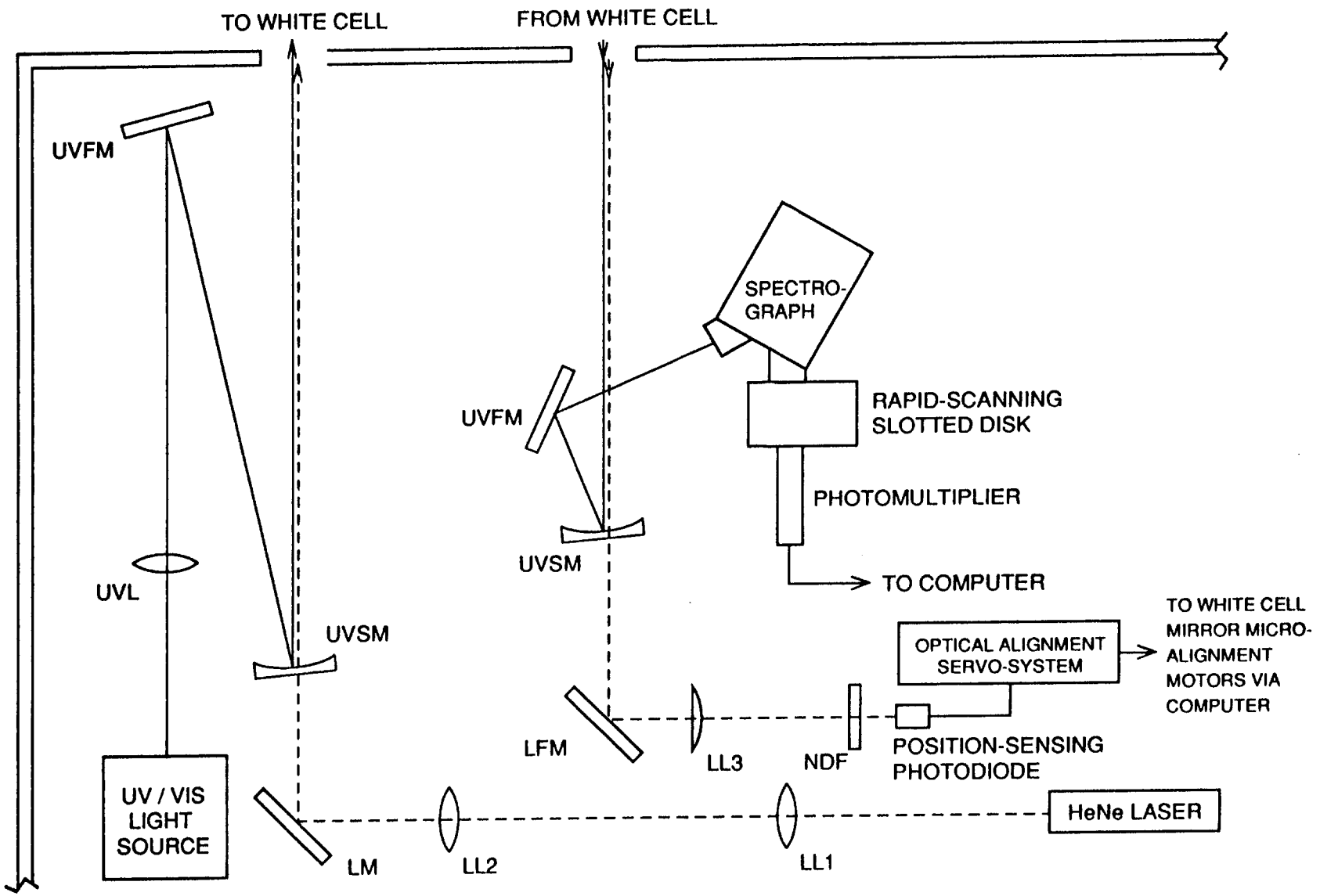

Figure IV-2. Arrangement of DOAS transfer optics.

In order to improve the light throughput of the multipath systems at the wavelengths of interest, we employed dielectric coatings, which offer a much higher reflectivity (although limiting the useful spectral width) on the White cell mirrors. For this purpose, the Newport Thin Film Company designed a custom coating for our special needs (i.e., high reflectivity around 350 and 660 nm). From the attached test sheet (Figure IV-3), it can be seen that in the region of the HONO and NO_3 radical absorption bands the reflectivity of this dielectric coating is approximately 99%.

With this dielectric coating the pathlength was no longer limited by the light losses, but rather by the stacking limit for the images on the mirror surface while preserving their separation from neighboring images. Furthermore, at high image densities, minute changes in the positioning of the mirror mounts due to large temperature changes at sunrise and sunset can cause misalignment of the optical system. For automatic scanning of spectra, we routinely employed 32 reflections (corresponding to pathlengths of 800 m.

After passing through the multiple reflection system, white light from the Xenon arc was focused onto the entrance slit of the spectrograph and the resulting intensity monitored by a photomultiplier (EMI 9659Q) whose output was acquired by a DEC MINC 11/23 minicomputer. The average light intensity within the multiple reflection system due to the Xenon arc was less than 1% of solar noon and therefore caused negligible photolysis of HONO. For NO_3 measurements in the 660 nm region, an orange filter was inserted in front of the Xenon arc as a further precaution against photolysis of this species at night and to eliminate spurious second order signals from the spectrograph grating.

In each DOAS system, the exit slit of the spectrograph was replaced by a rapid-scanning device rotating in the focal plane of the dispersed spectrum. This consisted of a thin metal disk into which slits 10 μm wide and 20 mm apart were etched radially. During each scan, one slit moved across an opening between two masks which blocked other slits, sweeping over a spectral range of ~50 nm. A single scan was completed in approximately 10 ms, minimizing noise in the spectra due to atmospheric turbulence.

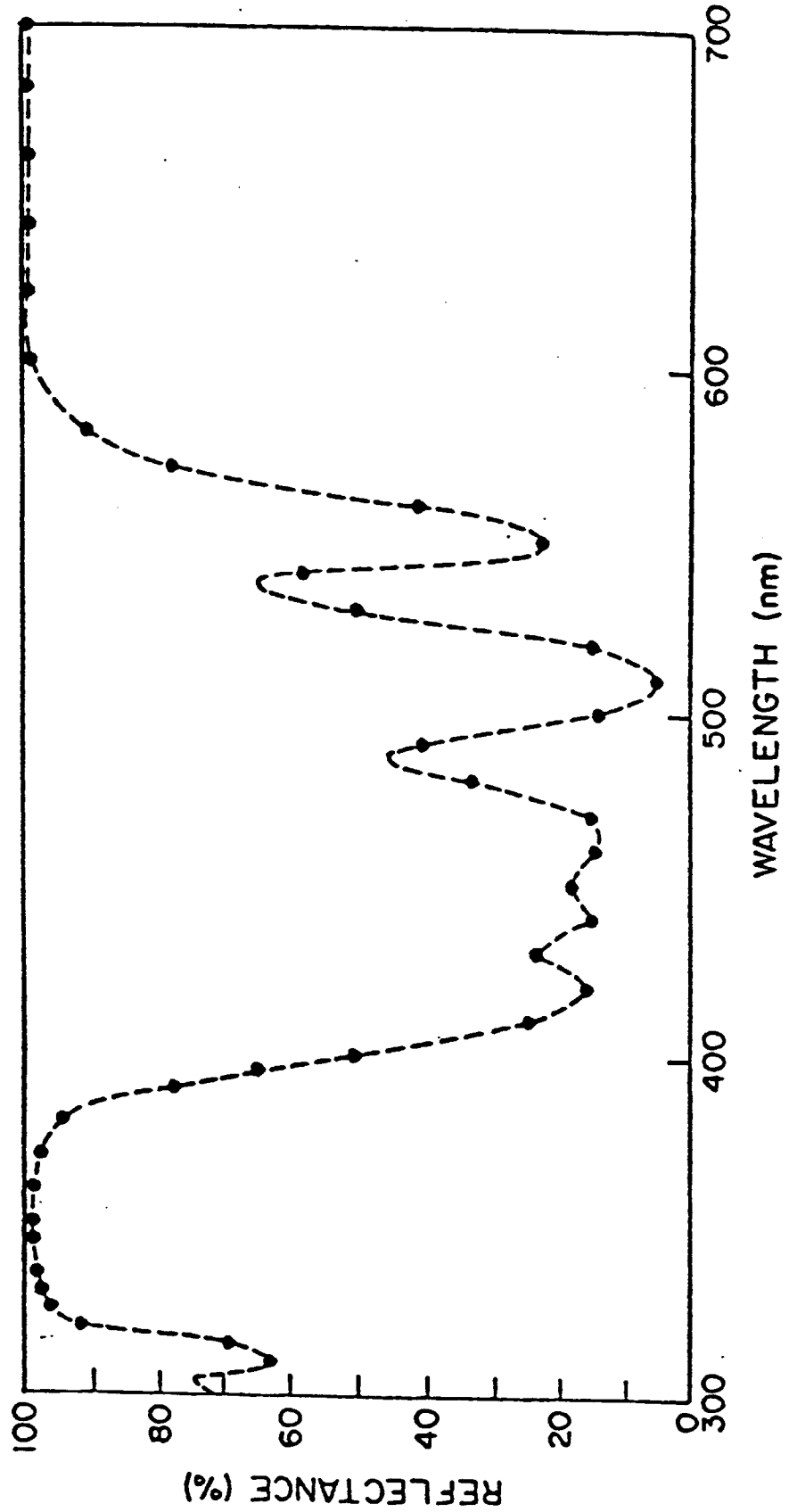

Figure IV-3. Reflectance properties of 37-layer dielectric coating employed in DOAS multiple reflection optical system.

2. Signal Averaging

The output signal was digitized by a high-speed analog-to-digital converter (data translation) and read by the minicomputer. In order to preserve spectral resolution while superimposing scans, the rotational speed of the slotted disk was maintained constant to within ±0.1%. During each 15 min measurement period, approximately 50,000-70,000 scans were added in the computer memory, providing a signal-to-noise ratio sufficiently high that optical densities as low as 3×10^{-4} (base 10) could be determined.

Since, as noted above, a single scan requires only ~10 msec, atmospheric scintillation has little effect on the signal. Moreover, since typically $(5\text{-}7) \times 10^4$ individual scans are recorded and signal-averaged over each several minute measurement period, even complete, but momentary, interruption of the light beam has no appreciable effect on the final spectrum. Except under the haziest conditions, stray light effects through the entrance slit are usually negligible due to the instrument's narrow field of view [$\sim 8 \times 10^{-5}$ steradians].

3. Derivation of Concentrations

The concentrations of atmospheric species were derived from Beer's Law. However, since the light intensity (I_o) in the absence of any absorption cannot be obtained with this technique, the differential optical density was employed and thus only those compounds which have structured absorption spectra could be measured. For such compounds

$$\log \frac{I_o'}{I} = \alpha \, C \, l$$

where I is the light intensity at the center of the absorption band (at wavelength λ_2) due to the compound of interest, I_o' is the intensity in the absence of well-structured absorption (ignoring any absorption continuum) by that compound, α is the "differential" absorption coefficient at λ_2 for the compound of interest, l is the optical path and C is the concentration of the absorbing molecule. I_o' is interpolated linearly from the intensities at wavelengths λ_1 and λ_3 at which there is no structured absorption due to the compound of interest, according to

$$I_o' = I(\lambda_1) + [I(\lambda_3) - I(\lambda_1)] \frac{\lambda_2 - \lambda_1}{\lambda_3 - \lambda_1}$$

4. Scan Protocol

As noted above, a given spectral region was scanned for approximately 15 minutes (50,000 to 70,000 scans) and this constituted the integration period for that measurement. At Long Beach, measurements were restricted to the 300-370 nm spectral region which contains prominent absorption features due to HONO, HCHO and NO_2 as shown in Figure IV-4. At Claremont there was the added complication of also scanning, at night, the 620-670 nm region containing two NO_3 radical absorption bands. For this purpose, the scan protocol employed at Claremont is shown in Table IV-1.

5. Calibration and Treatment of Data

The procedures used for calibration and treatment of the DOAS data are described below, and in additional detail elsewhere (Winer et al. 1987; Biermann et al. 1988a; Winer and Biermann 1990). Briefly, a background spectrum was synthesized from the original spectrum using a polynomial fit. After removal of the broadband contour, the remaining spectra were successively fitted, using a least squares method, to reference spectra generated in the field. The resulting optical densities were converted to concentrations using recommended literature values (DeMore et al. 1987) for the differential absorption cross sections for NO_2 and HONO of 1.0×10^{-19} (348 and 365 nm) [Bass et al. 1976] and 4.2×10^{-19} (354 nm[12]) [Stockwell and Calvert 1978] cm^2 $molecule^{-1}$, respectively. The absorptivities employed for HCHO and NO_3 were 6.8×10^{-20} [based on determinations in this laboratory (Green and Biermann 1987)] and 1.8×10^{-17} cm^2 $molecule^{-1}$ [from the literature (Graham and Johnston 1978)], respectively. As indicated in Table IV-2, based on the these absorption cross sections, an 800 m absorption pathlength, and the actual noise levels in the spectra, we calculated detection limits of 4, 0.8, and 5 ppb for NO_2, HONO, and HCHO, respectively, and approximately 30 ppt for NO_3. Accounting for noise levels, baseline drift, and data-processing effects, the error limits for NO_2 data were estimated at ±10% while for the HONO and HCHO data the corresponding errors were ±30% due to the more complex deconvolution. For NO_3 radical concentrations, the error is estimated to be ±15%.

Figure IV-5 gives an example of this data analysis procedure and the system performance (Winer et al. 1987). The top trace (a) is an actual, full-scale air spectrum obtained during the night of September 15, 1985

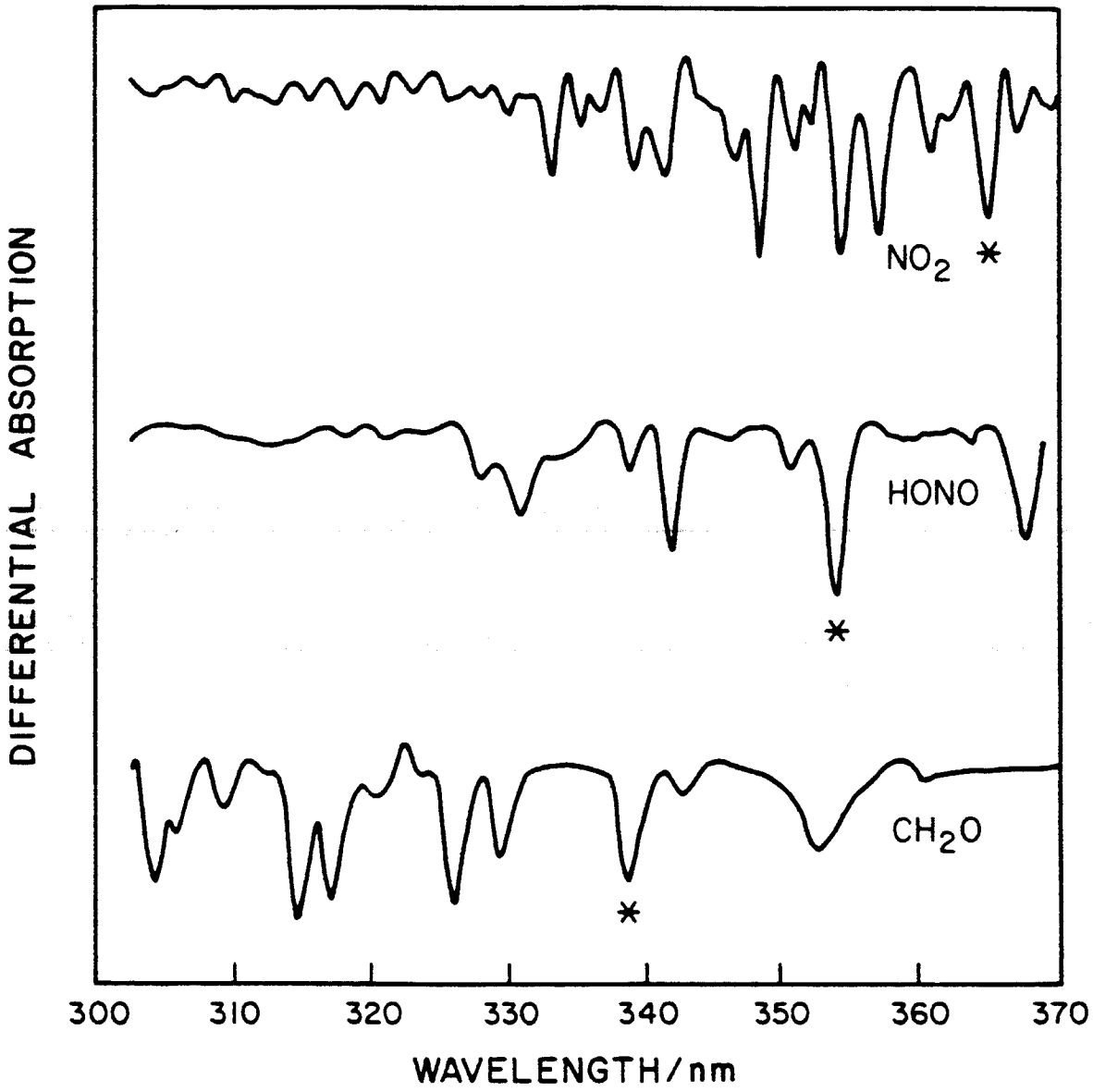

Figure IV-4. DOAS reference spectra generated for nitrogen dioxide, nitrous acid and formaldehyde, indicating principal absorption bands used for quantitative atmospheric measurements.

Table IV-1. Scan Protocol at Claremont

	Number of Scans for HONO/HCHO/NO_2 (per hour)	Number of Scans for NO_3 Radicals
0700-1900	4	-
1900-2400	2	2
2400-0700	2.7	1.3

Table IV-2. Calculated Detection Limits for 25-m Basepath Multiple-Reflection Cell DOAS System Operated at 800 m Pathlength

Compound	Differential Absorption Coefficient (atm^{-1} cm^{-1})	Absorption Wavelength (nm)	Detection Limit (ppb) for 3×10^{-4} O.D. (base 10)
NO_2	2.7	365	4
HONO	11	354	0.8
NO_3 Radical	480	662	0.03[a]
HCHO	2.1	339	5

[a]Based on 5×10^{-4} O.D.

(the zero intensity line overlaps trace (b)]. The broad, large-scale structure is due to a superposition of spectral response curves resulting from mirror reflectivity, lamp intensity, photomultiplier sensitivity, and other instrumental characteristics. Trace (b) shows the residual trace after the synthetic background was subtracted as described above. Trace (c) is the same spectrum magnified by a factor of 16 to depict more clearly the low optical densities involved. The predominant structure can be immediately recognized as being due to NO_2, a reference spectrum of which is shown in (d). After subtraction of the NO_2 features and further magnification by a factor of 4, the residual structure in trace (e) is unambiguously identified as HONO by comparison with its reference spectrum (f).

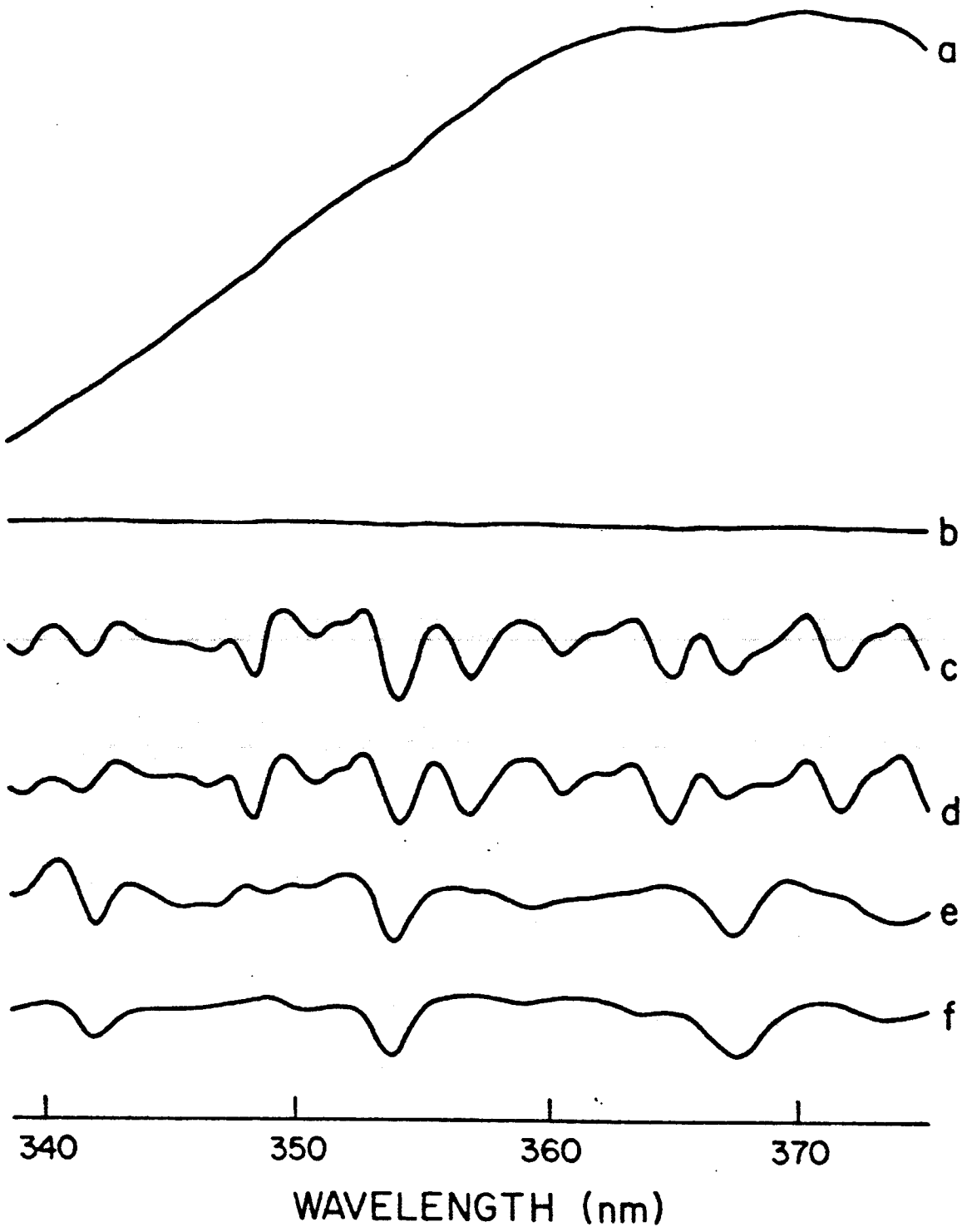

Figure IV-5. DOAS spectrum of ambient air covering the wavelength region ~340-375 nm from the night of September 15-16, 1985: (a) full-scale air spectrum [the zero intensity line overlaps trace (b)]; (b) after removal of background curvature; (c) same as (b), magnified by a factor of 16; (d) NO_2 reference; (e) after NO_2 subtraction, magnified by a factor of 4; (f) HONO reference spectrum.

6. Generation of Reference Spectra

Reference spectra for NO_2 were generated by inserting 10 cm cells into the beam exiting the transfer optics within the shed and recording approximately 50,000 spectra. These quartz cells had been filled with typically 1 or 3 torr of the respective gases (sometimes higher concentrations for HCHO) on a vacuum rack at the SAPRC laboratories using a Baratron gauge, then wrapped in black cloth and foil and transported to Claremont or Long Beach. The NO_2 cells were used as is, while the HCHO cells were sometimes heated with a hot air gun or warmed in the sun (while still wrapped in black cloth and foil to prevent photolysis). Spectra recorded over periods of days, and even weeks, exhibited little change in the NO_2 concentration, but a small continuous loss in HCHO in most cases.

Nitrous acid reference spectra were obtained by generating HONO in situ in free air inside the shed, in the transfer optics for the white light source exiting the shed to the multiple reflection cell. A dilute sulfuric acid solution (one part H_2SO_4 to five parts water) was added dropwise to a large watch glass containing a suitable sodium nitrite solution (15 gm $NaNO_2$ in 16 oz water) while scanning with the DOAS system. Typically, approximately 10,000 to 15,000 scans were recorded during the evolution of NO_2 and HONO gaseous vapors from this procedure.

Nitrate radical reference spectra were generated in-situ on the last day of the summer SCAQS campaign using a Welsbach ozonizer brought to the Claremont site. Ozone was added to one side of a 10 cm cell already containing NO_2 until approximately half the NO_2 had been displaced. Both stopcocks were quickly closed and the cell placed immediately in the transfer optics and scanning begun. Several spectra exhibiting the prominent 623 and 662 nm NO_3 radical absorptions were obtained in this fashion.

In most cases reference spectra were used only for fitting purposes and therefore the absolute concentrations of these samples did not need to be known, hence the use of HONO in situ samples. However, the cuvette samples of NO_2 and HCHO, prepared throughout the study, were useful in monitoring the performance of the DOAS spectrometer. The HONO and NO_3 concentrations obtained in this study would be subject to revision if the absorptivities reported in the literature for these two species are shown

to be different in future studies. For NO_2 and HCHO, however, we independently confirmed the absorption cross-sections.

C. Pre-episode Preparations and Performance During Episodes

The contract for this study was finalized on April 17, 1987, less than two months before the start of the nominal SCAQS episode window opened on June 15. During this two month period, all of the needed equipment and supplies not already available were ordered and obtained. Both DOAS systems and the field sheds which would house them at Long Beach and Claremont were pre-assembled and tested at SAPRC to minimize the time needed for subsequent set-up in the field.

In the last week in May, the massive cement supports for the DOAS spectrometers and multiple reflection mirror assemblies were delivered by the Pyramid Precast Company to the type A sites and placed at pre-marked positions corresponding to the base optical path of 25 m. The shed platforms were then constructed, followed by assembly of the sheds themselves and installation of the spectrometers and mirrors. The final week prior to the start of the study was spent optimizing the performance of the two DOAS spectrometers, dealing with computer malfunctions and testing of the new auto-sensing, laser-based alignment systems.

1. Summer Episodes

Both DOAS systems were fully operational for the commencement of episode monitoring on June 19, 1987 and operated with relatively little downtime, except for the final 12 hours of episode S-3 on June 25 during which there were repeated power failures to the Long Beach site which led to a pre-amplifier failure in the DOAS system. On July 16 the instruments were shutdown for what eventually proved to be a five week postponement of the summer phase of the SCAQS study. Both DOAS systems were left in their entirety at the two sites due to the uncertainty concerning the length of delay in the summer episodes, and because of the inadvisability of attempting to move the computers back to Riverside for what might be a short period. Thus, no data reduction took place during the five week postponement.

The summer study recommenced on the evening of August 26 and the DOAS systems were operated for two additional multi-day episodes in late August and early September during which generally high pollution levels were

encountered. For the first time during the SCAQS program NO_2 features appeared prominently in the instantaneous DOAS spectra at Long Beach for a significant fraction of the final episodes of the summer campaign. Both the Claremont and Long Beach systems operated successfully for more than 95% of the monitoring periods during these high pollution episodes. Summer experiments were completed on September 4, with the generation of reference spectra for all four atmospheric species investigated with the DOAS technique.

During the week of September 7, 1987, the DOAS systems were disassembled and returned to UCR. At Claremont the shed and platforms were also disassembled and the cement blocks removed for storage at the Pyramid Precast Company. The shed and blocks at Long Beach were left in place for the fall phase of the SCAQS program. The PDP-11/23 diskettes on which the original data were recorded were backed up on 8 in diskettes and on 20 MB hard disks.

2. Fall Episodes

During the fall study period, only the DOAS system at Long Beach was operated since pollution levels were expected to be low at the Claremont receptor site during November and December.

During the weeks of October 19 and 26 the components of the DOAS system needed for the fall study were assembled and prepared for transfer to to the SCAQS site in Long Beach. Repair and refurbishment of the shed and platforms at the site were also completed during this period. On October 29 and 30 the optical table and other large equipment were moved to Long Beach and after security began at the site on November 2, the DOAS system itself. Several modifications were made to reduce the possibility of stray light interferences, and the system was demonstrated to be fully operational by November 5, after two days of uninterrupted scanning.

Preparations for the first winter episode (W-1) were made on the evening of November 10, with official start of the episode at midnight. Conditions for the DOAS system at the beginning of the winter study were 800 m pathlength, 10 micron nominal slit width, and a scanned spectral region between about 310 and 370 nm, with 15-minute averaging times corresponding to approximately 68,000 scans.

During the first morning of episode W-1, it was found that the rising sun faced directly into the far out-of-focus mirrors causing serious misalignment problems due to heating of the mirrors and mirror mounts.

A shield was subsequently created to prevent sunlight from striking the mirrors. Appropriate reference spectra were taken for NO_2 and HCHO on the first morning and each morning thereafter for all three winter episodes.

The DOAS system performed well throughout the first episode until shortly after midnight of November 12/13, at which time heavy fog completely obliterated both the UV source light and the HeNe laser. From approximately 0230 until about 0500 there was low signal after which there was good UV signal until the formal end of the first episode at midnight. The system was left running and spectra obtained until 1030 the following morning, at which time reference spectra were obtained not only for formaldehyde and nitrogen dioxide, but also for nitrous acid.

The DOAS system was restarted on the afternoon of December 2 for the second winter episode (W-2) and operated under the same standard conditions as for episode W-1. Again there were periods during the early morning hours when fog curtailed the UV signal, but the DOAS system was attended throughout the night and, during those periods when the fog cleared, spectra were obtained under optimized conditions. Although the fog conditions were deleterious to DOAS operation, they may have also contributed to the observed elevated levels of nitrous acid. The stagnant air conditions encountered during this period were also conducive to the buildup of elevated aldehyde levels.

On the morning of December 4, for the first time in either the summer or winter episode periods of the SCAQS program, an opportunity occurred to obtain clean air background spectra with the DOAS system. This occurred when light rain fell during the morning following the official end of episode W-2. Whereas fog had earlier led to severely attenuated signals, the UV signal during the rain and drizzle was the strongest observed during the study. Clean air background spectra were obtained following several hours of very light rain and, in fact, light sprinkles fell during at least some periods when the clean air spectra were being recorded. In addition to these background spectra, reference spectra were again obtained for HONO, HCHO and NO_2.

Preparation for the final winter episode (W-3) began on the afternoon of December 9, and spectra were recorded continuously for the next 48 hours until the formal conclusion of the winter SCAQS study at midnight December 11/12. Ambient air spectra and reference spectra for all three compounds of interest were obtained the following morning for various concentrations of HCHO and NO_2 in 10 cm cuvettes and for free HONO vapor generated by the dropwise addition of diluted H_2SO_4 to $NaNO_2$ solution.

During the following week, the DOAS instrument and computer, as well as the ancillary instrumentation and optical system were dismantled and removed from the site. Subsequently, the shed and platform were removed, as were the Hi-Vol samplers and Tenax sampling system employed in a related study.

V. RESULTS

A. Introduction

The gaseous pollutant concentration data obtained by DOAS measurements during eleven intensive days in the summer at Claremont and Long Beach, and during six intensive days in the fall of 1987 at Long Beach are summarized in this Section in graphical form. Generally, the data are plotted either as individual 15-minute values, representing the approximate integration time employed in this study, or as 1-hr average values. Although for simplicity, the integration time for the DOAS data is referred to throughout this section (including the figure captions) as being "15 min," the integration times in some cases were in the range of 14 to 16 minutes (except in the evenings at Claremont where scans were shortened to permit the spectrometer grating to be moved between the HONO and NO_3 radical spectral regions). The actual scan times for each individual cumulative spectrum obtained in this study are given in the Appendices to this report.

The 1-hr averages are for each of the 24 hours of an episode day, the first hour being 0000-0100 (labeled 0000) and the last hour being 2300-0000 (labeled 2300) Pacific Standard Time. Where scan times for a given spectrum fell across an hour point, simple linear weighting was used for the purpose of calculating 1-hr averages. Unless otherwise noted, values below the detection limit were counted as zero in calculating 1-hr averages.

All of the individual numerical values of the 15-min DOAS concentrations obtained in this study are presented in tabular form in Appendices A, B and C which contain the data for the summer Claremont, summer Long Beach and fall Long Beach episodes, respectively. In addition, these data have been forwarded to the ARB and ENSR in machine-readable form.

The data presented here are organized first by the site and measurement season (i.e., summer or fall), then by pollutant, and finally by specific episode days, usually grouping the multi-day episodes data. Table V-1 provides the episode day identification, and corresponding calendar and Julian dates, for the summer and fall measurement days.

A limited amount of discussion is provided in this Section of the general features of these data, including times and ranges of daily maxima

Table V-1. Episode Day Identification and Corresponding Dates (1987)

Season	Episode	Date	Julian Day
Summer	S-1	June 19	170
	S-2	June 24	175
	S-3	June 25	176
	S-4	July 13	194
	S-5	July 14	195
	S-6	July 15	196
	S-7	August 27	239
	S-8	August 28	240
	S-9	August 29	241
	S-10	September 2	245
	S-11	September 3	246
Fall	F-1	November 11	315
	F-2	November 12	316
	F-3	November 13	317
	F-4	December 3	337
	F-5	December 10	344
	F-6	December 11	345

for 1-hr averaging times, highest 15-min values, times and ranges of daily minima, and other qualitative or semi-quantitative observations resulting from these measurements. Additional interpretations and conclusions concerning these DOAS data, including implications for atmospheric chemistry, intercomparison with other measurements made during the SCAQS program (where available at the time this report was prepared), and regulatory approaches are given in Section VI.

B. Claremont Summer Episodes

At Claremont all four atmospheric species accessible to the DOAS technique during this project were measured, including the nitrate radical. The scanning protocol during evening hours at Claremont, divided between the 320-370 nm spectral region for NO_2, HONO and HCHO and the 640-670 nm region for NO_3, is given in Table IV-1. Sections 1 to 4 below present the 15-min values for NO_2, HONO, HCHO and the NO_3 radical, respectively, while section 5 contains the 1-hr average data for all species except the NO_3 radical.

As can be seen from Table V-1, there was only one single-day episode during the summer measurement period, June 19. In the following sections, data for June 19 are presented on a full-page plot, while for all other multi-day episodes the data are grouped into two- or three-day periods.

1. Nitrogen Dioxide

Figures V-1 through V-3 present the 15-min DOAS measurements for NO_2 during the summer Claremont episodes. Perhaps the most striking feature of these data is the regularity with which the daily peak NO_2 concentration occurred at almost exactly 0800 each morning (with the exception of episode S-6, a lower pollution day). Clearly, these morning NO_2 peaks correlate well with the morning traffic peaks, which may have been dominated by the local traffic in the vicinity of, and on, the Claremont campus.

The 15-min NO_2 concentration maxima observed at Claremont ranged between approximately 70 ppb and 120 ppb, with minima in the early morning hours and at around noon generally in the range from 10 to 40 ppb. A secondary maximum also well correlated with traffic patterns was generally observed in the NO_2 data at about 2000. Periods of missing data, primarily for a few hours in the afternoon of several episodes, were usually due to high noise levels or other manifestations of what is believed to have been a stray light problem during that time of the day. [Evidence of this problem was only obtained at the conclusion of the summer study.]

2. Nitrous Acid

Figures V-4 through V-6 present the 15-min HONO concentrations measured by DOAS at Claremont. These data exhibit the characteristic buildup of HONO at night, either shortly after sunrise or, for a few of the episodes, beginning around midnight. Concentrations typically reached peaks or plateaus in the early morning hours, followed by rapid loss of HONO due to photolysis shortly after sunrise.

Peak HONO concentrations observed at Claremont ranged from ~2 ppb to as high as 7 ppb. Both the diurnal pattern in HONO concentrations, and the peak concentrations observed during these eleven episode periods, were consistent with the patterns and peak concentrations observed in earlier DOAS measurements at receptor sites in the SoCAB such as Claremont and Glendora (Winer et al. 1987; Biermann et al. 1988a).

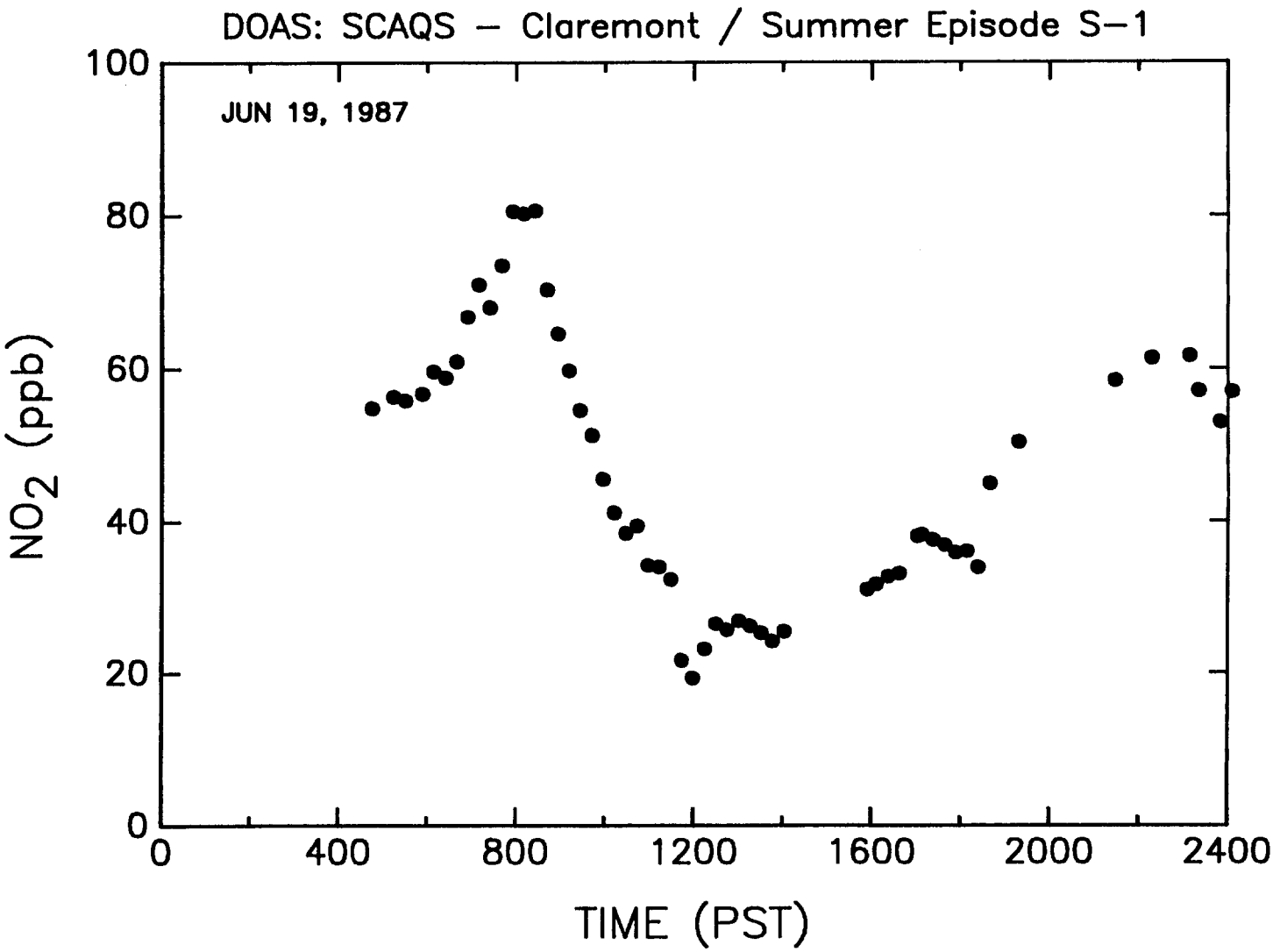

Figure V-1. DOAS 15-min NO_2 concentrations observed at Claremont during summer episode S-1.

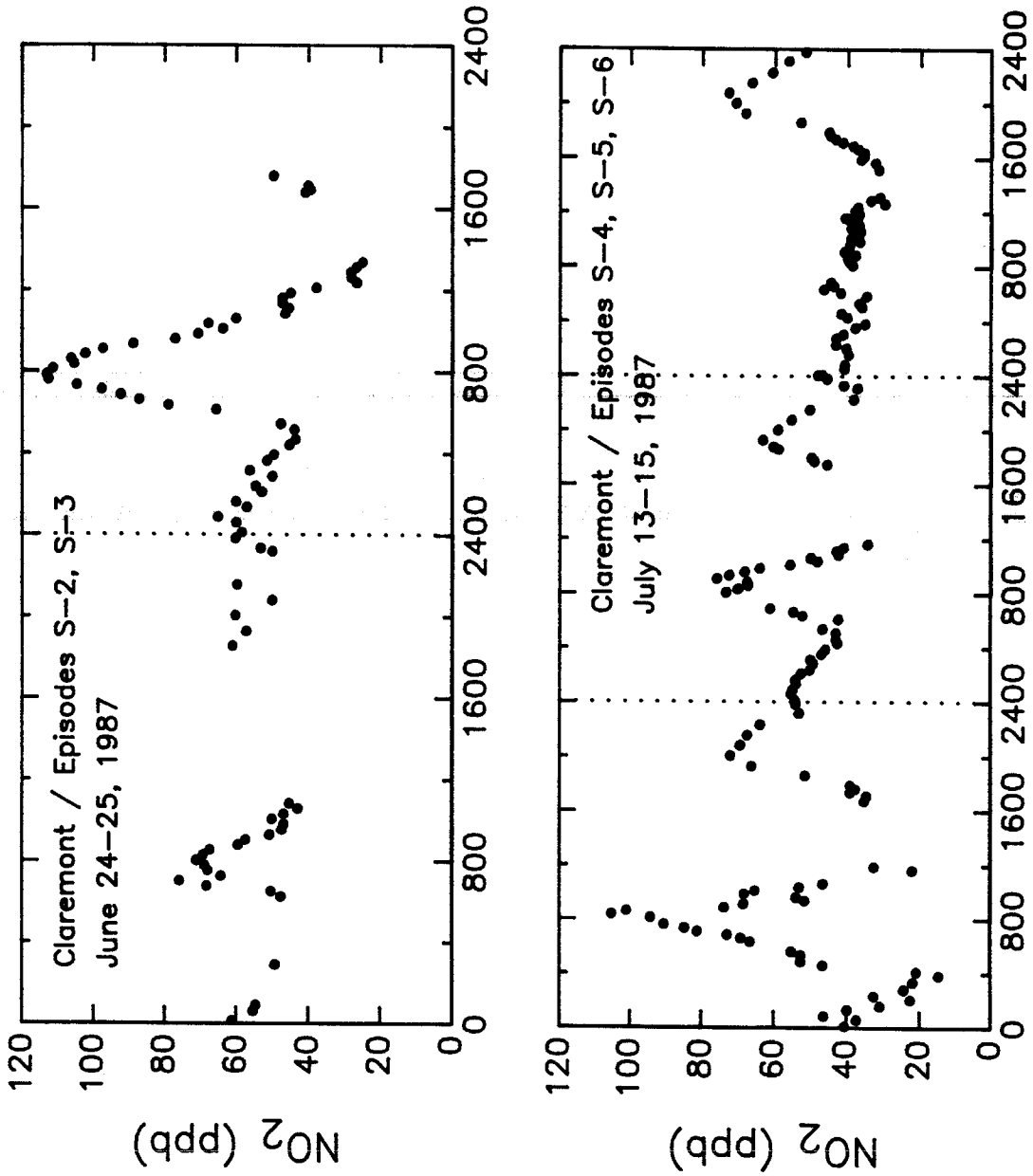

Figure V-2. DOAS 15-min NO_2 concentrations observed at Claremont during summer episodes S-2 through S-6.

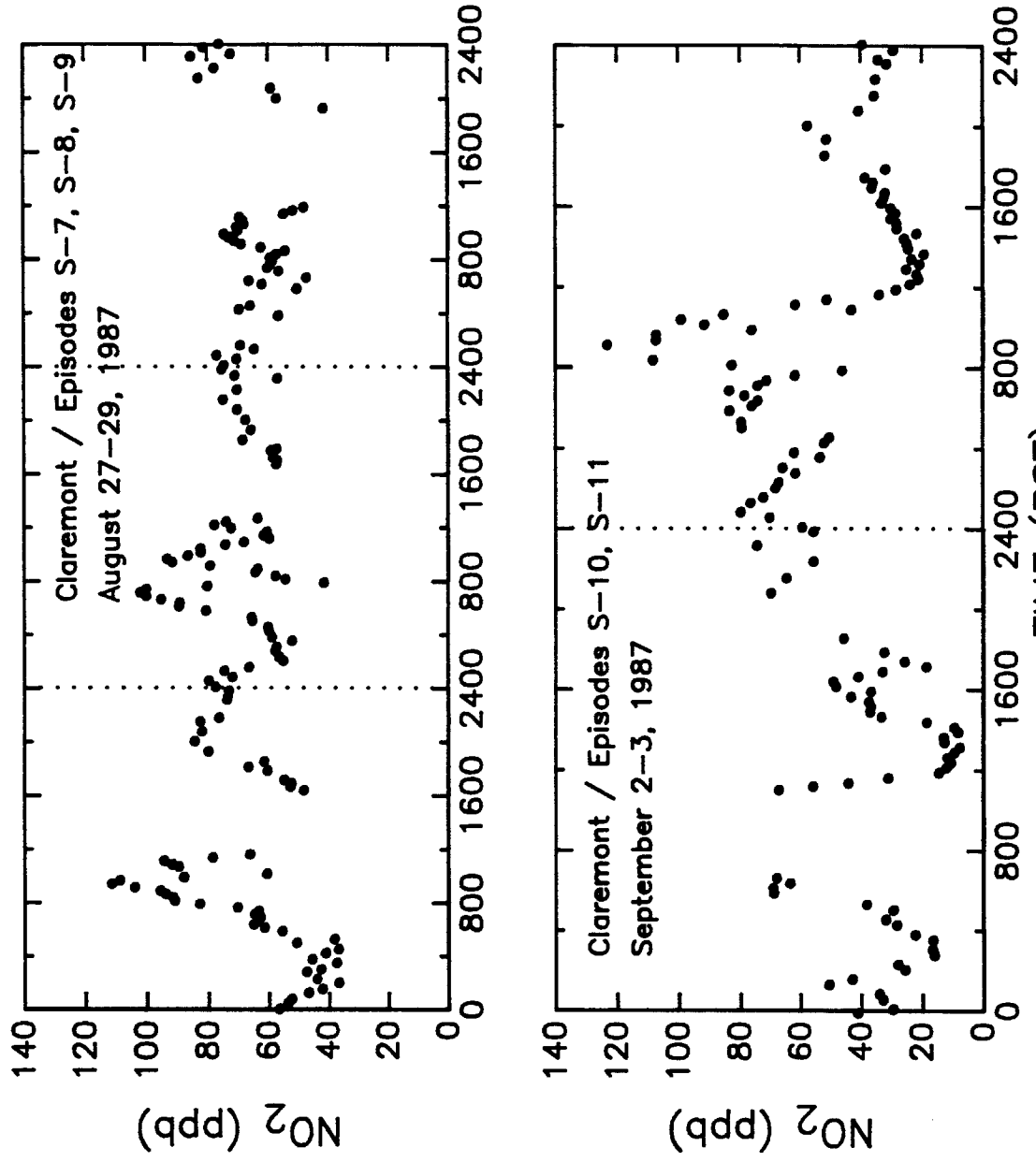

Figure V-3. DOAS 15-min NO_2 concentrations observed at Claremont during summer episodes S-7 through S-11.

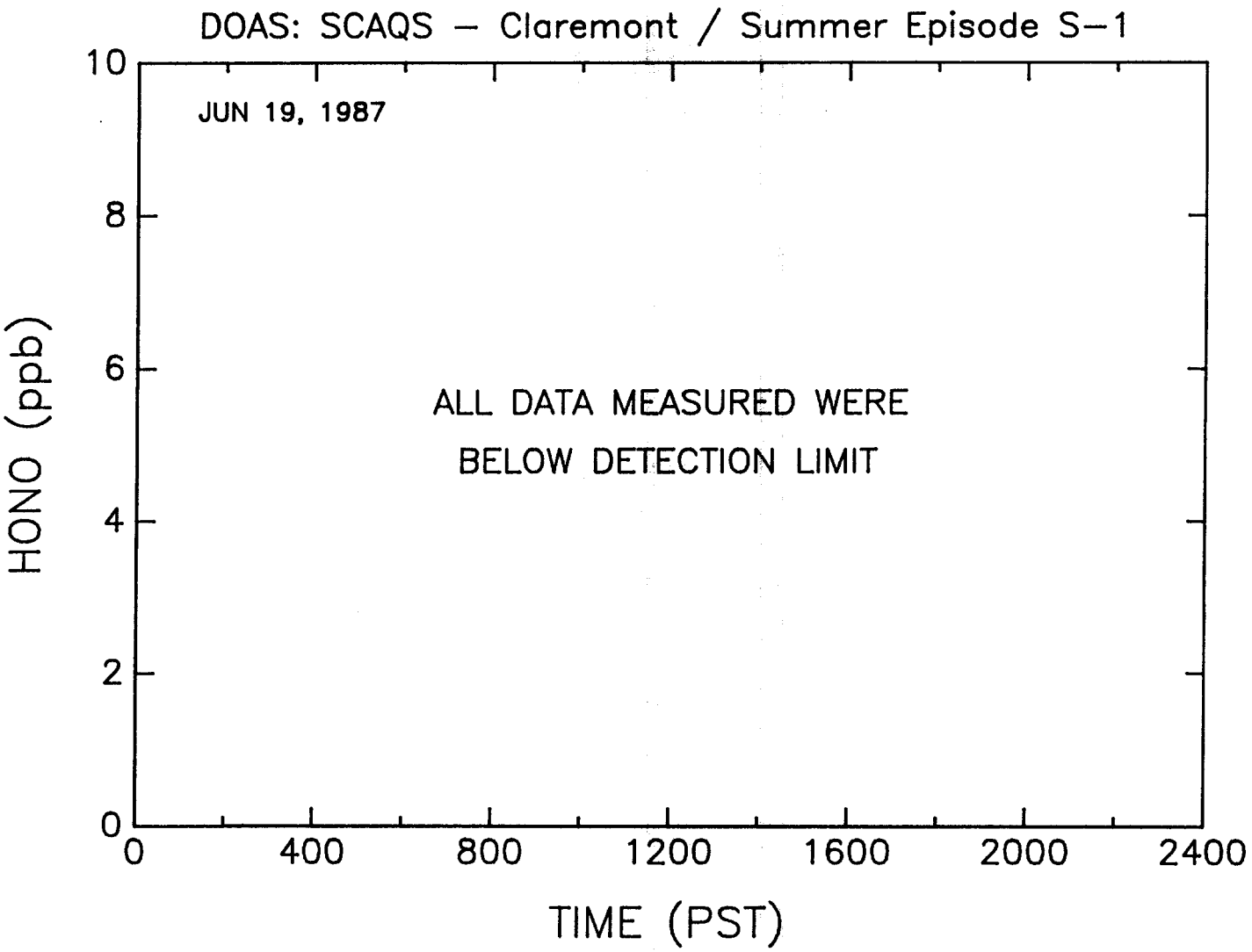

Figure V-4. DOAS 15-min HONO concentrations observed at Claremont during summer episode S-1.

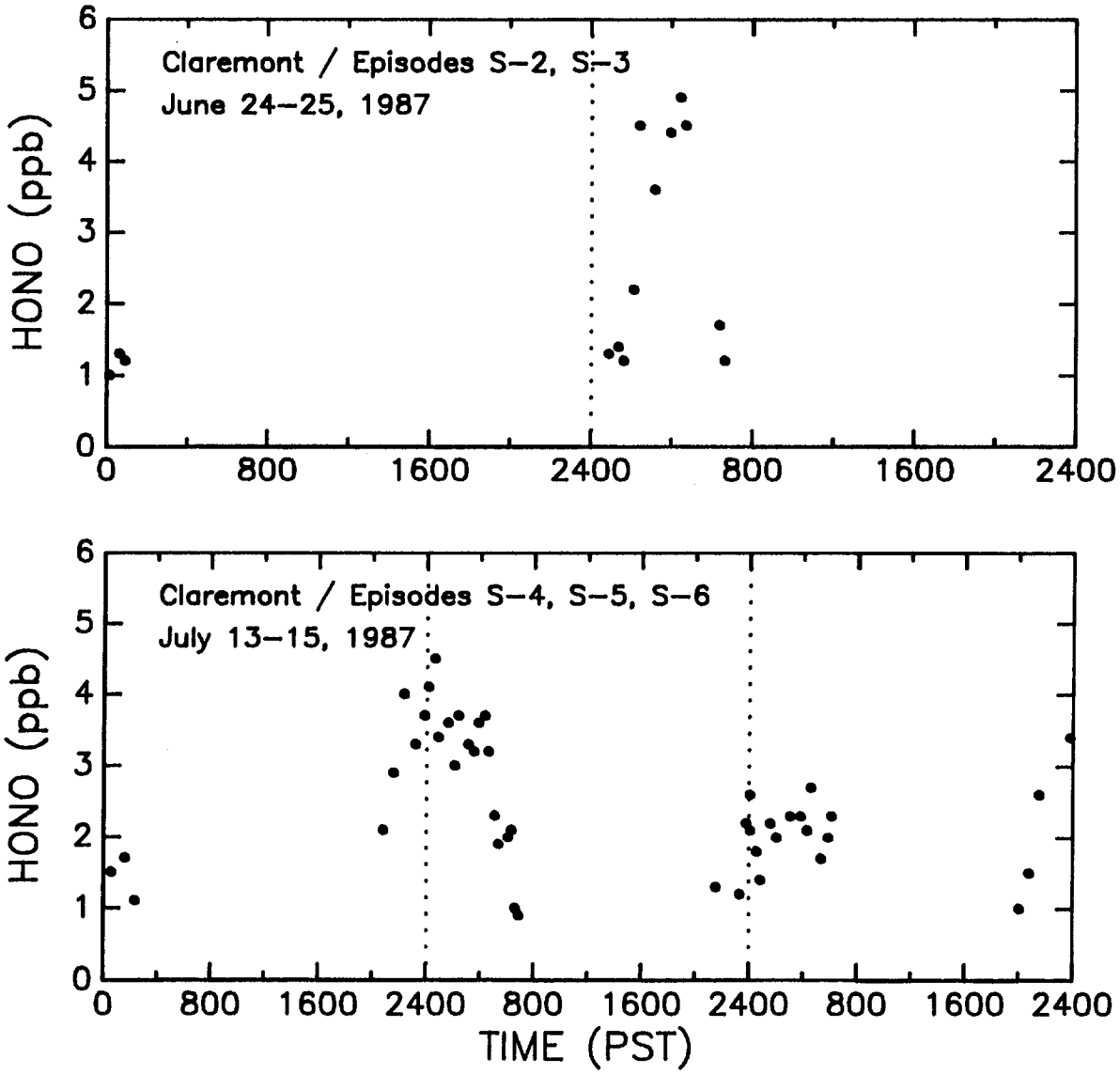

Figure V-5. DOAS 15-min HONO concentrations observed at Claremont during summer episodes S-2 through S-6.

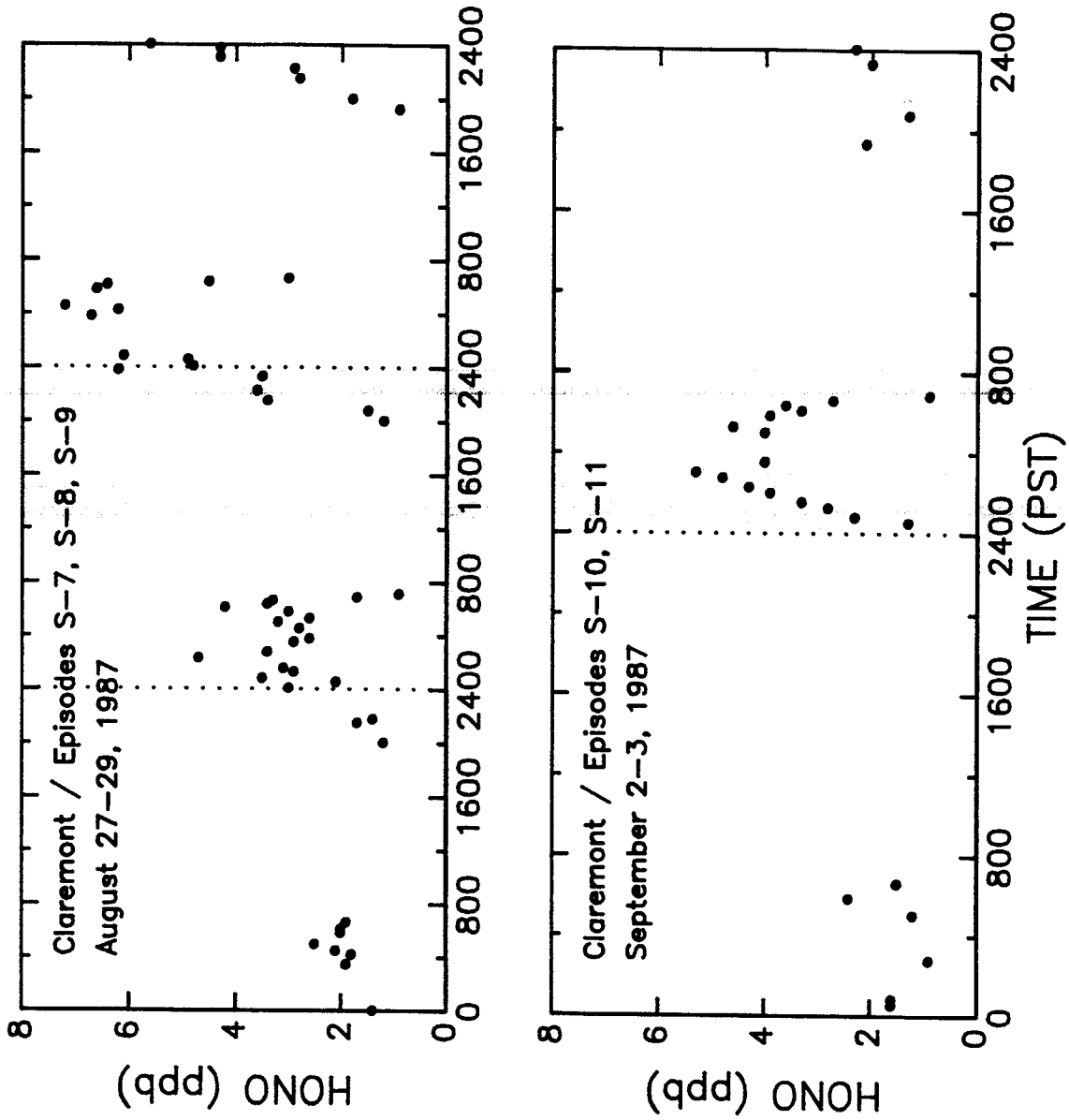

Figure V-6. DOAS 15-min HONO concentrations observed at Claremont during summer episodes S-7 through S-11.

Further interpretation of the HONO data obtained in this study are discussed in Section VI.

3. Formaldehyde

The 15-min HCHO concentrations observed at Claremont are shown in Figures V-7 through V-9. Although the apparent peak in the HCHO diurnal variation occurred generally between 0800 and 1600, the frequent absence of data for several mid-afternoon hours limits what can be concluded in this regard. Peak 15-min HCHO concentrations during the Claremont episodes as measured by DOAS ranged from approximately 12-15 ppb to a high of ~25 ppb on June 25. Daily minima in HCHO concentrations occurred at night and were always less than the 5 ppb detection limit for these DOAS measurements.

4. Nitrate Radical

Figure V-10 displays the nitrate radical concentrations measured at Claremont during the summer episodes. Concentrations above the approximately 30 ppt detection limit for this study were observed in the evenings following sunset for episodes S-2, S-5, S-7, S-8, S-9 and S-10. The maximum NO_3 radical concentrations were in the range of 150 to 170 ppt on the evenings of August 29 (S-9) and September 2, 1987 (S-10).

As in the case of HONO, the behavior of NO_3 radical concentrations was characteristic of that observed in previous DOAS measurements at SoCAB receptor sites such as Claremont and Riverside. As can be seen in Figure V-10, NO_3 radical concentrations peaked between approximately 1900 and 2000, and then declined rapidly to values below the DOAS detection limit by 2200. The observation of measurable NO_3 radical concentrations corresponded, as expected, to those nights for which there were significant concentrations of both of the NO_3 radical precursors, ozone and nitrogen dioxide.

At the Claremont receptor site during intensive episodes O_3, concentrations were typically declining rapidly around the time of sunset (a process accelerated by emissions of nitric oxide during the latter part of the afternoon traffic peak). Concentrations of NO_2 were also generally declining into the early evening hours (see Figures V-2 and V-3). Thus, the rate of formation of NO_3 radicals would be decreasing rapidly into the early evening hours. On most of the nights, nitric oxide (NO) concentrations measured by the chemiluminescence method by GM researchers

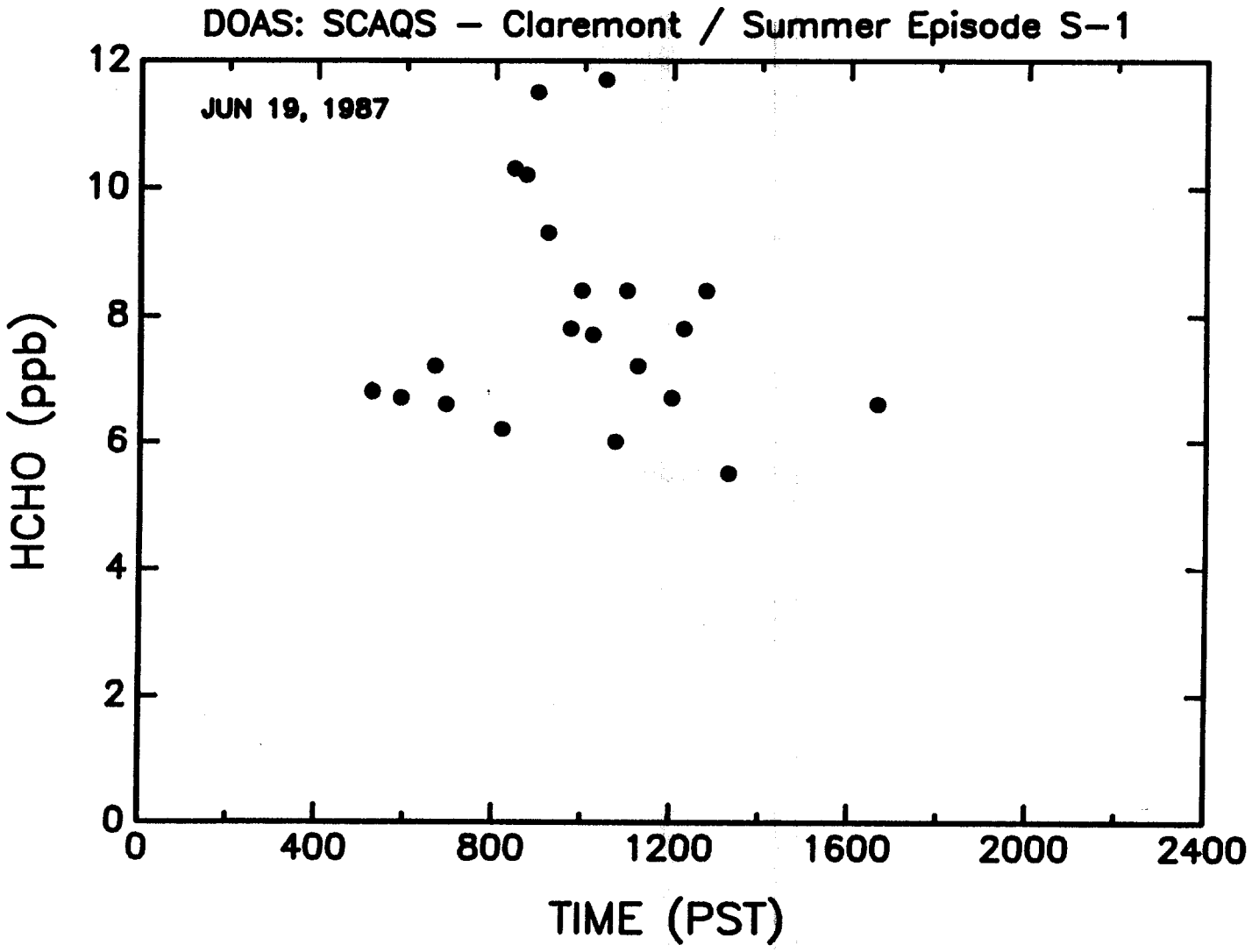

Figure V-7. DOAS 15-min HCHO concentrations observed at Claremont during summer episode S-1.

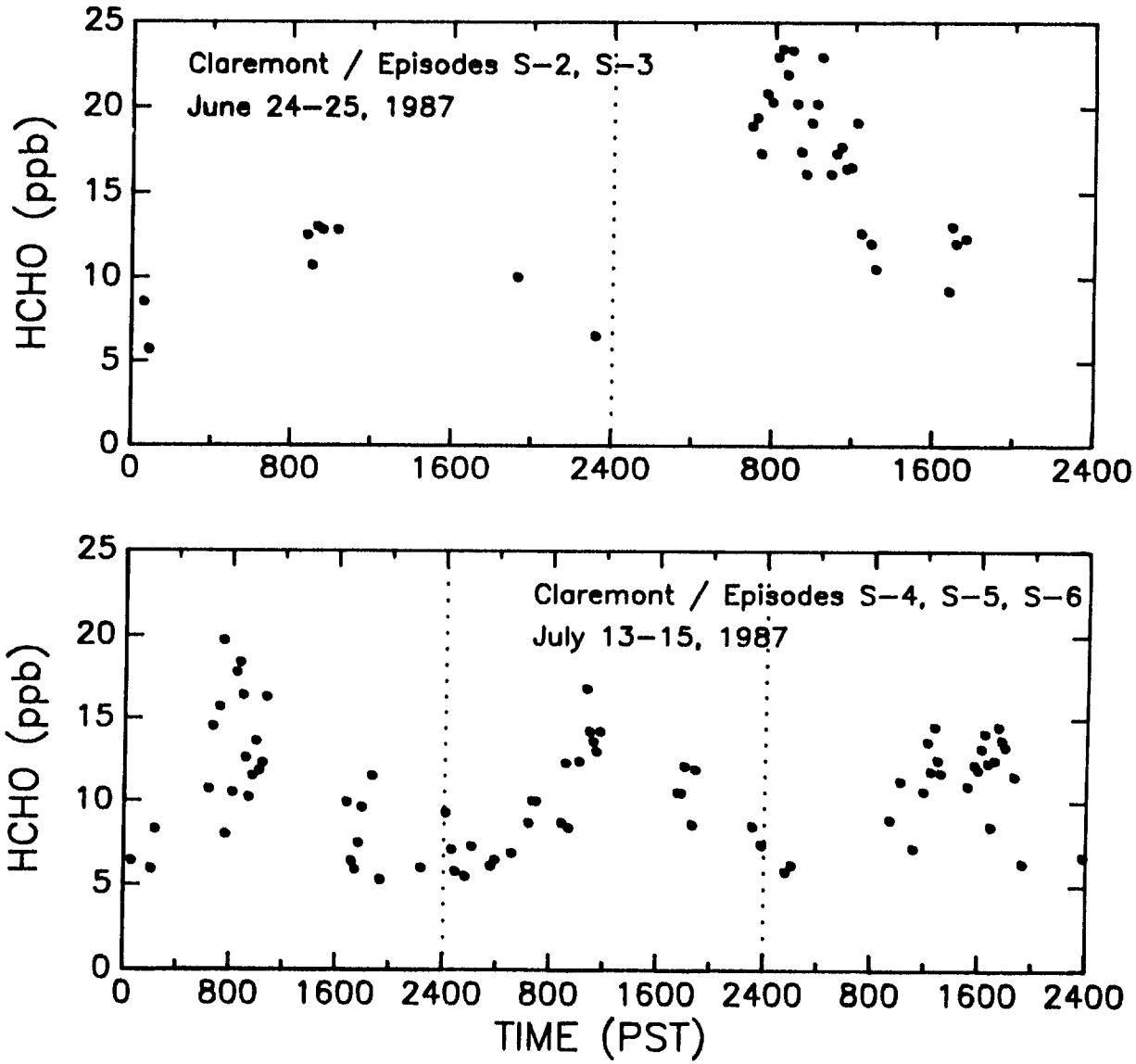

Figure V-8. DOAS 15-min HCHO concentrations observed at Claremont during summer episodes S-2 through S-6.

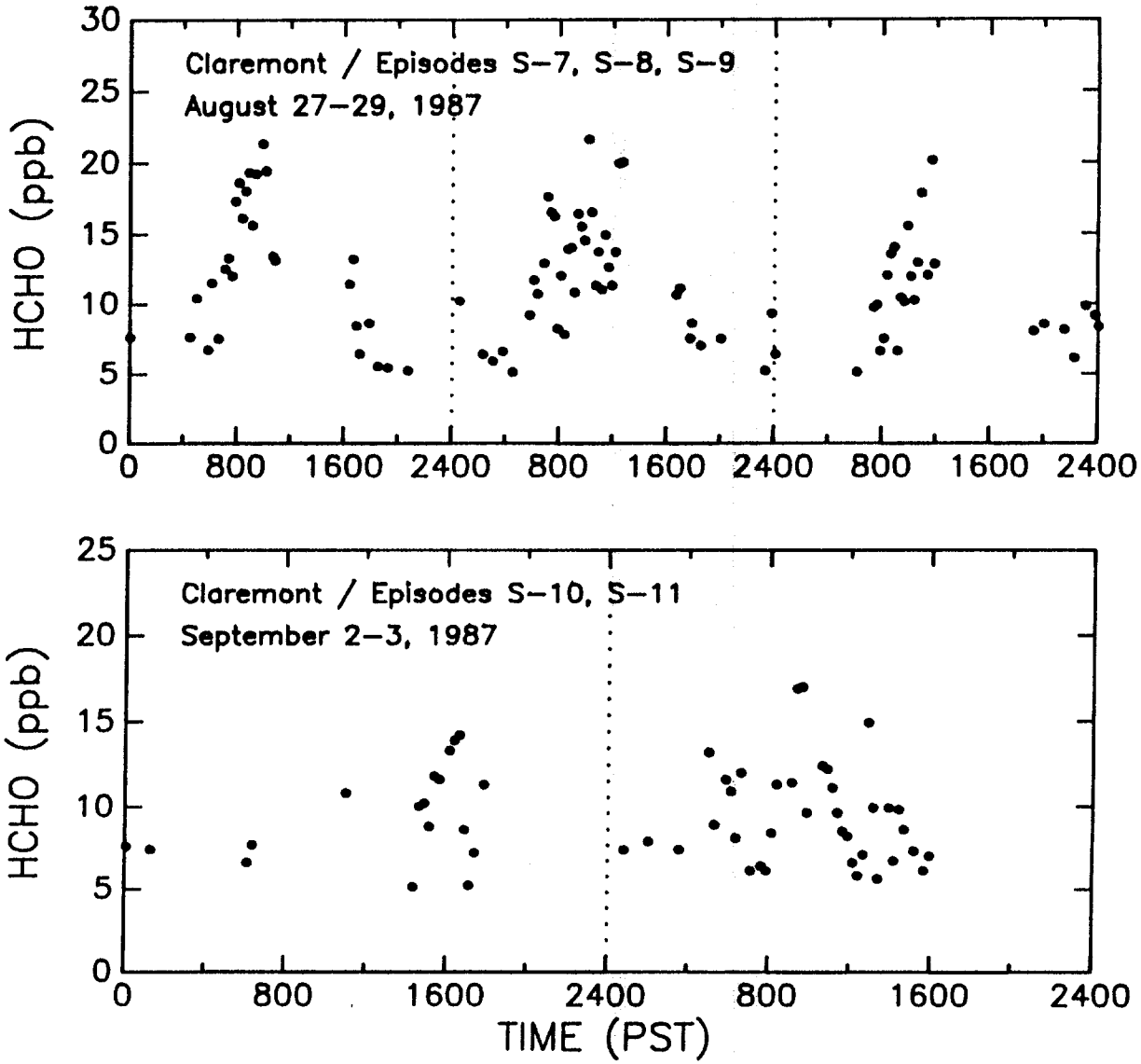

Figure V-9. DOAS 15-min HCHO concentrations observed at Claremont during summer episodes S-7 through S-11.

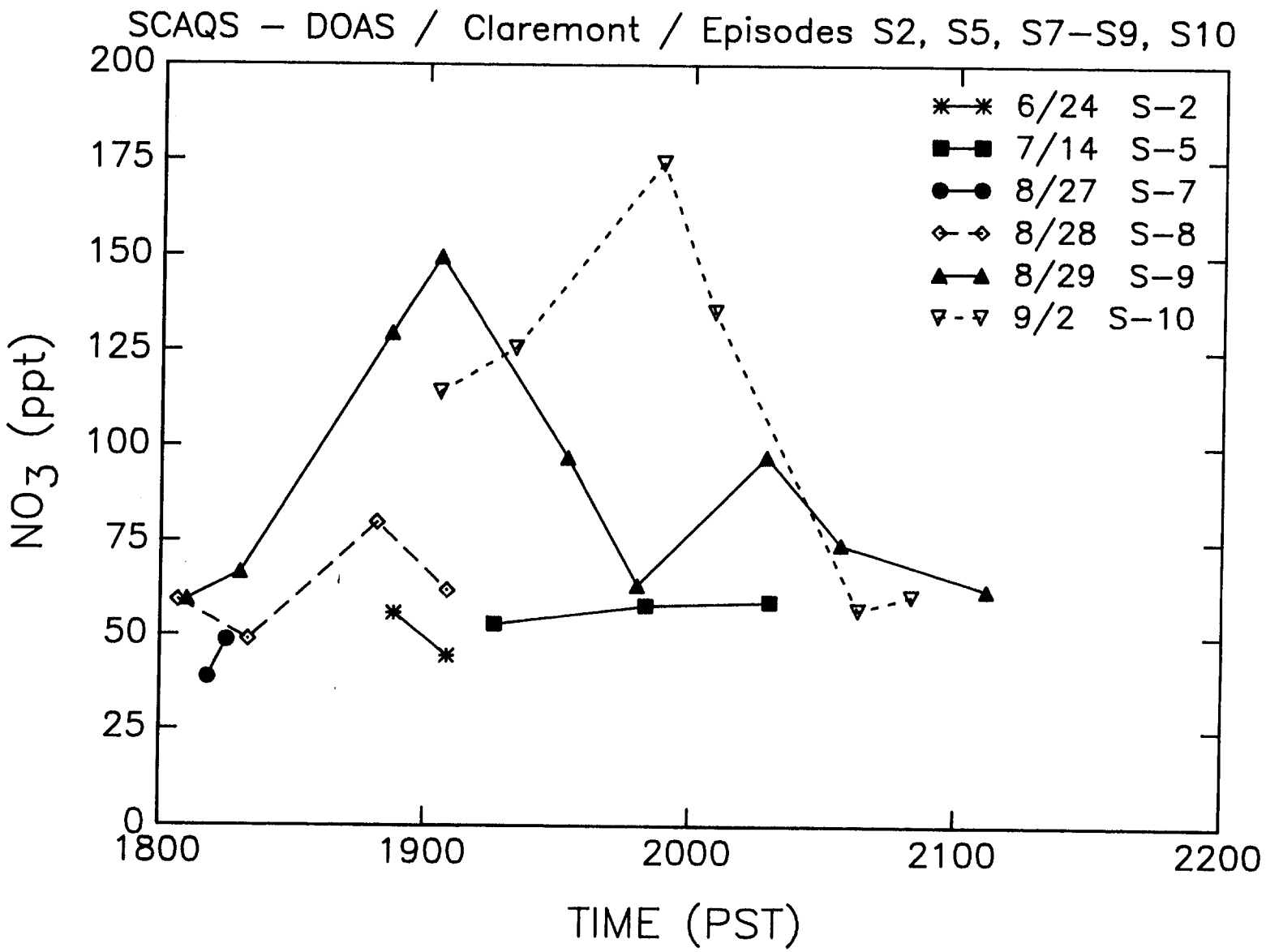

Figure V-10. DOAS 15-min nitrate radical concentrations measured at Claremont during summer episodes.

increased above the 0-5 ppb level by ~2200 hr and remained elevated for the rest of the evening. Due to the rapid rate of reaction between NO and NO_3 radicals, NO serves as an efficient sink for NO_3. The combination of decreasing rates of formation of NO_3 radicals, and rapid loss due to reaction with increasing NO concentrations, accounts for the time-concentration profiles for NO_3 radicals observed in Figure V-10. The values of the NO_3 radical concentrations which were above the DOAS detection limit are given in Table V-2.

5. 1-Hr Average Data

Figures V-11 to V-21 contain 1-hr average concentrations measured at Claremont for NO_2, HONO and HCHO for each of the eleven summer episodes. The corresponding numerical values are provided in Tables V-3 through V-5. The influence on NO_2 concentrations of the major traffic peak at approximately 0800, and the secondary late afternoon-early evening traffic peak are evident in the 1-hr average data as they were in the individual 15-min concentrations discussed above. Similarly, the occurrence of HCHO concentration maxima in the period from 0800 to 1600 is apparent in many of these figures.

The paucity of 1-hr average values for HONO for several of the episodes, and for HCHO during many evening periods, reflects the generally low pollution levels encountered during these periods, resulting in average concentration below the DOAS detection limits for these compounds, particularly during the June and July episodes. These conditions were not favorable for DOAS measurements, especially for HCHO, a weakly absorbing species in the near UV spectral region.

Note that while in some cases individual 15-min concentrations may have been above the detection limits for HONO or HCHO during these periods, if the 1-hr average concentration was below the detection limit that value is not plotted in Figures V-11 to V-21. Due to its rapid photolysis in the actinic UV region below approximately 370 nm, HONO concentrations were below the 0.8 ppb detection limit from shortly after sunrise until after sunset, as expected during these summer episodes. Gaps in 1-hr average HCHO data during mid-day periods were usually due to computer malfunction or stray light or temperature influences which degraded the signal, particularly at short wavelengths where HCHO is measured, rather than because HCHO concentrations were below the 5 ppb

Table V-2. NO_3 Radical Concentrations Above Detection Limit Measured by DOAS During 1987 SCAQS Study, Summer Episodes at Claremont

Episode	Date	Time Period (PST)	Concentration (ppt)
S-2	June 24	18:46:32 - 18:58:34	56
		18:58:34 - 19:10:42	40
S-5	July 14	19:26:53 - 19:43:12	53
		19:43:12 - 19:55:06	58
		20:11:32 - 20:27:52	59
S-6	July 15	18:58:48 - 10:10:34	72
S-7	August 27	18:06:46 - 18:18:44	39
		18:18:44 - 18:25:30	49
S-8	August 28	17:57:10 - 18:13:30	59
		18:13:30 - 18:25:26	49
		18:42:17 - 18:58:36	80
		18:58:36 - 19:10:34	62
S-9	August 29	17:59:58 - 18:11:44	60
		18:11:53 - 18:23:42	67
		18:45:00 - 18:56:49	129
		18:56:49 - 19:08:46	150
		19:25:29 - 19:41:50	97
		19:41:50 - 19:53:45	63
		20:10:32 - 20:26:52	97
		20:27:01 - 20:38:50	74
		21:00:05 - 21:11:50	62
S-10	September 2	17:56:50 - 18:13:10	114
		18:13:18 - 18:25:09	126
		18:46:33 - 18:58:20	174
		18:58:24 - 19:10:20	135
		19:31:18 - 19:43:08	57
		19:43:08 - 19:55:05	61
S-11	September 3	03:57:12 - 04:09:02	59

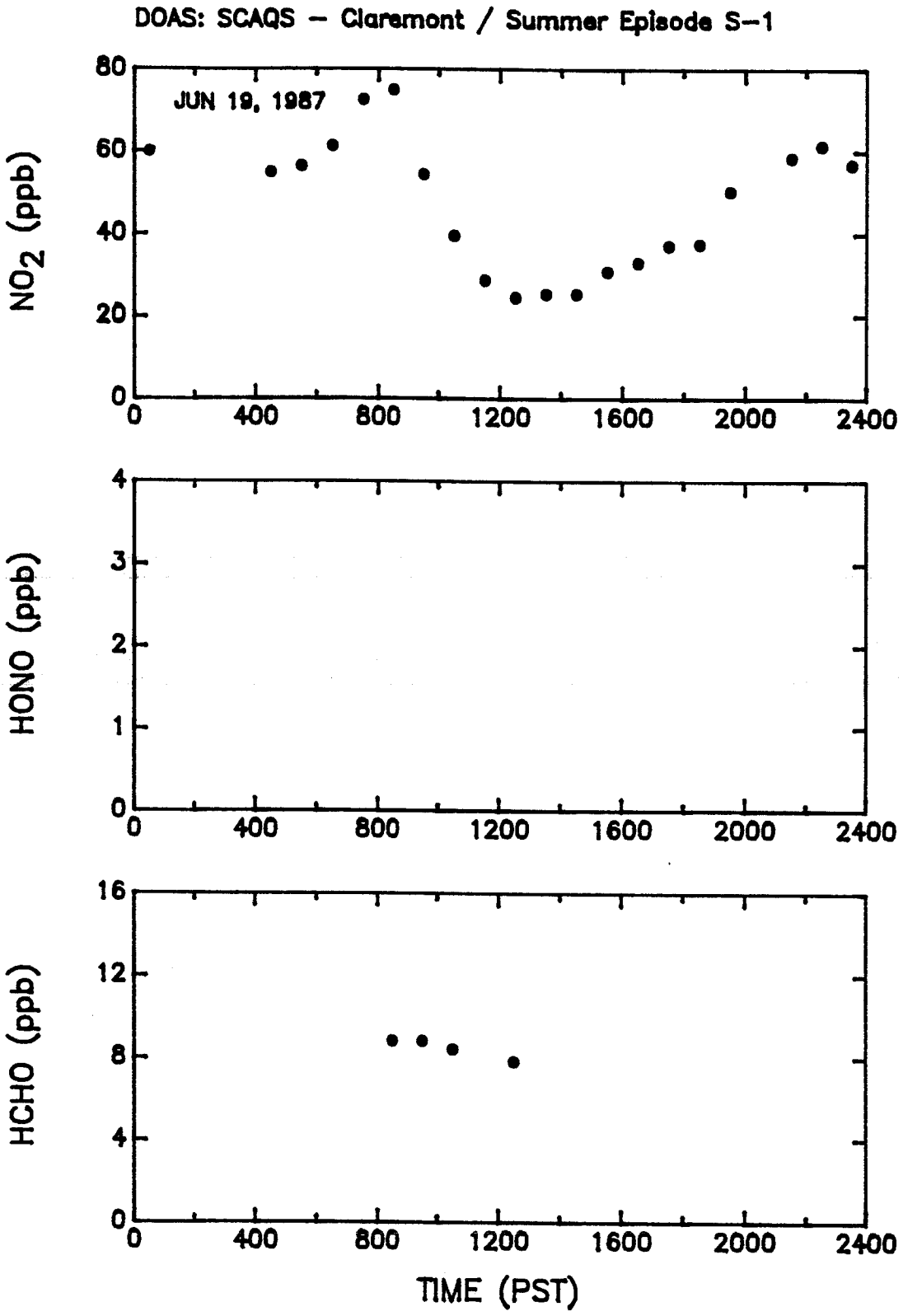

Figure V-11. DOAS 1-hr average concentrations observed at Claremont during summer episode S-1.

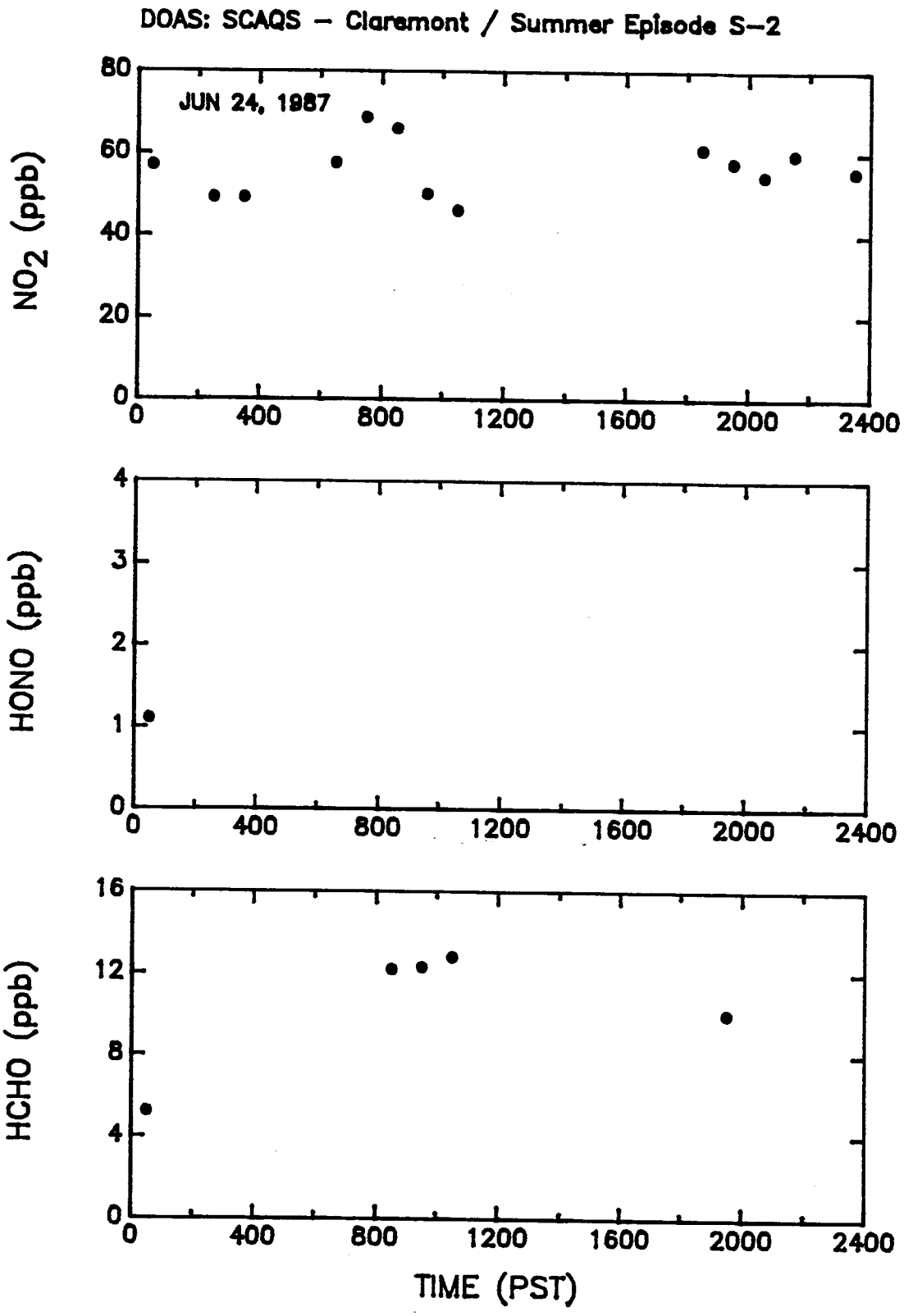

Figure V-12. DOAS 1-hr average concentrations observed at Claremont during summer episode S-2.

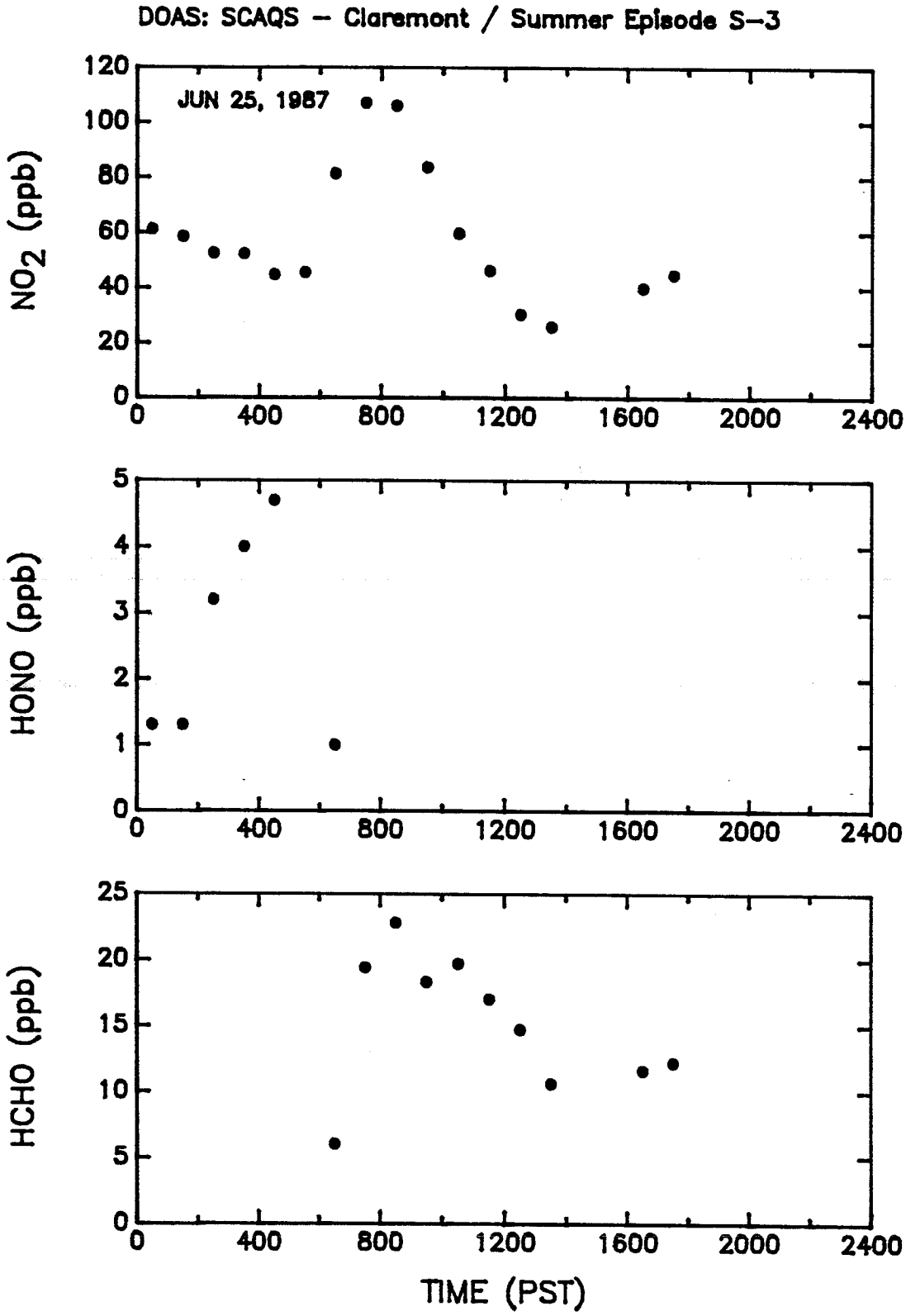

Figure V-13. DOAS 1-hr average concentrations observed at Claremont during summer episode S-3.

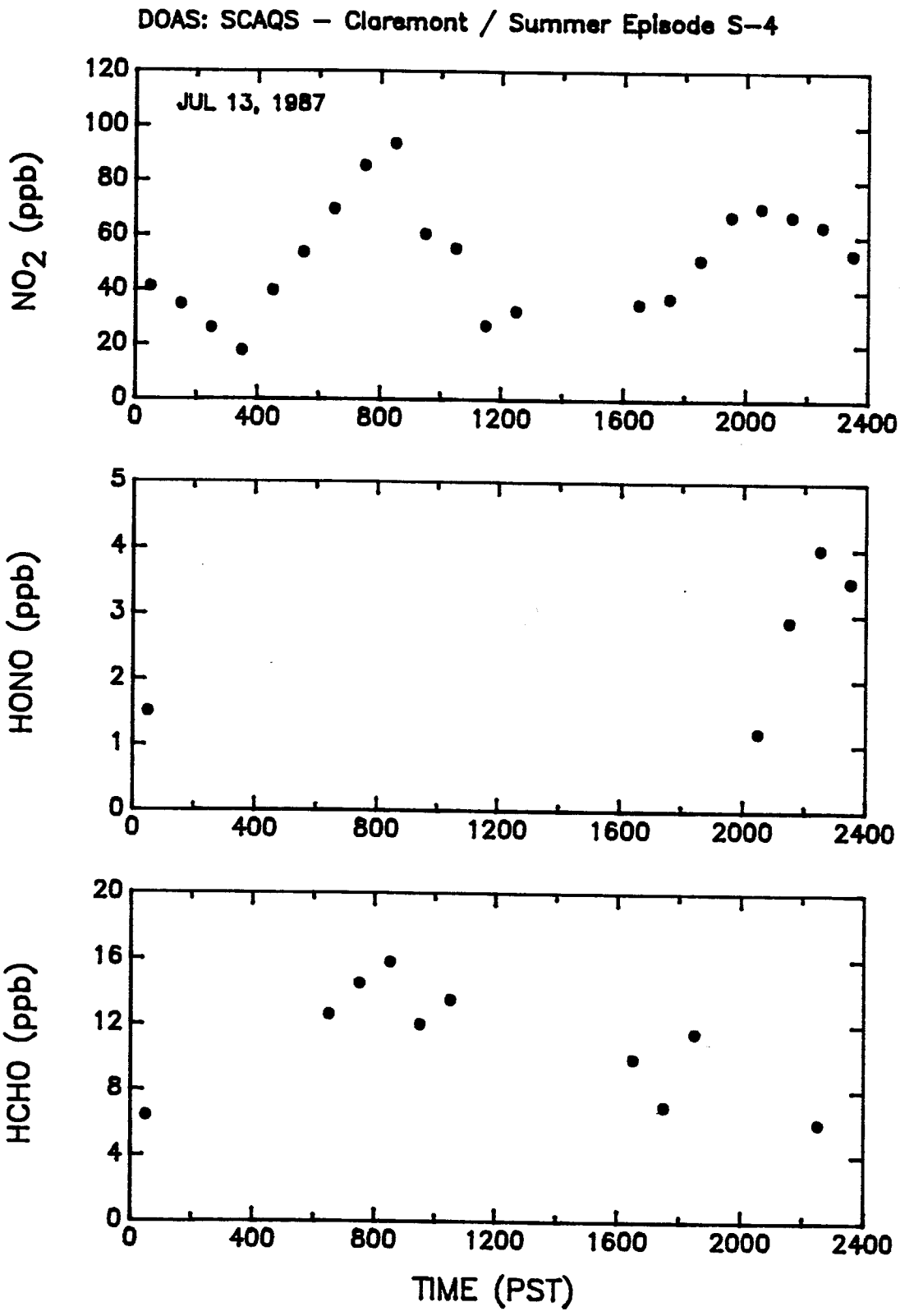

Figure V-14. DOAS 1-hr average concentrations observed at Claremont during summer episode S-4.

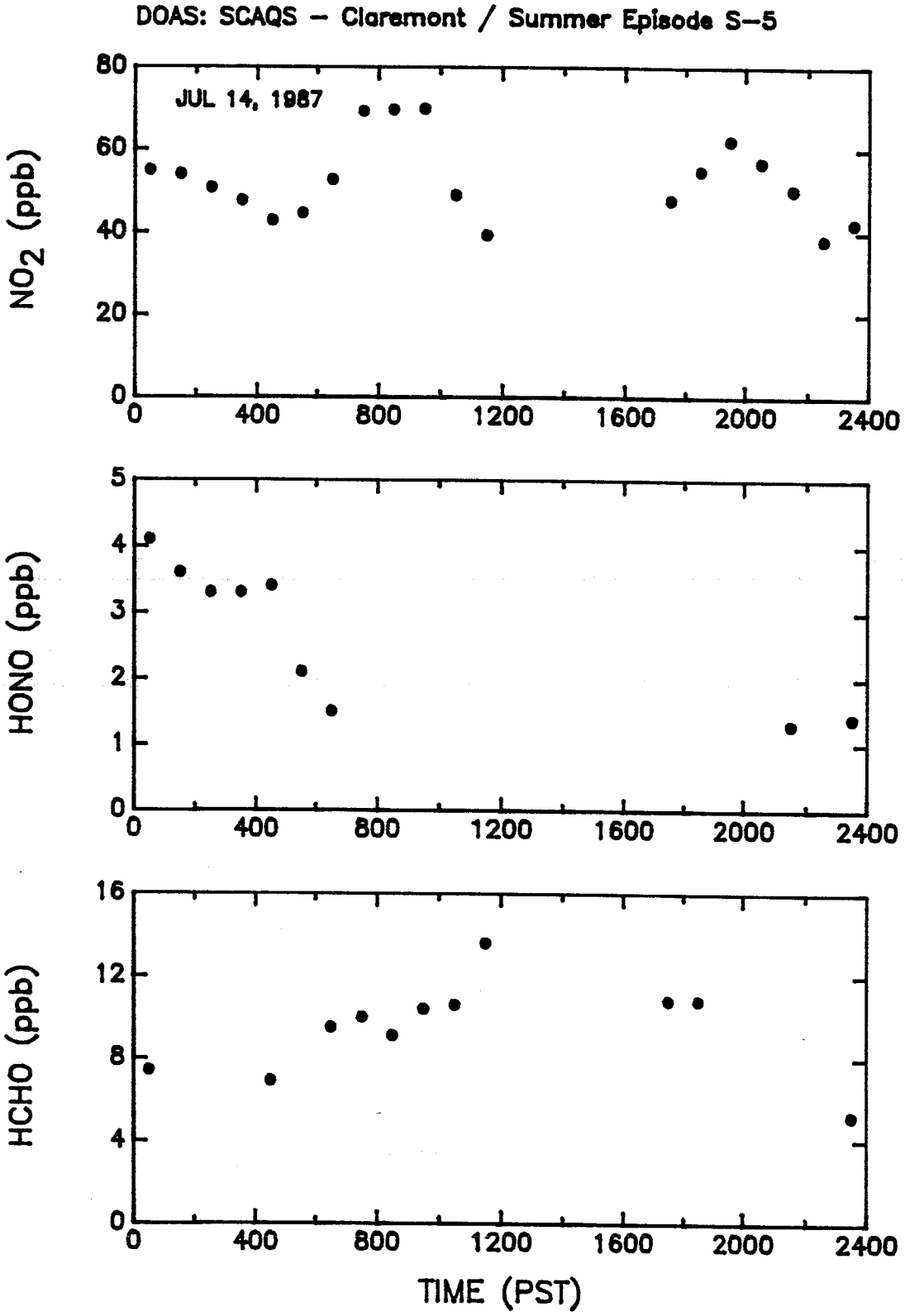

Figure V-15. DOAS 1-hr average concentrations observed at Claremont during summer episode S-5.

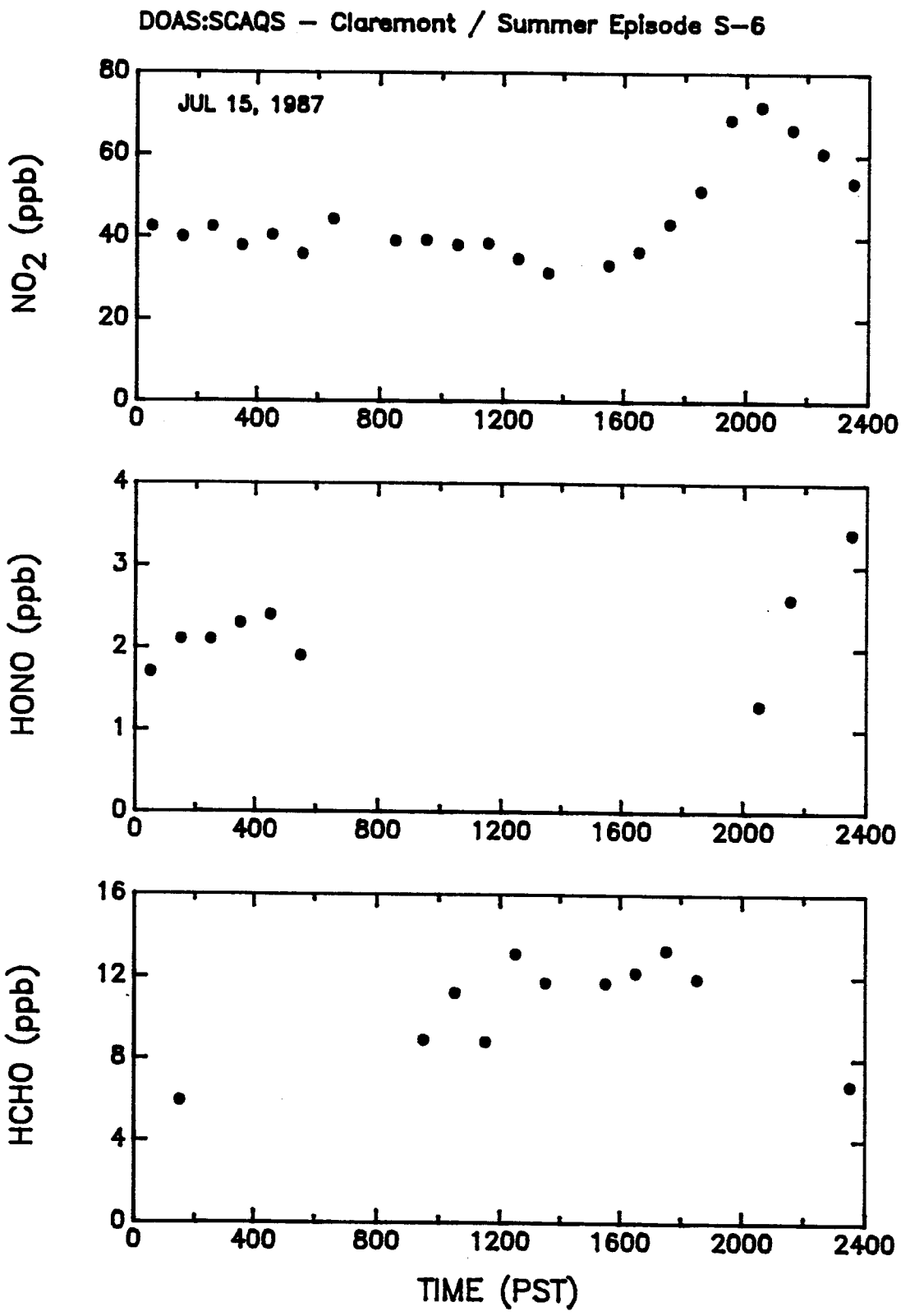

Figure V-16. DOAS 1-hr average concentrations observed at Claremont during summer episode S-6.

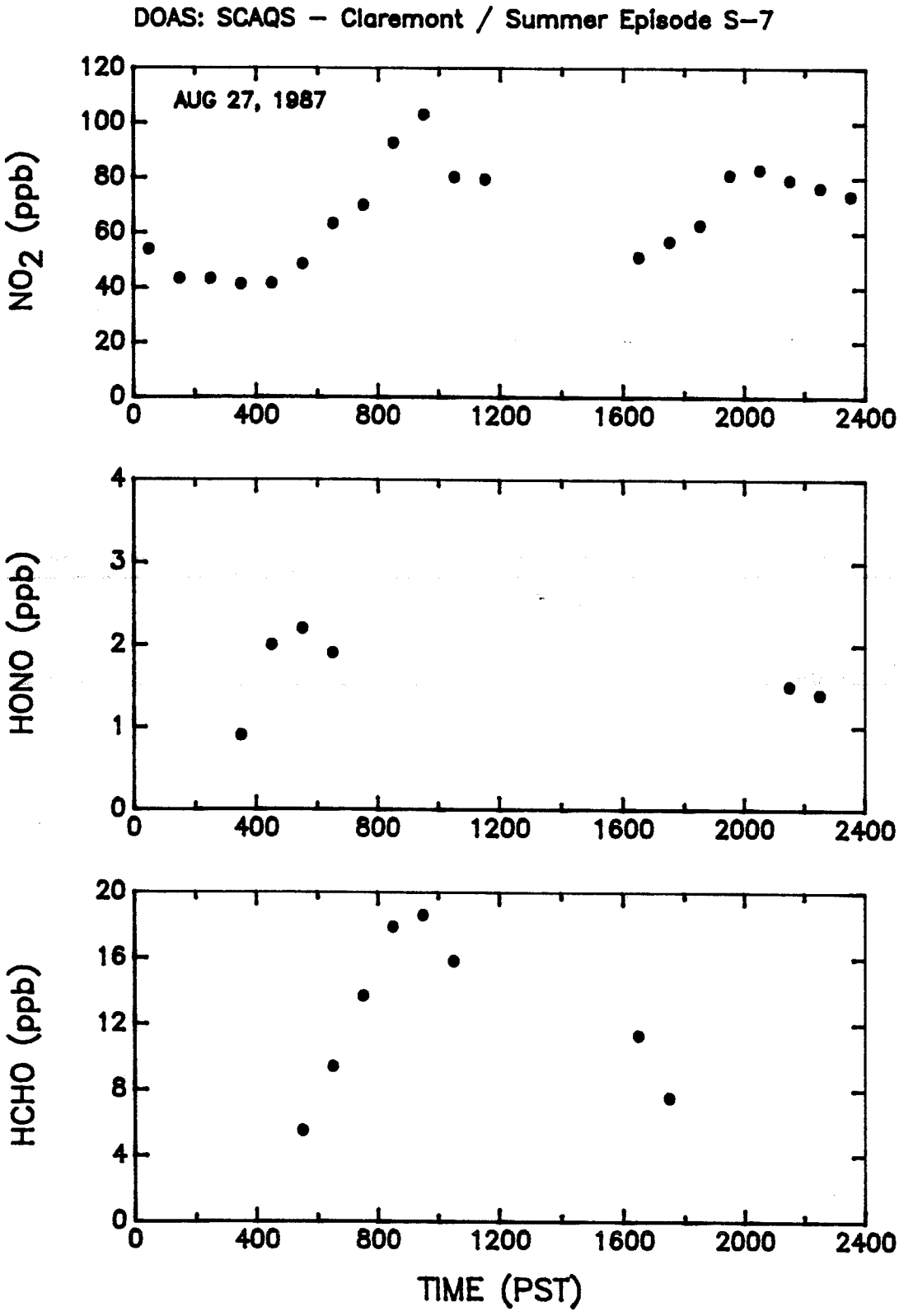

Figure V-17. DOAS 1-hr average concentrations observed at Claremont during summer episode S-7.

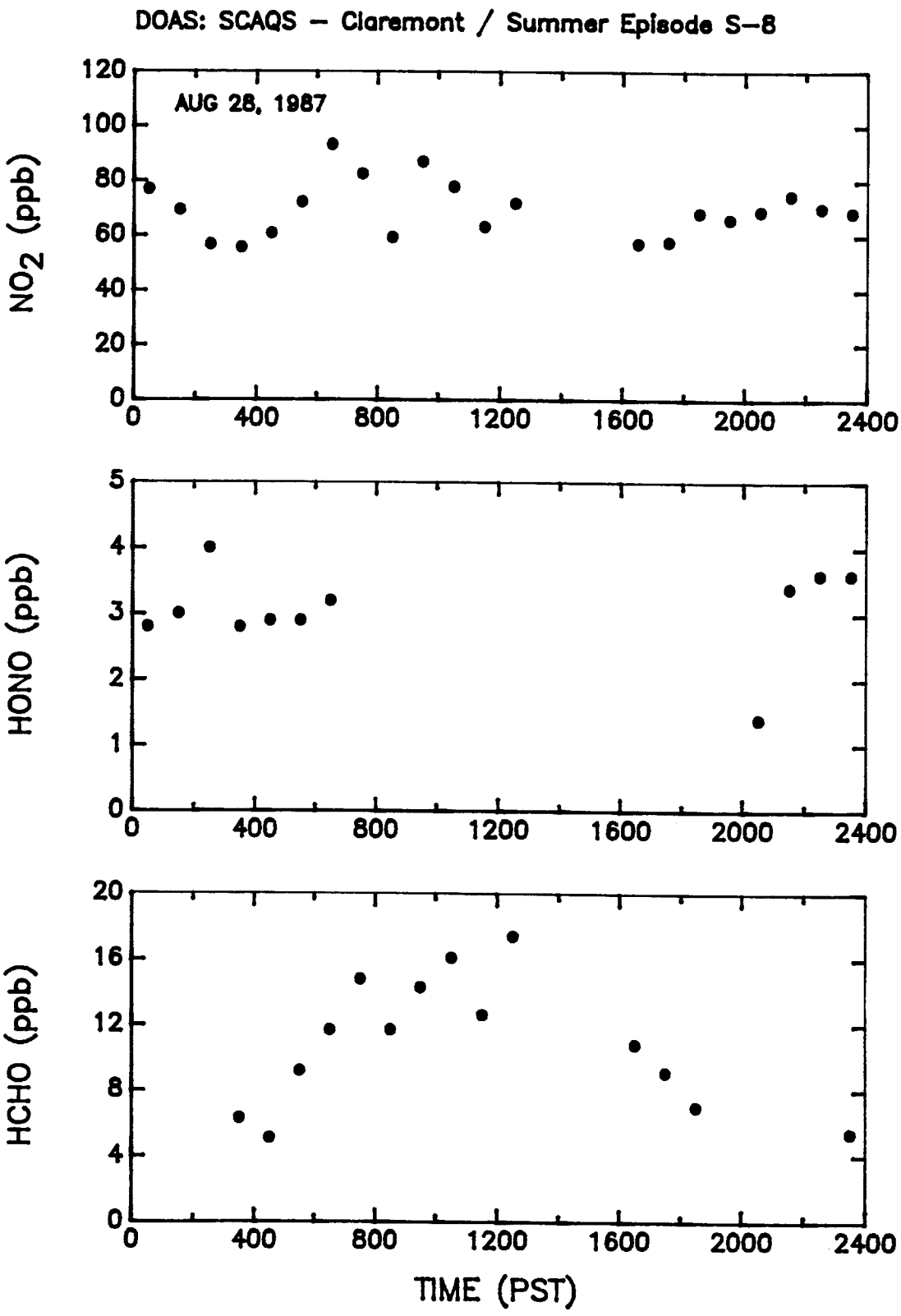

Figure V-18. DOAS 1-hr average concentrations observed at Claremont during summer episode S-8.

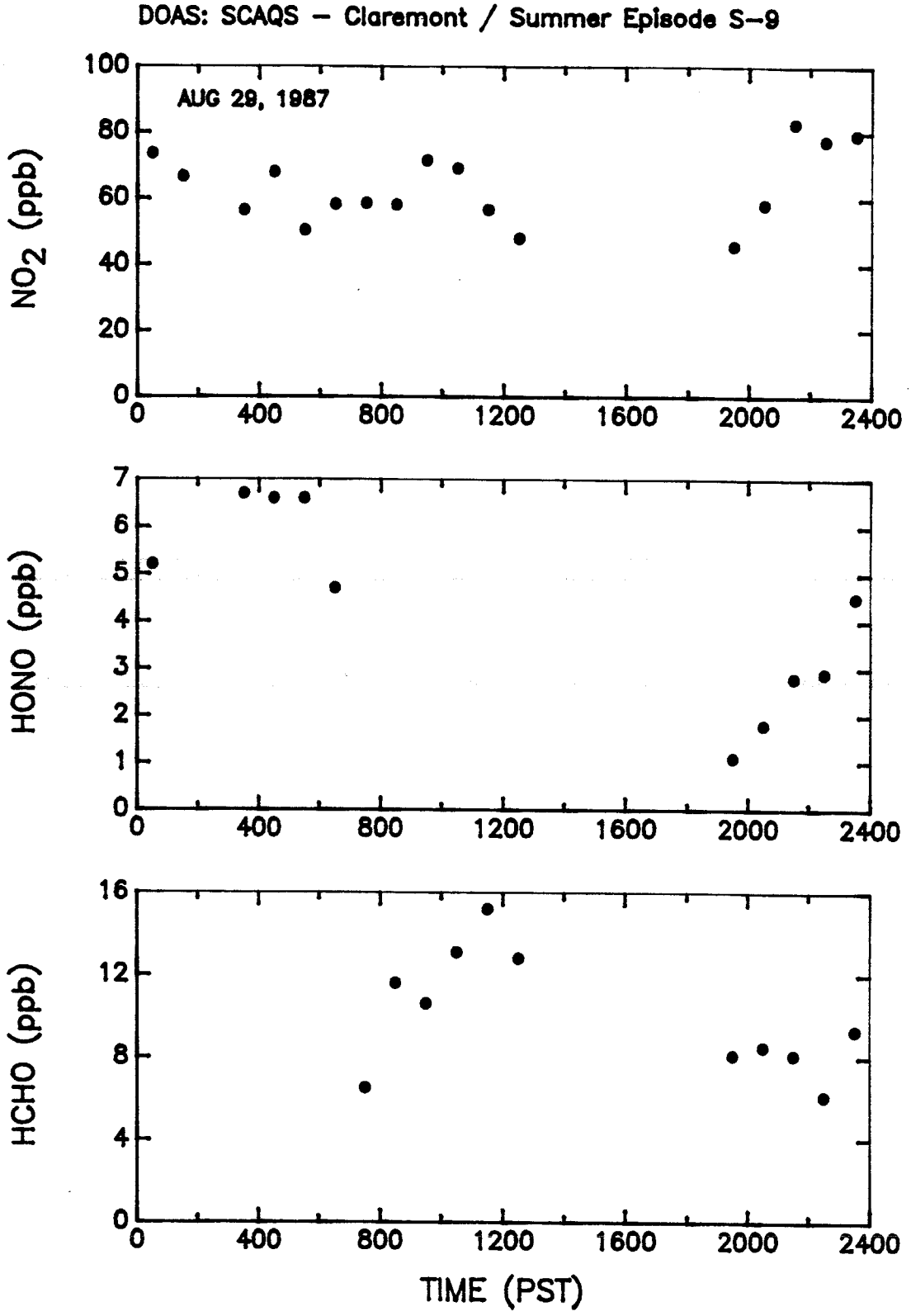

Figure V-19. DOAS 1-hr average concentrations observed at Claremont during summer episode S-9.

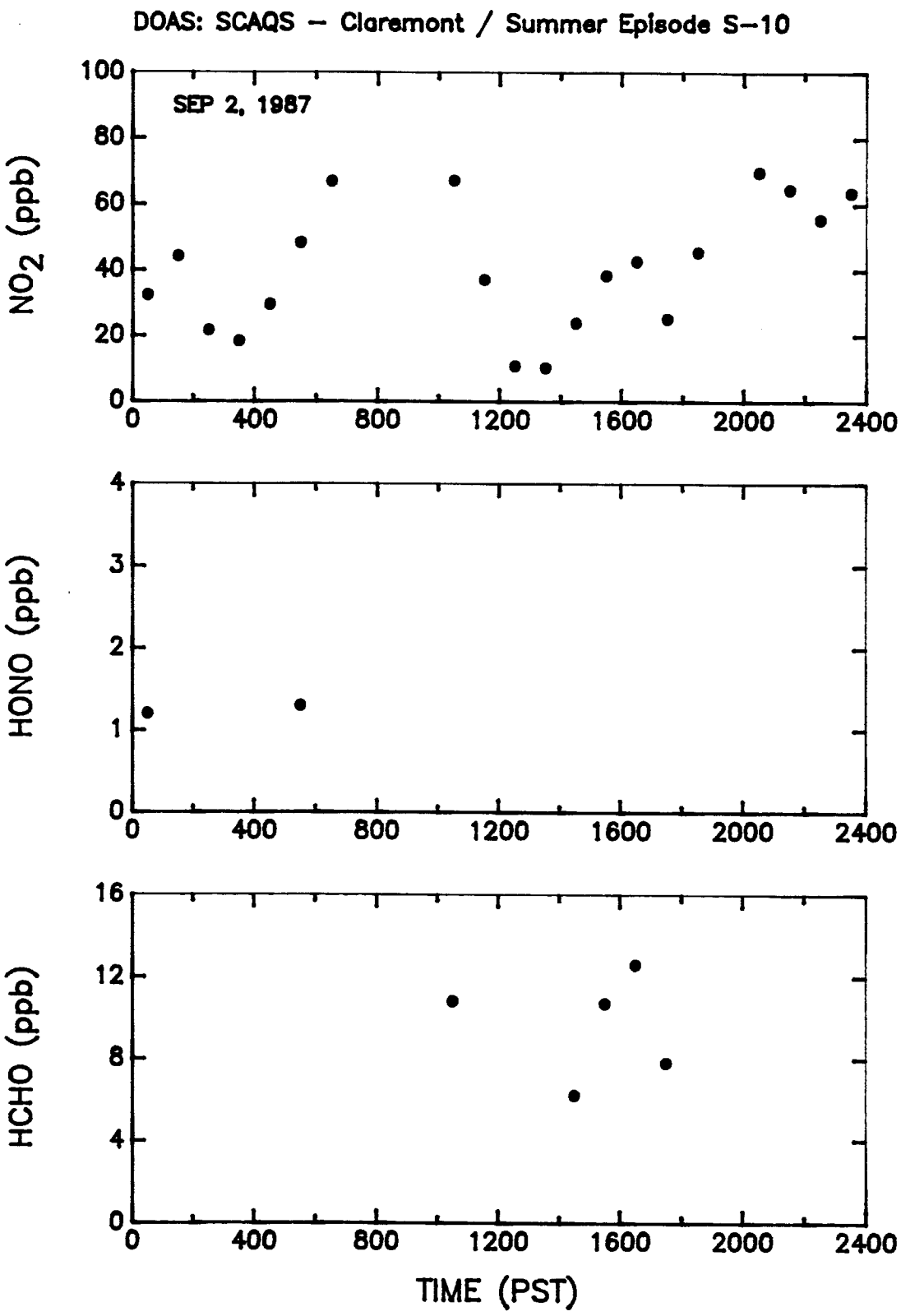

Figure V-20. DOAS 1-hr average concentrations observed at Claremont during summer episode S-10.

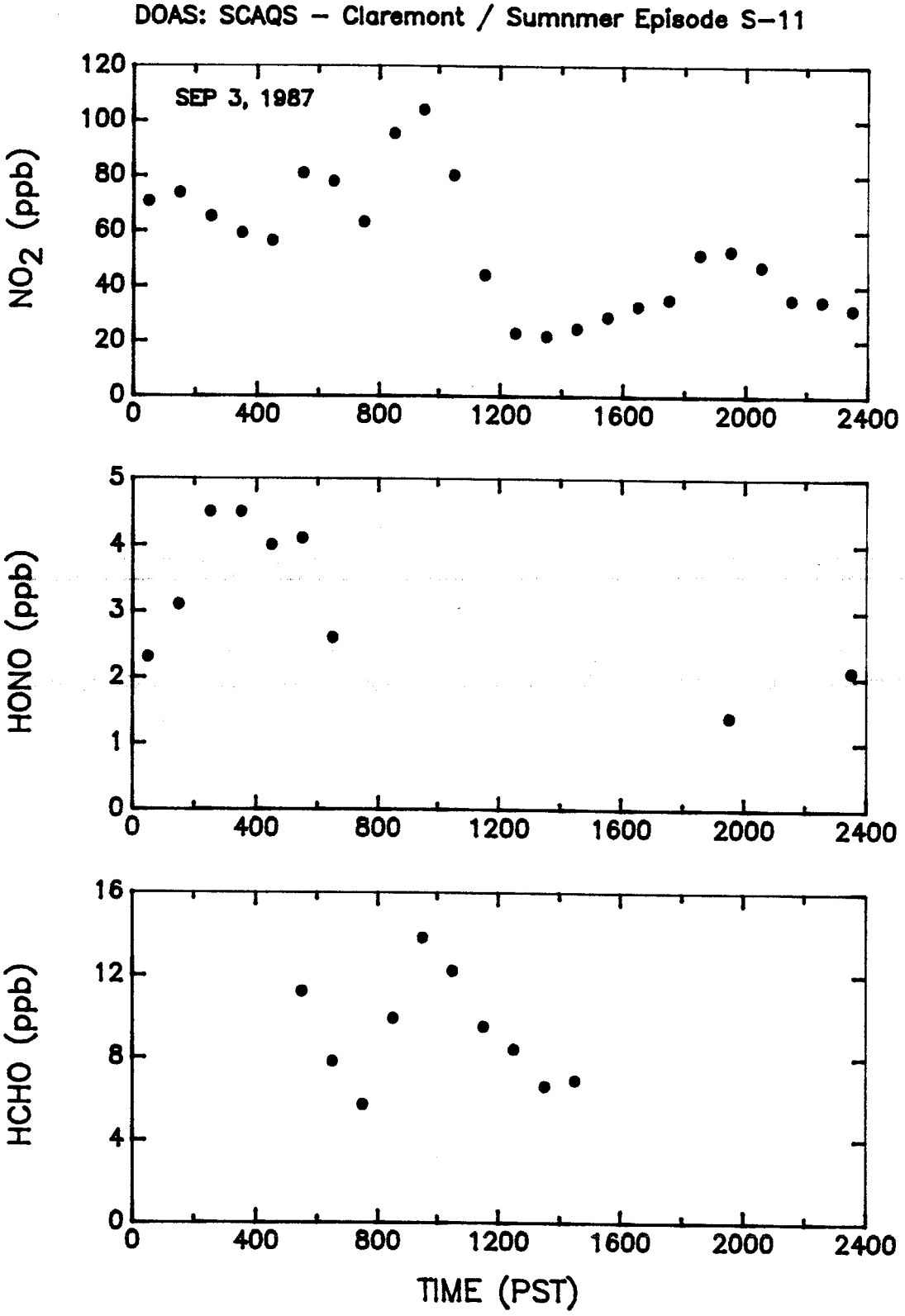

Figure V-21. DOAS 1-hr average concentrations observed at Claremont during summer episode S-11.

Table V-3. Hourly Average NO_2 Concentrations (ppb) Measured by DOAS During the 1987 SCAQS Study, Summer Episodes at Claremont

Hourly Period (PST)	S-1 Jun 19	S-2 Jun 24	S-3 Jun 25	S-4 Jul 13	S-5 Jul 14	S-6 Jul 15	S-7 Aug 27	S-8 Aug 28	S-9 Aug 29	S-10 Sep 2	S-11 Sep 3
0000-0100	60	57	61	41	55	42	54	77	73	32	70
0100-0200	ND	ND	58	35	54	40	43	69	66	44	74
0200-0300	ND	49	52	26	51	42	43	57	ND	22	65
0300-0400	ND	49	52	18	48	38	41	56	56	18	59
0400-0500	55	ND	45	40	43	40	41	61	68	30	56
0500-0600	56	ND	45	54	44	36	48	72	50	48	81
0600-0700	61	58	81	70	53	44	63	93	58	67	78
0700-0800	72	69	107	85	69	ND	70	82	58	ND	63
0800-0900	75	66	106	93	70	39	93	59	58	ND	95
0900-1000	54	50	84	60	70	39	103	87	72	ND	104
1000-1100	40	46	60	55	49	38	80	78	69	67	80
1100-1200	29	ND	46	27	39	38	79	63	57	37	44
1200-1300	24	ND	30	32	ND	35	ND	72	48	11	23
1300-1400	25	ND	26	ND	ND	31	ND	ND	ND	10	22
1400-1500	25	ND	ND	ND	ND	ND	ND	ND	ND	24	25
1500-1600	31	ND	ND	ND	ND	33	ND	ND	ND	38	29
1600-1700	33	ND	40	35	ND	36	51	57	ND	43	33
1700-1800	37	ND	45	37	48	43	57	58	ND	25	35
1800-1900	38	61	ND	51	55	51	63	68	ND	46	52
1900-2000	50	58	ND	67	62	69	81	66	46	ND	53
2000-2100	ND	54	ND	70	57	72	83	69	58	70	47
2100-2200	58	60	ND	67	50	66	79	75	83	64	35
2200-2300	61	ND	ND	64	38	61	76	70	78	55	35
2300-2400	57	55	ND	54	42	53	73	69	79	64	32

BDL - Below detection limit.
ND - No data available.

Table V-4. Hourly Average HONO Concentrations (ppb) Measured by DOAS During the 1987 SCAQS Study, Summer Episodes at Claremont

Hourly Period (PST)	S-1 Jun 19	S-2 Jun 24	S-3 Jun 25	S-4 Jul 13	S-5 Jul 14	S-6 Jul 15	S-7 Aug 27	S-8 Aug 28	S-9 Aug 29	S-10 Sep 2	S-11 Sep 3
0000-0100	BDL	1	1	2	4	2	BDL	3	5	1	2
0100-0200	ND	ND	1	BDL	4	2	BDL	3	ND	BDL	3
0200-0300	ND	ND	3	BDL	3	2	BDL	4	ND	BDL	4
0300-0400	ND	ND	4	ND	3	2	1	3	7	BDL	4
0400-0500	BDL	ND	5	ND	3	2	2	3	7	BDL	4
0500-0600	BDL	ND	ND	BDL	2	2	2	3	7	1	4
0600-0700	BDL	BDL	1	BDL	2	BDL	2	3	5	BDL	3
0700-0800	BDL	BDL	BDL	BDL	BDL	ND	BDL	BDL	BDL	ND	BDL
0800-0900	BDL	BDL	BDL	BDL	BDL	BDL	BDL	BDL	BDL	ND	BDL
0900-1000	BDL	BDL	BDL	BDL	BDL	BDL	BDL	BDL	BDL	ND	BDL
1000-1100	BDL	BDL	BDL	BDL	BDL	BDL	BDL	BDL	BDL	BDL	BDL
1100-1200	BDL	ND	BDL	BDL	BDL	BDL	BDL	BDL	BDL	BDL	BDL
1200-1300	BDL	ND	BDL	BDL	ND	BDL	ND	BDL	BDL	BDL	BDL
1300-1400	BDL	ND	BDL	ND	ND	BDL	ND	ND	ND	BDL	BDL
1400-1500	BDL	ND	ND	ND	ND	ND	ND	ND	ND	BDL	BDL
1500-1600	BDL	ND	ND	ND	ND	BDL	ND	ND	ND	BDL	BDL
1600-1700	BDL	ND	BDL	BDL	ND	BDL	BDL	BDL	ND	BDL	BDL
1700-1800	BDL	ND	BDL	BDL	BDL	BDL	BDL	BDL	ND	BDL	BDL
1800-1900	BDL	BDL	ND	BDL	BDL	BDL	BDL	BDL	ND	BDL	BDL
1900-2000	BDL	BDL	ND	BDL	BDL	BDL	BDL	BDL	1	ND	1
2000-2100	ND	ND	ND	1	BDL	1	BDL	1	2	BDL	BDL
2100-2200	BDL	ND	ND	3	1	3	2	3	3	BDL	ND
2200-2300	BDL	ND	ND	4	ND	ND	1	4	3	ND	ND
2300-2400	BDL	BDL	ND	4	1	3	BDL	4	4	ND	2

BDL - Below detection limit.
ND - No data available.

Table V-5. Hourly Average HCHO Concentrations (ppb) Measured by DOAS During the 1987 SCAQS Study, Summer Episodes at Claremont

Hourly Period (PST)	S-1 Jun 19	S-2 Jun 24	S-3 Jun 25	S-4 Jul 13	S-5 Jul 14	S-6 Jul 15	S-7 Aug 27	S-8 Aug 28	S-9 Aug 29	S-10 Sep 2	S-11 Sep 3
0000-0100	BDL	5	BDL	6	7	BDL	BDL	BDL	BDL	BDL	BDL
0100-0200	ND	ND	BDL	BDL	BDL	6	BDL	BDL	BDL	BDL	BDL
0200-0300	ND	ND	BDL	BDL	BDL	BDL	BDL	BDL	ND	BDL	BDL
0300-0400	ND	ND	BDL	ND	BDL	BDL	BDL	6	BDL	BDL	BDL
0400-0500	BDL	ND	BDL	ND	7	BDL	BDL	5	BDL	BDL	BDL
0500-0600	BDL	ND	ND	ND	BDL	ND	6	9	ND	BDL	11
0600-0700	BDL	BDL	6	13	10	ND	9	12	BDL	BDL	8
0700-0800	BDL	ND	19	15	10	ND	14	15	6	ND	BDL
0800-0900	9	12	23	16	9	ND	18	12	12	ND	10
0900-1000	9	12	18	12	10	9	19	14	11	ND	14
1000-1100	8	13	20	14	11	11	16	16	13	11	12
1100-1200	BDL	ND	17	ND	14	9	ND	13	15	BDL	10
1200-1300	8	ND	15	ND	ND	13	ND	17	13	BDL	8
1300-1400	BDL	ND	11	ND	ND	12	ND	ND	ND	BDL	7
1400-1500	BDL	ND	ND	ND	ND	ND	ND	ND	ND	6	7
1500-1600	BDL	ND	ND	ND	ND	12	ND	ND	ND	11	BDL
1600-1700	BDL	ND	12	10	ND	12	11	11	ND	13	BDL
1700-1800	BDL	ND	12	7	11	13	8	9	ND	8	BDL
1800-1900	BDL	ND	ND	12	11	12	BDL	7	ND	ND	BDL
1900-2000	BDL	10	ND	BDL	BDL	BDL	BDL	BDL	8	ND	BDL
2000-2100	ND	ND	ND	BDL	BDL	BDL	BDL	BDL	8	BDL	BDL
2100-2200	BDL	ND	ND	BDL	BDL	ND	BDL	BDL	8	BDL	BDL
2200-2300	BDL	ND	ND	6	ND	ND	BDL	BDL	6	ND	BDL
2300-2400	BDL	BDL	ND	BDL	5	7	BDL	5	9	ND	BDL

BDL - Below detection limit.
ND - No data available.

detection limit (see Appendix A to identify specific reasons for missing data).

As can be seen in these figures, maximum 1-hr average NO_2 concentrations fell in the range from 70 to 100 ppb. Plateau or peak HONO concentration at Claremont during the summer episodes generally fell in the range from 3 to 5 ppb, except for episode S-9 when the 1-hr average HONO concentration reached a plateau of nearly 7 ppb. Maximum 1-hr average HCHO concentrations fell in the range from 10 to 20 ppb, except for episode S-3 when HCHO peaked at nearly 25 ppb for a 1-hr average.

These results are consistent with data obtained in previous DOAS studies at Claremont (Winer et al. 1987; Biermann et al. 1988a) for periods of lower pollution.

C. Long Beach Summer Episodes

Based on our earlier experience during the 1986 study at El Camino Community College in Torrance (Winer et al. 1987), no measurements of NO_3 radical concentrations were made at Long Beach during the summer SCAQS episodes, due to the expected occurrence of low O_3 concentrations, and NO concentrations which were expected to always be in excess of 10 ppb, sufficient to scavenge NO_3 radical concentrations to levels below the DOAS detection limit. This permitted continuous monitoring of NO_2, HONO and HCHO in the 320 to 370 nm region throughout each 24-hr period. With the exceptions discussed below, sections 1-3 present the 15-min pollutant concentrations measured by DOAS for NO_2, HONO and HCHO, respectively, while section 4 presents the 1-hr average data for these three pollutants.

1. Nitrogen Dioxide

Figures V-22 to V-24 show the 15-min NO_2 concentrations measured at Long Beach during the eleven summer episodes. Although, like the NO_2 data obtained at Claremont, there was clear evidence in the Long Beach measurements of the influence of morning and evening traffic peaks, the results were less uniform at Long Beach. In the three June episodes, the late afternoon-early evening traffic peak produced the highest NO_2 concentrations for those days (between 1600 and 2000), while on August 27 (S-7) the morning and evening NO_2 concentration maxima were essentially identical at ~75 ppb. For the remaining episodes, the morning traffic peak produced the highest NO_2 concentrations, ranging as low as ~20 ppb on July

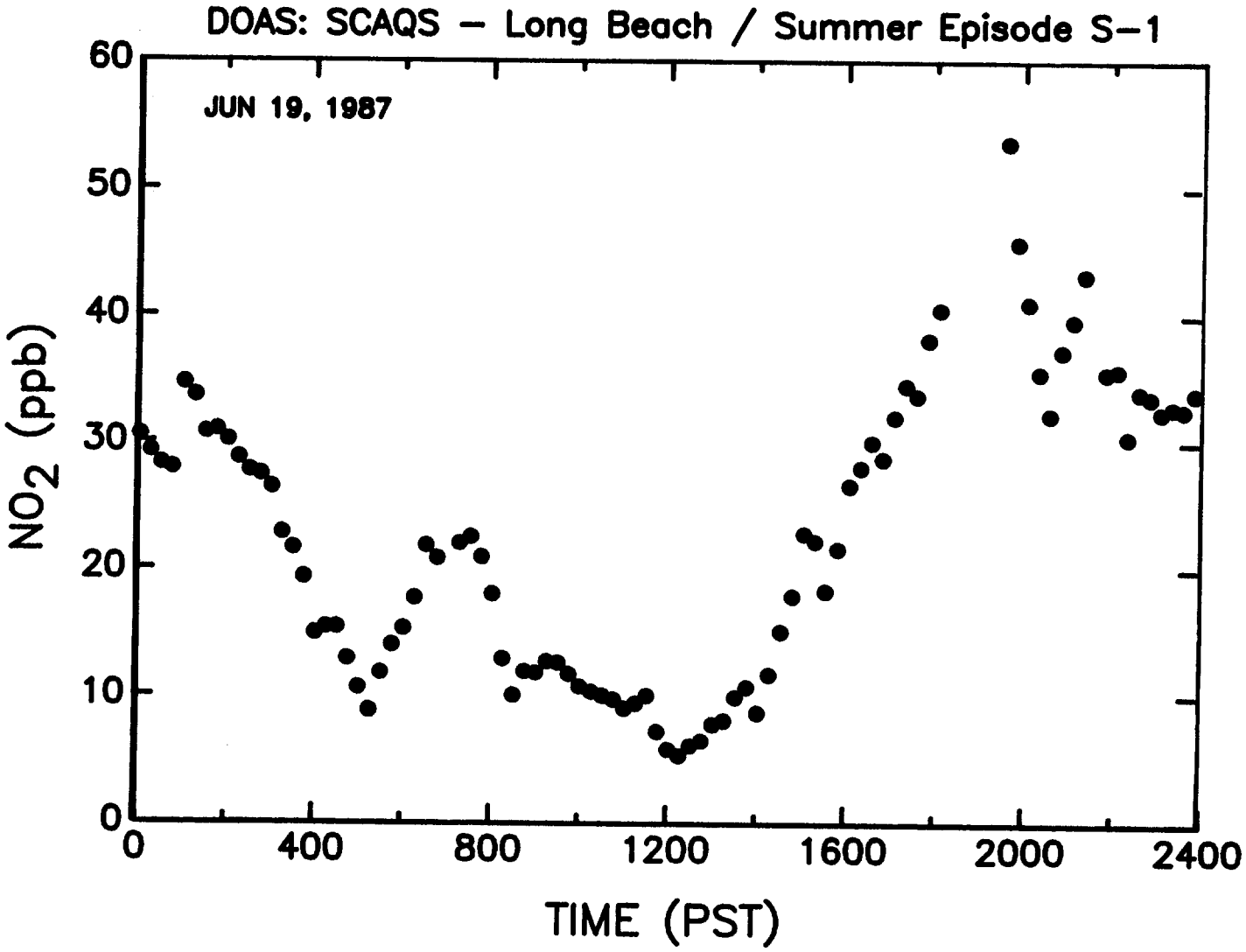

Figure V-22. DOAS 15-min NO_2 concentrations observed at Long Beach during summer episode S-1.

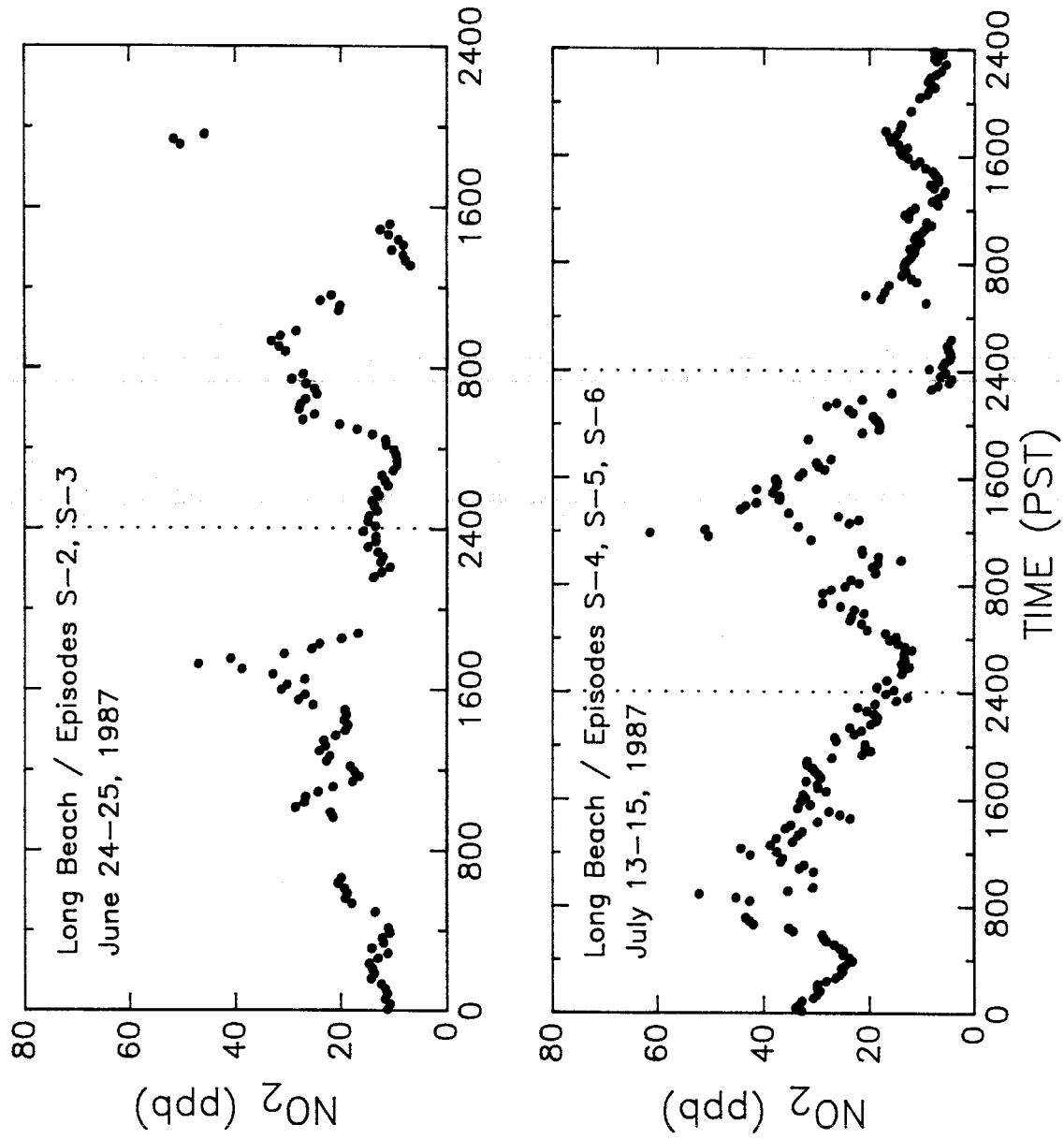

Figure V-23. DOAS 15-min NO_2 concentrations observed at Long Beach during summer episodes S-2 through S-6.

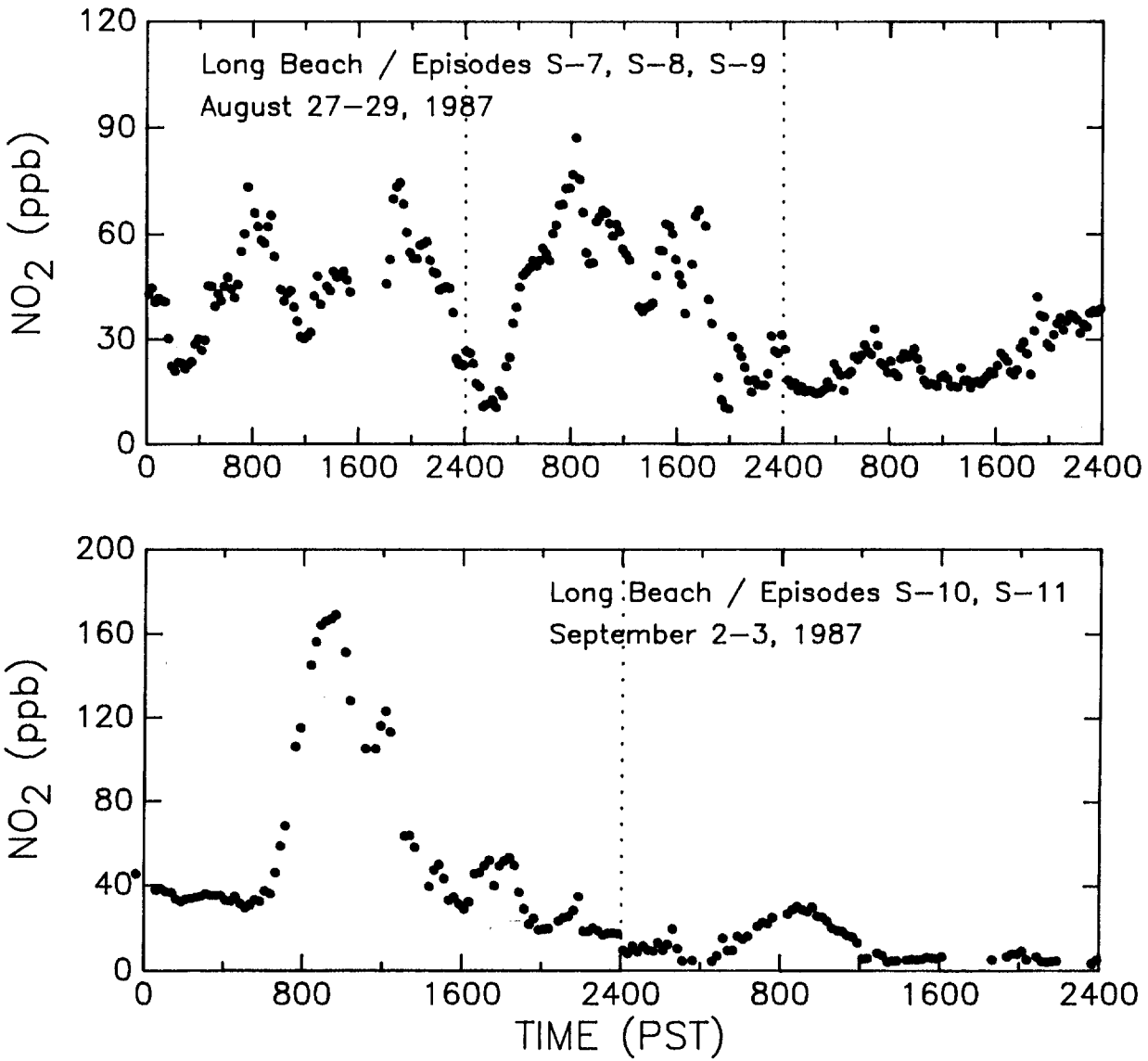

Figure V-24. DOAS 15-min NO_2 concentrations observed at Long Beach during summer episodes S-7 through S-11.

15 and September 3 (S-6 and S-11) to as high as ~170 ppb on September 2 (S-10).

2. Nitrous Acid

As can be seen from Figures V-25 and V-26, 15 min HONO concentrations were above the 0.8 detection limit for extended periods of time only during the evenings of four episodes: July 13, August 27 and 28, and September 2. Only two 15-min periods (at 2100) exhibited measurable HONO concentrations (1 ppb) during the entire June 19 (S-1) episode and therefore no plot is included. The highest HONO concentration observed at Long Beach during the summer episodes, 3.4 ppb, occurred shortly before sunrise on September 2. These data provide additional evidence that meteorological conditions during the SCAQS summer episodes, especially in June and July, were not favorable for high pollution episodes. As a result, the principal utility of the summer Long Beach HONO data is expected to provide upper limits to the HONO concentrations during most episodes as inputs to airshed models.

3. Formaldehyde

Because the HCHO concentration was above the detection limit for only one 15-min period (nearly 8 ppb at 1700) on June 19, no plot is included for episode S-1. The 15-min HCHO concentrations observed by DOAS during the remaining ten episodes are shown in Figures V-27 and V-28. Due to the more difficult operational conditions at Long Beach during the summer (as opposed to the fall period), including greater extremes in temperature, higher sunlight intensities and greater potential for stray light interferences, the detection limit for HCHO for these measurements was taken to be ~6-7 ppb during most periods. Conditions encountered at Long Beach during the summer also led to somewhat higher scatter in the generally low concentrations (i.e., between ~7 and ~12 ppb) observed. Only during the episodes on July 14 and September 2 were profiles resembling diurnal maxima observed, with maximum concentrations of ~18 and nearly 25 ppb, respectively.

4. 1-Hr Average Data

Figures V-29 and V-30 show the 1-hr average NO_2 concentrations for the first six summer episodes at Long Beach. The corresponding data for HONO and HCHO for these six episodes are not plotted since, for all but a few hours (notably on July 14 for HCHO), these 1-hr average

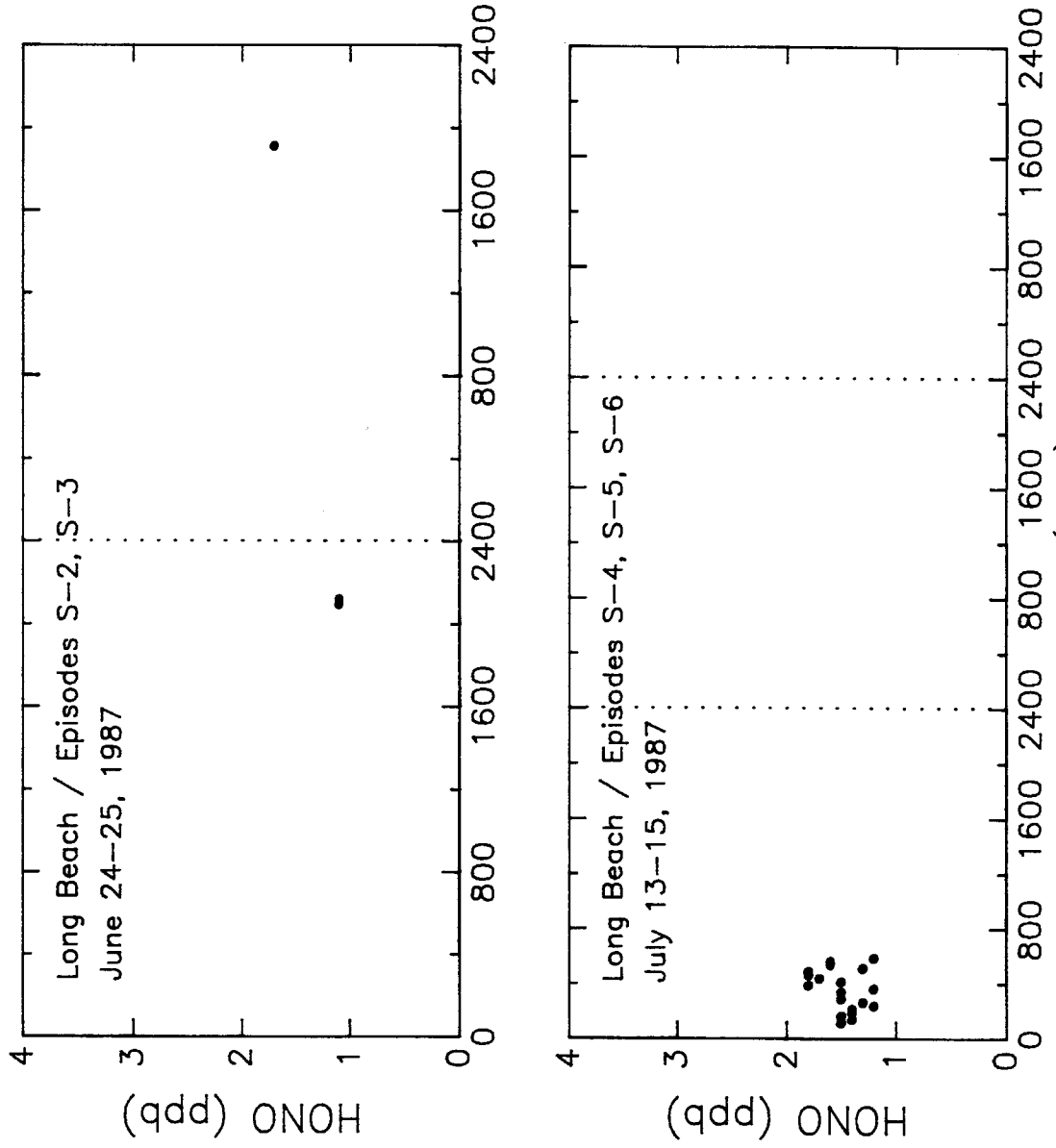

Figure V-25. DOAS 15-min HONO concentrations observed at Long Beach during summer episodes S-2 through S-6.

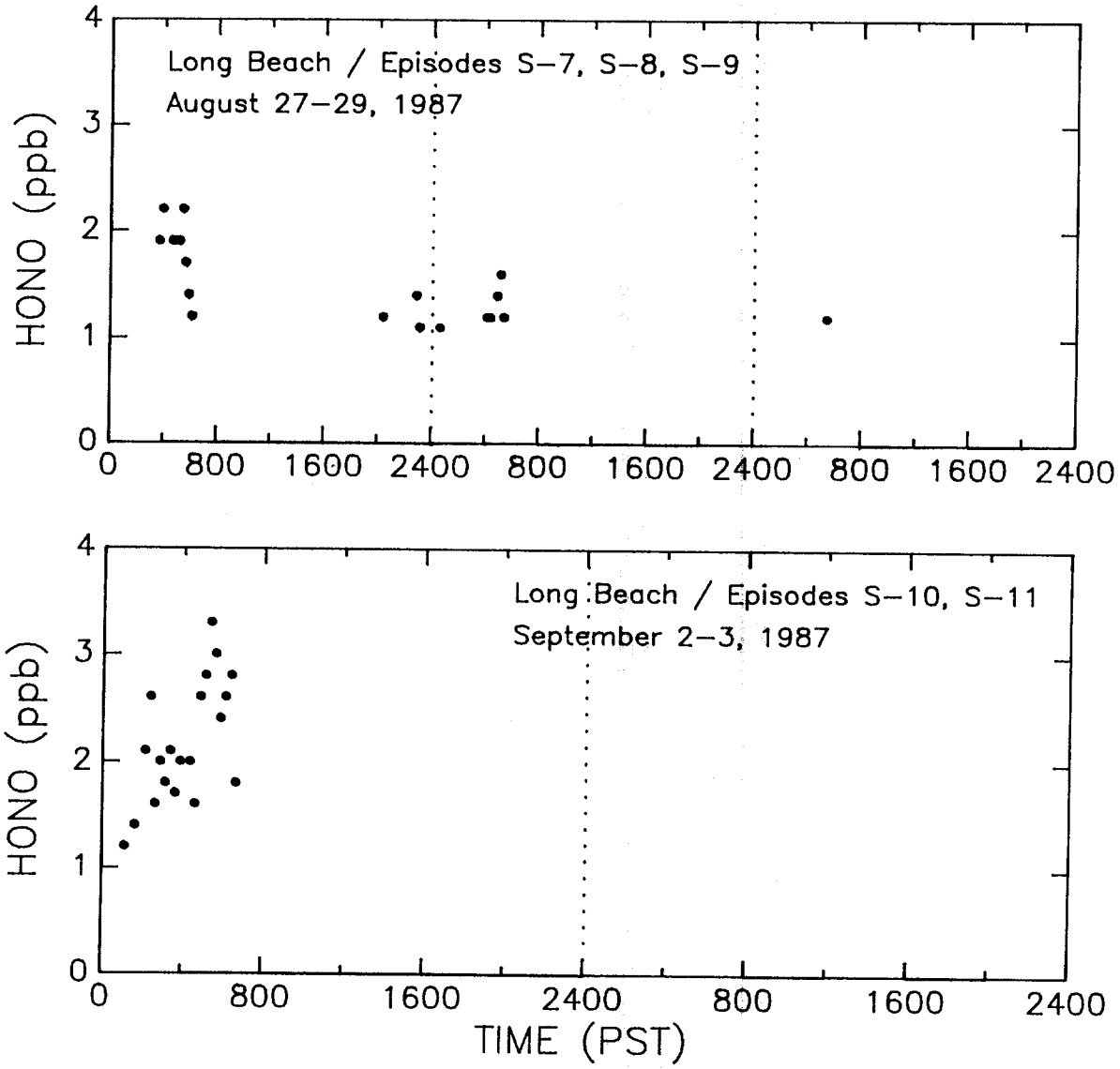

Figure V-26. DOAS 15-min HONO concentrations observed at Long Beach during summer episodes S-7 through S-11.

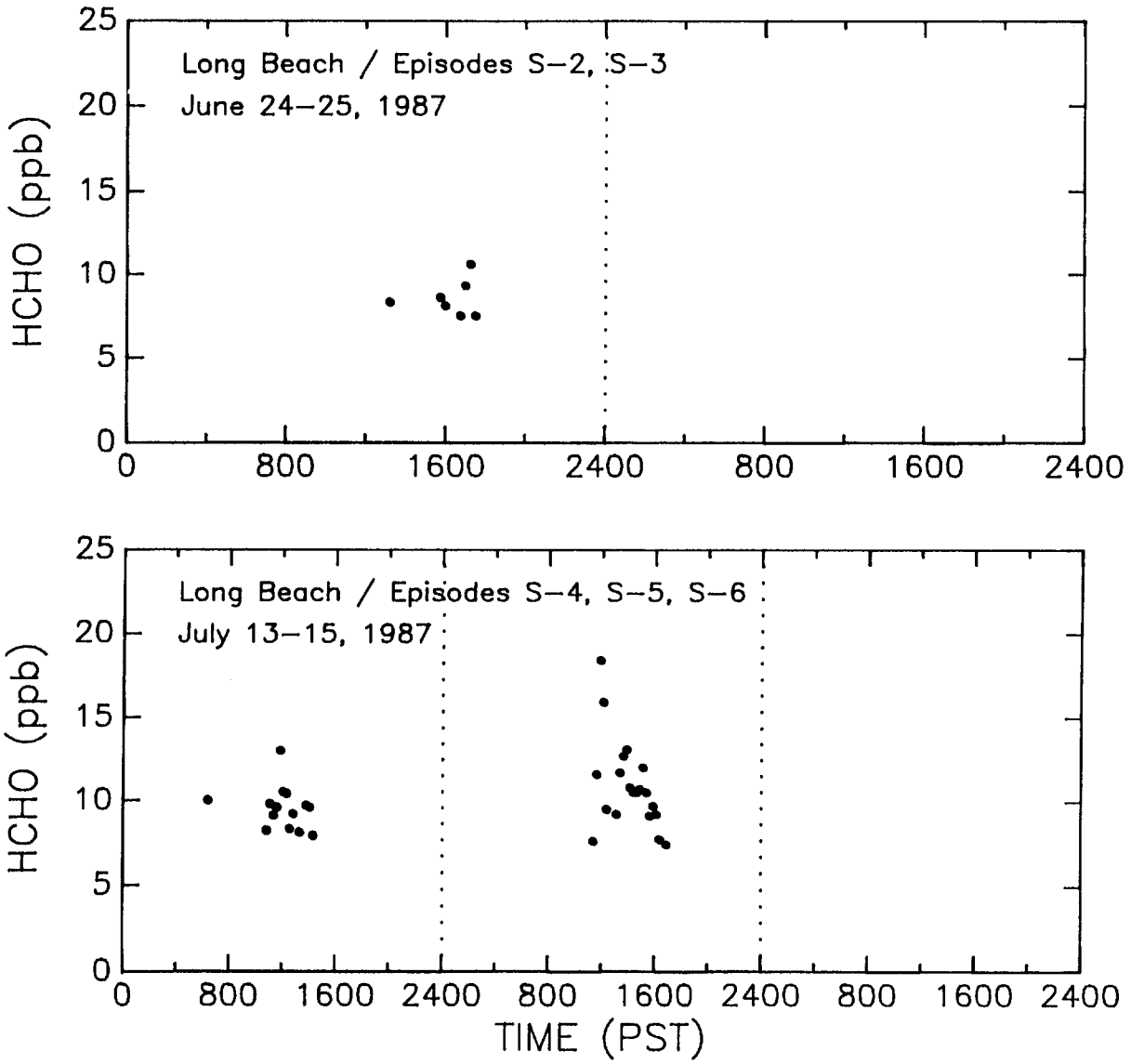

Figure V-27. DOAS 15-min HCHO concentrations observed at Long Beach during summer episodes S-2 through S-6.

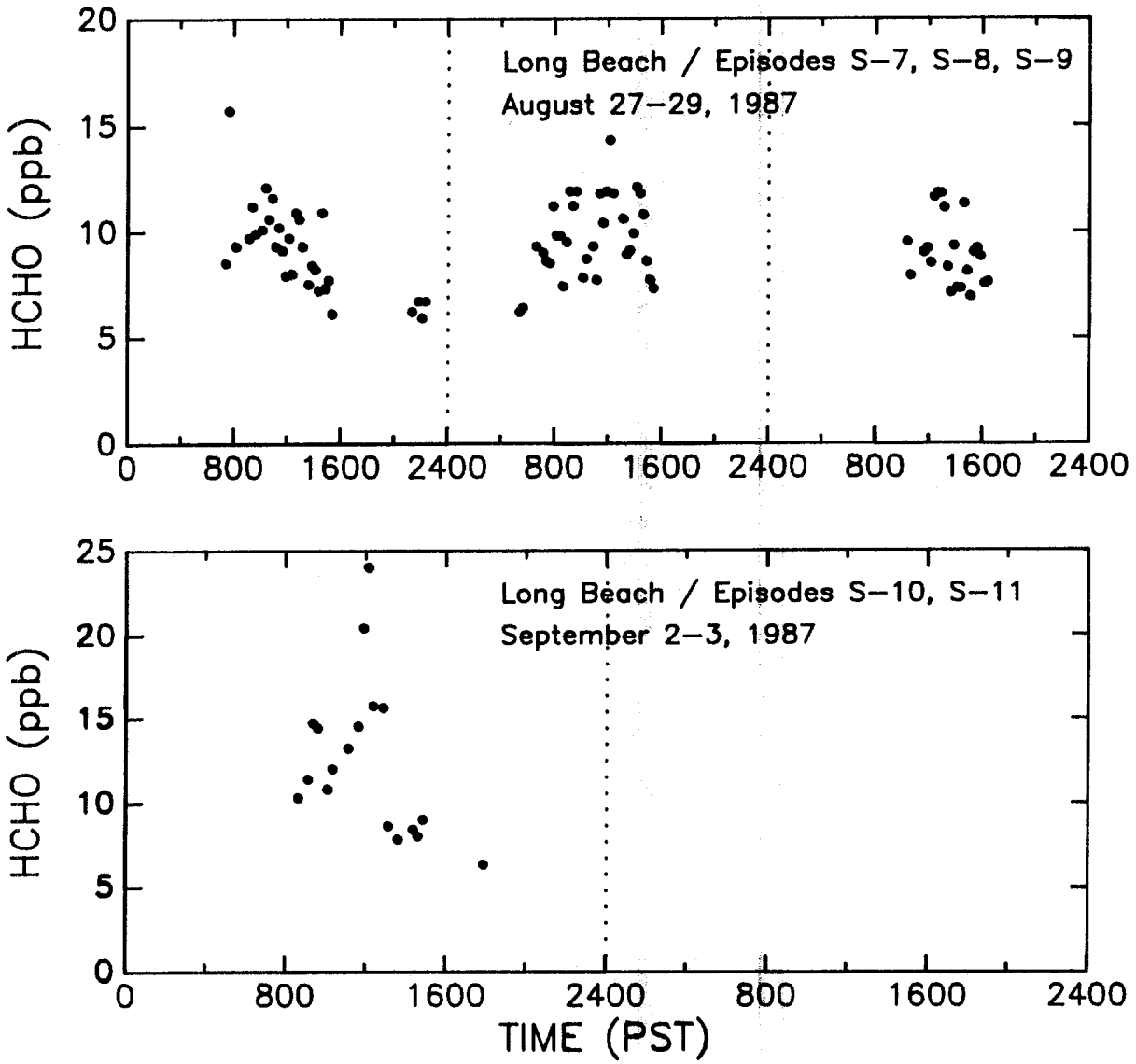

Figure V-28. DOAS 15-min HCHO concentrations observed at Long Beach during summer episodes S-7 through S-11.

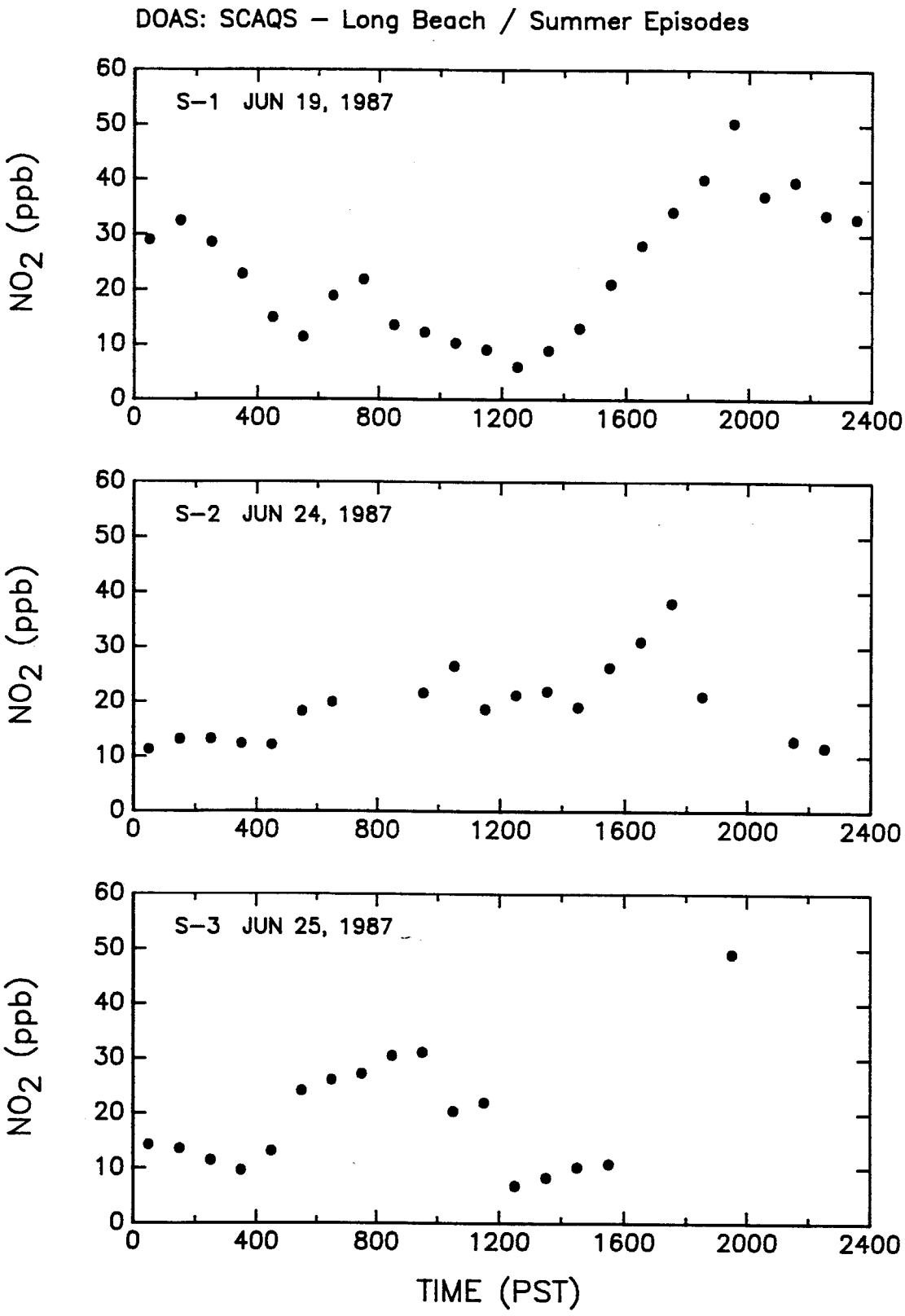

Figure V-29. DOAS 1-hr average NO_2 concentrations observed at Long Beach during summer episodes S-1 through S-3.

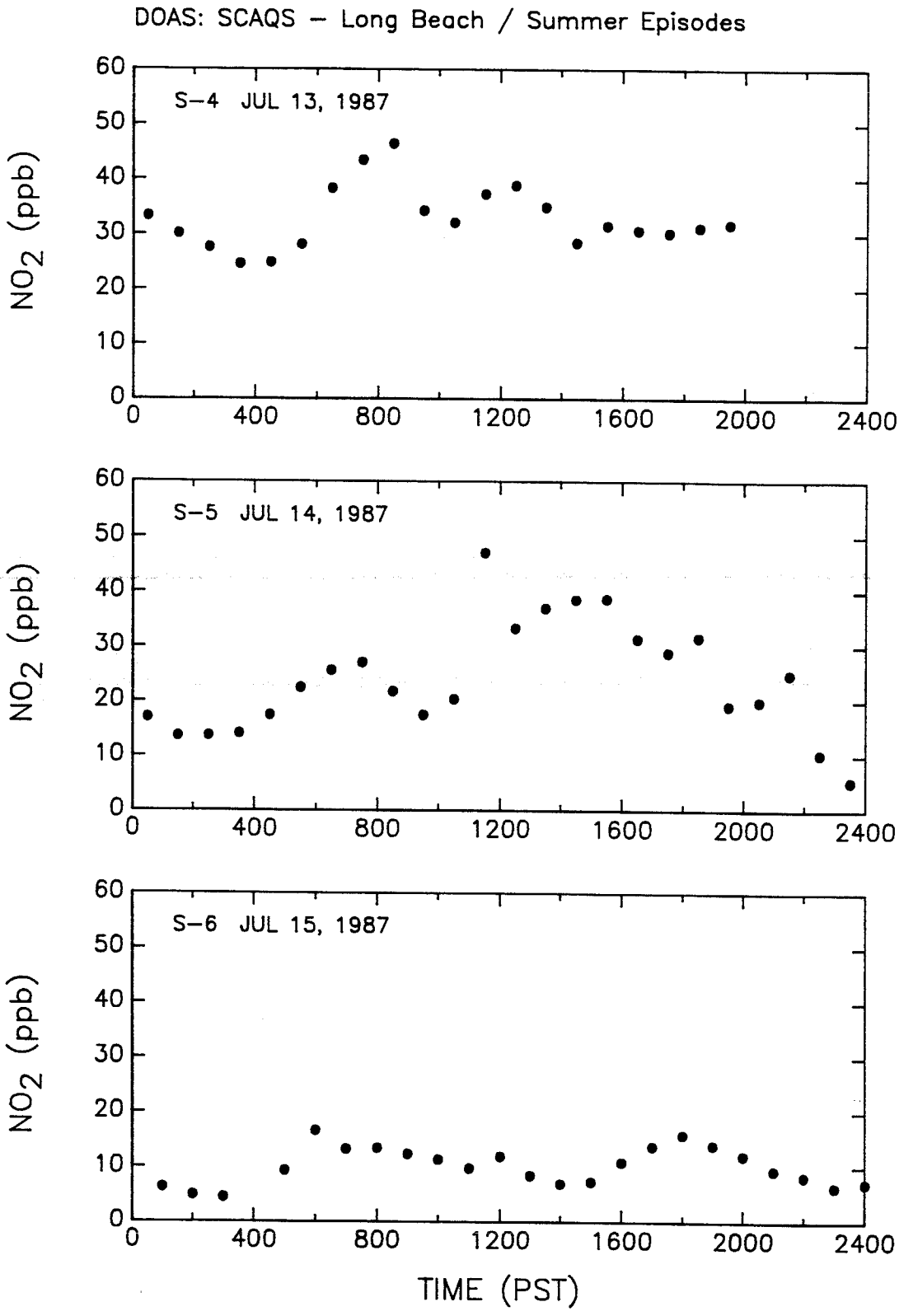

Figure V-30. DOAS 1-hr average NO_2 concentrations observed at Long Beach during summer episodes S-4 through S-6.

concentrations were below the respective detection limits throughout the 24-hr monitoring periods. As can be seen from Figures V-29 and V-30, maximum 1-hr NO_2 concentrations ranged from ~15 to 50 ppb, in marked contrast to the highly elevated NO_2 concentrations monitored during the fall episodes at Long Beach (see below).

For the remaining summer episodes, Figures V-31 through V-35 show the hourly average concentrations for NO_2, HONO and HCHO, respectively and Tables V-6 through V-8 provide the corresponding numerical concentrations. The smoothed diurnal profiles for NO_2, and their apparent dependence on traffic-associated emissions, are evident in these data. Maxima in HCHO hourly average concentrations occur between ~0800 and ~1400.

D. Long Beach Fall Episodes

As in the summer, NO_3 radical concentrations were not measured in Long Beach during the fall episodes since NO (an NO_3 scavenger) levels were expected to be highly elevated throughout most measurement periods and ozone (an NO_3 precursor) were expected to be quite low. In contrast to the predominant conditions during the summer phase of the SCAQS program, highly polluted conditions were encountered in most of the fall episodes at the Long Beach site. For this reason, we present in sections 1-3 below, individual full page plots of the 15 min concentrations measured by DOAS for NO_2, HONO and HCHO for the six fall episodes. In section 4, the corresponding 1-hr average data are plotted.

1. Nitrogen Dioxide

Figures V-36 to V-41 present the 15-min DOAS measurements for NO_2 during the fall Long Beach episodes. These data exhibit pronounced diurnal patterns and high NO_2 concentrations, ranging up to nearly 250 ppb near noon on December 3, 1987 (F-4). A comparable maximum in NO_2 concentration also occurred during mid-day on December 10 (F-5), while maximum NO_2 concentrations reached approximately 150 ppb during three other episodes (F-1, F-2 and F-6). In the case of the latter three episodes, the NO_2 maxima were associated with the afternoon traffic peak, rather than the morning. Typically, during the night NO_2 concentrations declined to more or less constant levels in the range from approximately 40 to 80 ppb.

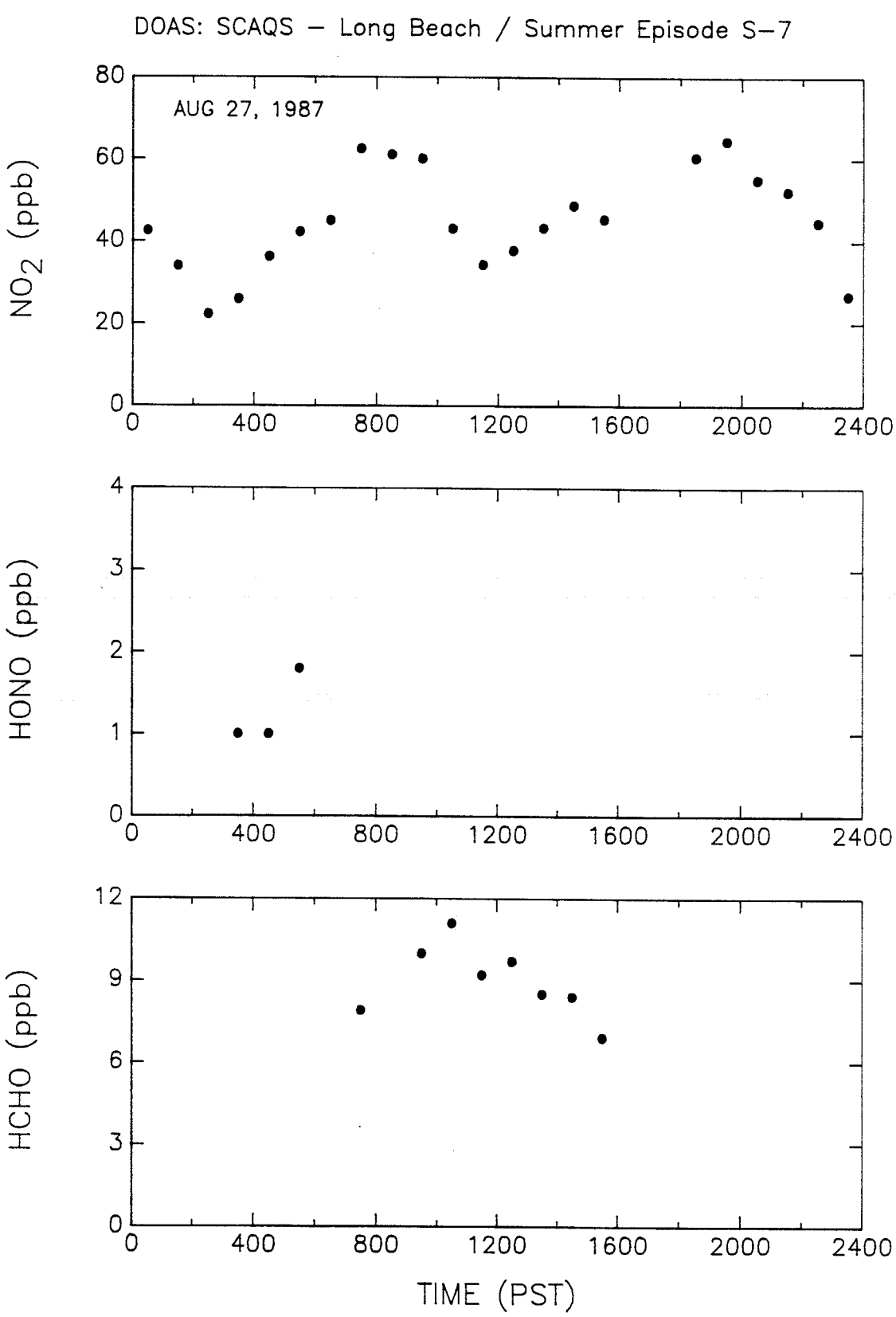

Figure V-31. DOAS 1-hr average concentrations observed at Long Beach during summer episode S-7.

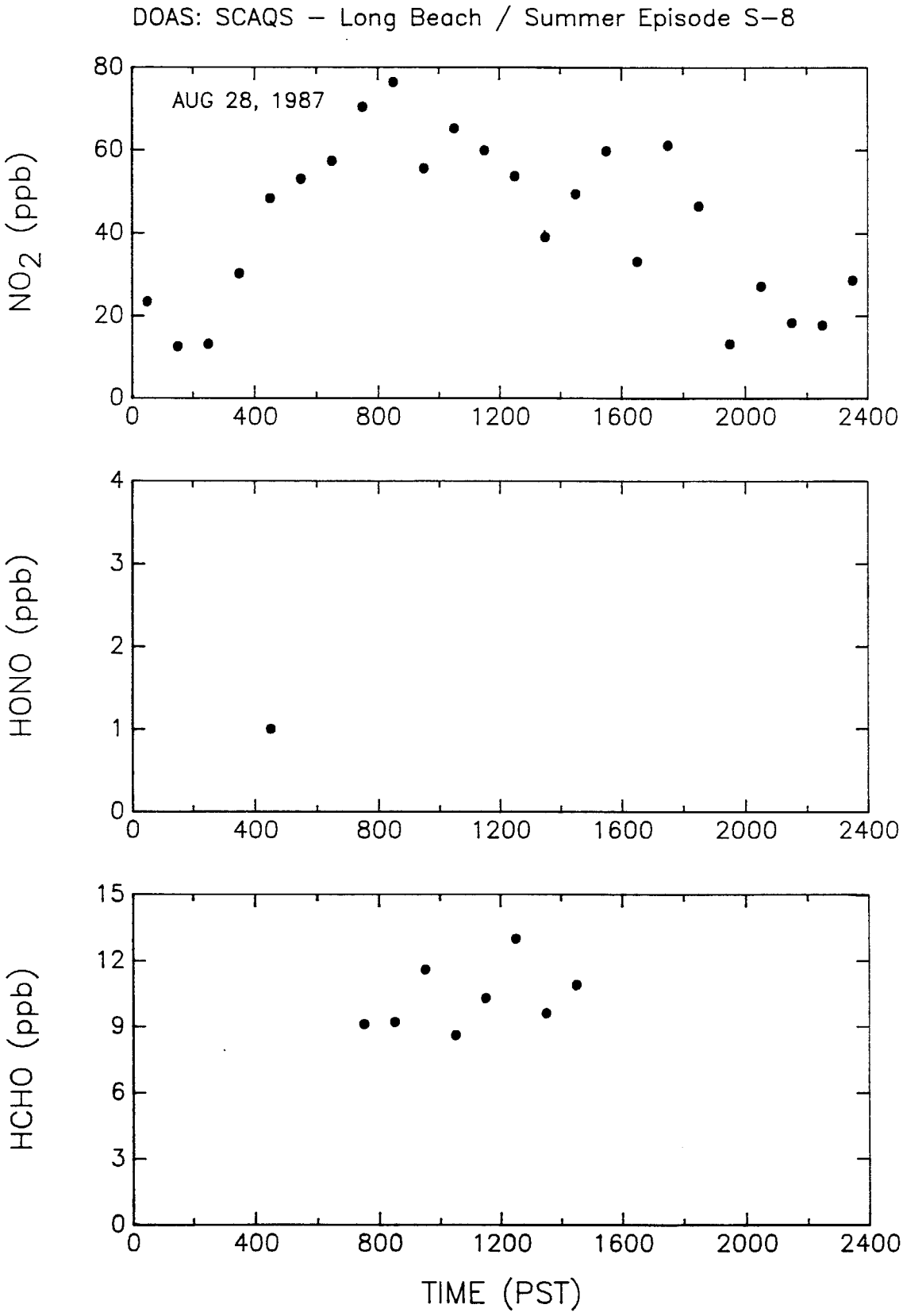

Figure V-32. DOAS 1-hr average concentrations observed at Long Beach during summer episode S-8.

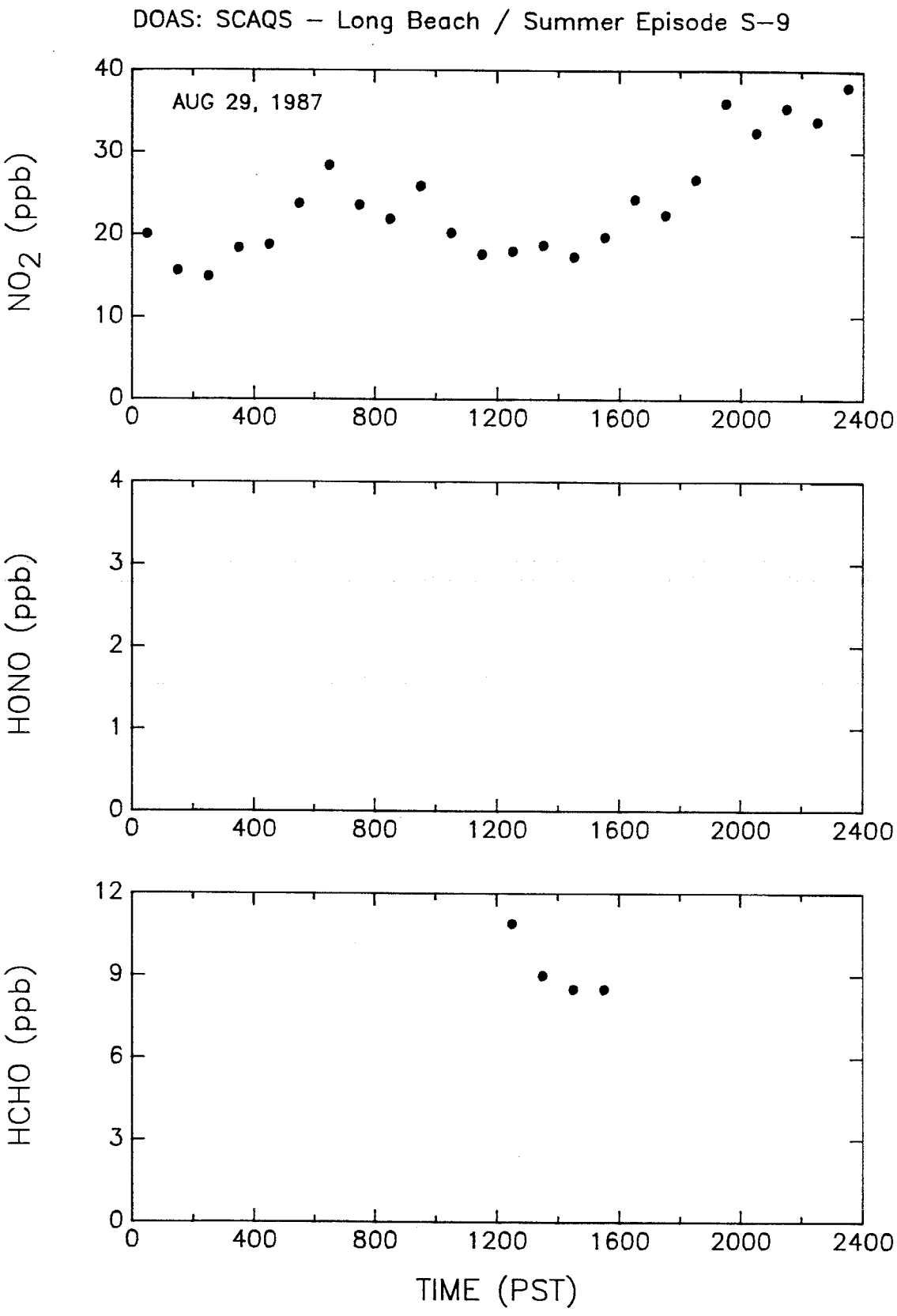

Figure V-33. DOAS 1-hr average concentrations observed at Long Beach during summer episode S-9.

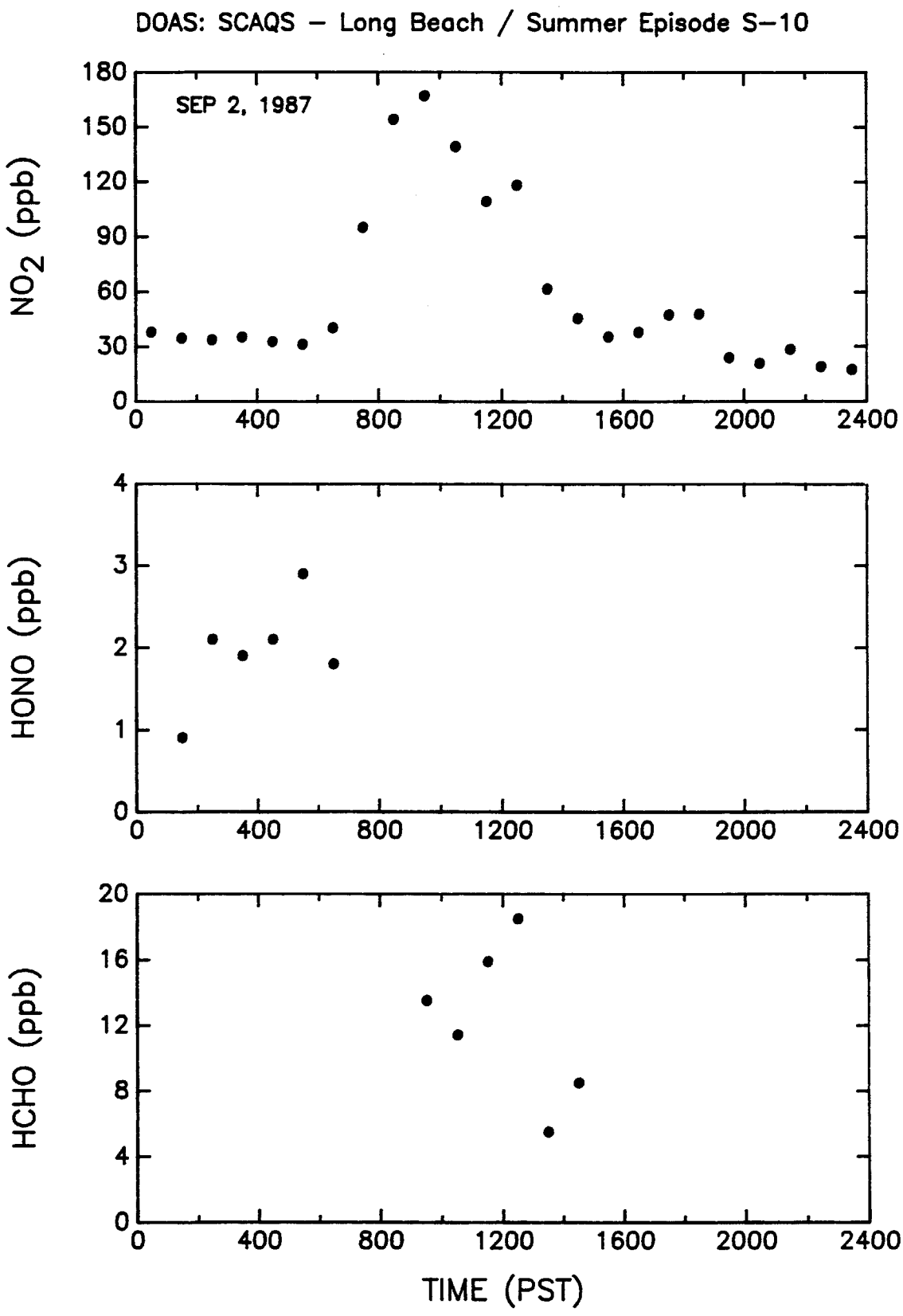

Figure V-34. DOAS 1-hr average concentrations observed at Long Beach during summer episode S-10.

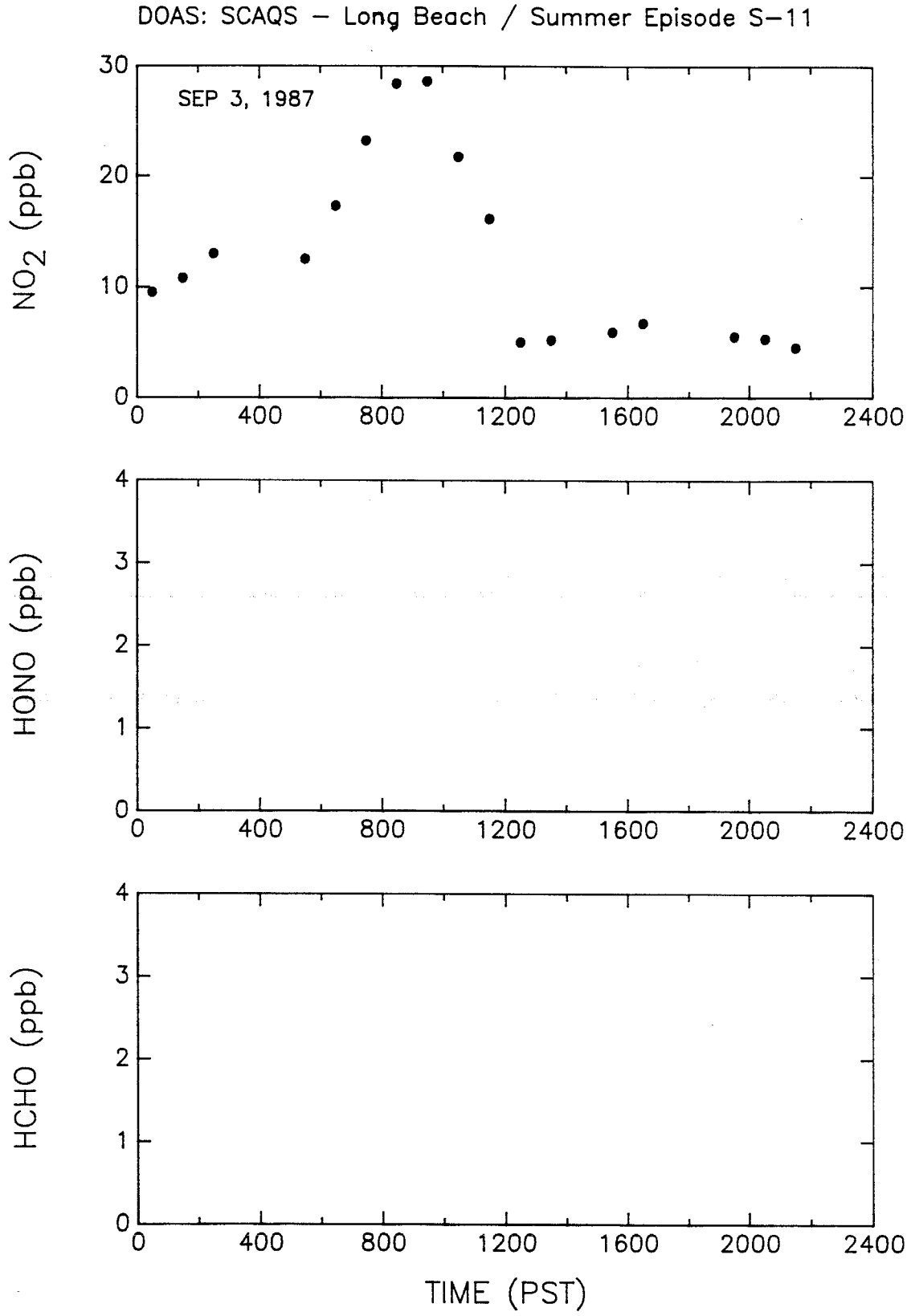

Figure V-35. DOAS 1-hr average concentrations observed at Long Beach during summer episode S-11.

Table V-6. Hourly Average NO_2 Concentrations (ppb) Measured by DOAS During the 1987 SCAQS Study, Summer Episodes at Long Beach

Hourly Period (PST)	S-1 Jun 19	S-2 Jun 24	S-3 Jun 25	S-4 Jul 13	S-5 Jul 14	S-6 Jul 15	S-7 Aug 27	S-8 Aug 28	S-9 Aug 29	S-10 Sep 2	S-11 Sep 3
0000-0100	29	11	14	33	17	6	42	23	20	38	10
0100-0200	32	13	14	30	14	5	34	12	16	34	11
0200-0300	28	13	11	28	14	4	22	13	15	34	13
0300-0400	23	12	10	24	14	BDL	26	30	18	35	BDL
0400-0500	15	12	13	25	17	9	36	48	19	33	BDL
0500-0600	11	18	24	28	22	17	42	53	24	31	12
0600-0700	19	20	26	38	26	13	45	57	28	44	17
0700-0800	22	ND	27	43	27	13	62	70	24	95	23
0800-0900	14	ND	30	46	22	12	61	76	22	154	28
0900-1000	12	22	31	34	17	11	60	56	26	167	29
1000-1100	10	26	20	32	20	10	43	65	20	139	22
1100-1200	9	19	22	37	47	12	34	60	18	109	16
1200-1300	6	21	7	39	33	8	38	54	18	118	5
1300-1400	9	22	8	35	37	7	43	39	19	61	5
1400-1500	13	19	10	28	38	7	49	49	17	45	BDL
1500-1600	21	26	11	32	39	11	45	60	20	35	6
1600-1700	28	31	ND	31	31	14	RS	33	24	38	7
1700-1800	34	38	ND	30	29	16	RS	61	22	47	ND
1800-1900	40	21	ND	31	32	14	60	46	27	48	BDL
1900-2000	50	ND	49	32	19	12	64	13	36	24	6
2000-2100	37	ND	ND	ND	20	9	55	27	32	21	5
2100-2200	40	13	ND	ND	25	8	52	18	35	28	4
2200-2300	34	12	ND	ND	10	6	45	18	34	19	BDL
2300-2400	33	ND	ND	ND	5	7	27	29	38	17	BDL

BDL - Below detection limit.
ND - No data avaliable.

Table V-7. Hourly Average HONO Concentrations (ppb) Measured by DOAS During the 1987 SCAQS Study, Summer Episodes at Long Beach

Hourly Period (PST)	S-1 Jun 19	S-2 Jun 24	S-3 Jun 25	S-4 Jul 13	S-5 Jul 14	S-6 Jul 15	S-7 Aug 27	S-8 Aug 28	S-9 Aug 29	S-10 Sep 2	S-11 Sep 3
0000-0100	BDL	BDL	BDL	BDL	BDL	BDL	BDL	BDL	BDL	BDL	BDL
0100-0200	BDL	BDL	BDL	2	BDL	BDL	BDL	BDL	BDL	1	BDL
0200-0300	BDL	BDL	BDL	1	BDL	BDL	BDL	BDL	BDL	2	BDL
0300-0400	BDL	BDL	BDL	1	BDL	BDL	1	BDL	BDL	2	BDL
0400-0500	BDL	BDL	BDL	2	BDL	BDL	1	1	BDL	2	BDL
0500-0600	BDL	BDL	BDL	1	BDL	BDL	2	BDL	BDL	3	BDL
0600-0700	BDL	BDL	BDL	BDL	BDL	BDL	BDL	BDL	BDL	2	BDL
0700-0800	BDL	ND	BDL	BDL	BDL	BDL	BDL	BDL	BDL	BDL	BDL
0800-0900	BDL	ND	BDL	BDL	BDL	BDL	BDL	BDL	BDL	BDL	BDL
0900-1000	BDL	BDL	BDL	BDL	BDL	BDL	BDL	BDL	BDL	BDL	BDL
1000-1100	BDL	BDL	BDL	BDL	BDL	BDL	BDL	BDL	BDL	BDL	BDL
1100-1200	BDL	BDL	BDL	BDL	BDL	BDL	BDL	BDL	BDL	BDL	BDL
1200-1300	BDL	BDL	BDL	BDL	BDL	BDL	BDL	BDL	BDL	BDL	BDL
1300-1400	BDL	BDL	BDL	BDL	BDL	BDL	BDL	BDL	BDL	BDL	BDL
1400-1500	BDL	BDL	BDL	BDL	BDL	BDL	BDL	BDL	BDL	BDL	BDL
1500-1600	BDL	BDL	BDL	BDL	BDL	BDL	BDL	BDL	BDL	BDL	BDL
1600-1700	BDL	BDL	ND	BDL	BDL	BDL	RS	BDL	BDL	BDL	BDL
1700-1800	BDL	BDL	ND	BDL	BDL	BDL	RS	BDL	BDL	BDL	ND
1800-1900	BDL	BDL	ND	BDL	BDL	BDL	BDL	BDL	BDL	BDL	BDL
1900-2000	BDL	ND	BDL	BDL	BDL	BDL	BDL	BDL	BDL	BDL	BDL
2000-2100	BDL	ND	ND	ND	BDL	BDL	BDL	BDL	BDL	BDL	BDL
2100-2200	BDL	BDL	ND	ND	BDL	BDL	BDL	BDL	BDL	BDL	BDL
2200-2300	BDL	BDL	ND	ND	BDL	BDL	BDL	BDL	BDL	BDL	BDL
2300-2400	BDL	ND	ND	ND	BDL	BDL	BDL	BDL	BDL	BDL	BDL

BDL - Below detection limit.
ND - No data available.

Table V-8. Hourly Average HCHO Concentrations (ppb) Measured by DOAS During the 1987 SCAQS Study, Summer Episodes at Long Beach

Hourly Period (PST)	S-1 Jun 19	S-2 Jun 24	S-3 Jun 25	S-4 Jul 13	S-5 Jul 14	S-6 Jul 15	S-7 Aug 27	S-8 Aug 28	S-9 Aug 29	S-10 Sep 2	S-11 Sep 3
0000-0100	BDL	BDL	BDL	BDL	BDL	BDL	BDL	BDL	BDL	BDL	BDL
0100-0200	BDL	BDL	BDL	BDL	BDL	BDL	BDL	BDL	BDL	BDL	BDL
0200-0300	BDL	BDL	BDL	BDL	BDL	BDL	BDL	BDL	BDL	BDL	BDL
0300-0400	BDL	BDL	BDL	BDL	BDL	BDL	BDL	BDL	BDL	BDL	BDL
0400-0500	BDL	BDL	BDL	BDL	BDL	BDL	BDL	BDL	BDL	BDL	BDL
0500-0600	BDL	BDL	BDL	BDL	BDL	BDL	BDL	BDL	BDL	BDL	BDL
0600-0700	BDL	BDL	BDL	BDL	BDL	BDL	BDL	BDL	BDL	BDL	BDL
0700-0800	BDL	ND	BDL	ND	BDL	BDL	8	9	BDL	BDL	BDL
0800-0900	BDL	ND	BDL	BDL	BDL	BDL	BDL	9	BDL	BDL	BDL
0900-1000	BDL	BDL	BDL	BDL	BDL	BDL	10	12	BDL	14	BDL
1000-1100	BDL	BDL	BDL	BDL	BDL	BDL	11	9	BDL	11	BDL
1100-1200	BDL	BDL	BDL	10	12	BDL	9	10	BDL	16	BDL
1200-1300	BDL	BDL	BDL	9	7	BDL	10	13	11	18	BDL
1300-1400	BDL	BDL	BDL	BDL	12	BDL	8	10	9	6	BDL
1400-1500	BDL	BDL	BDL	BDL	11	BDL	8	11	8	8	BDL
1500-1600	BDL	BDL	BDL	BDL	10	BDL	7	BDL	8	BDL	BDL
1600-1700	BDL	BDL	ND	BDL	6	BDL	RS	BDL	BDL	BDL	BDL
1700-1800	BDL	6	ND	BDL	BDL	BDL	RS	BDL	BDL	BDL	ND
1800-1900	BDL	BDL	ND	BDL	BDL	BDL	BDL	BDL	BDL	BDL	BDL
1900-2000	BDL	ND	BDL	BDL	BDL	BDL	BDL	BDL	BDL	BDL	BDL
2000-2100	BDL	ND	ND	ND	BDL	BDL	BDL	BDL	BDL	BDL	BDL
2100-2200	BDL	BDL	ND	ND	BDL	BDL	BDL	BDL	BDL	BDL	BDL
2200-2300	BDL	BDL	ND	ND	BDL	BDL	BDL	BDL	BDL	BDL	BDL
2300-2400	BDL	ND	ND	ND	BDL	BDL	BDL	BDL	BDL	BDL	BDL

BDL - Below detection limit.
ND - No data available.
RS - Reference Spectrum acquired this period.

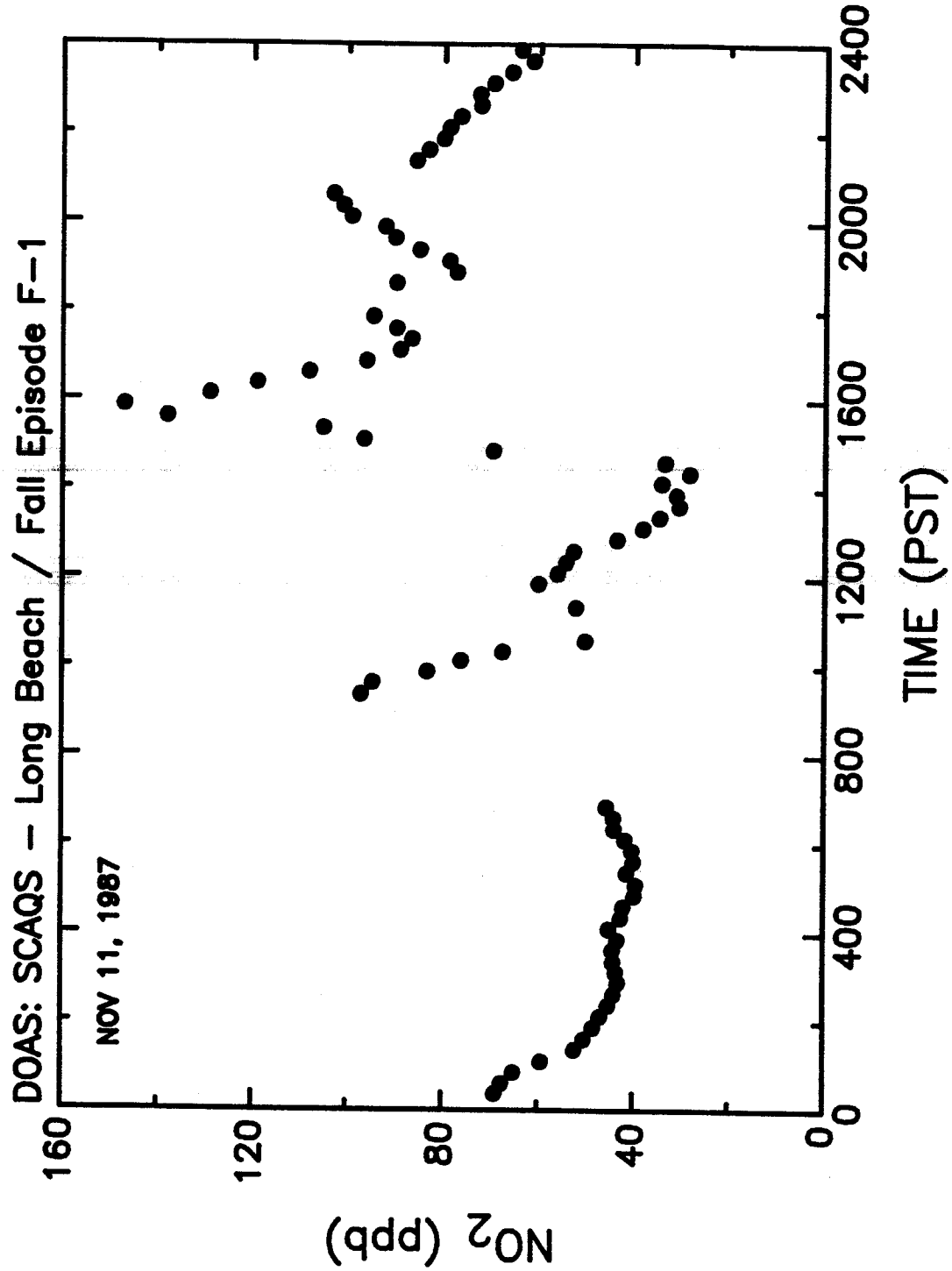

Figure V-36. DOAS 15-min NO_2 concentrations observed at Long Beach during fall episode F-1.

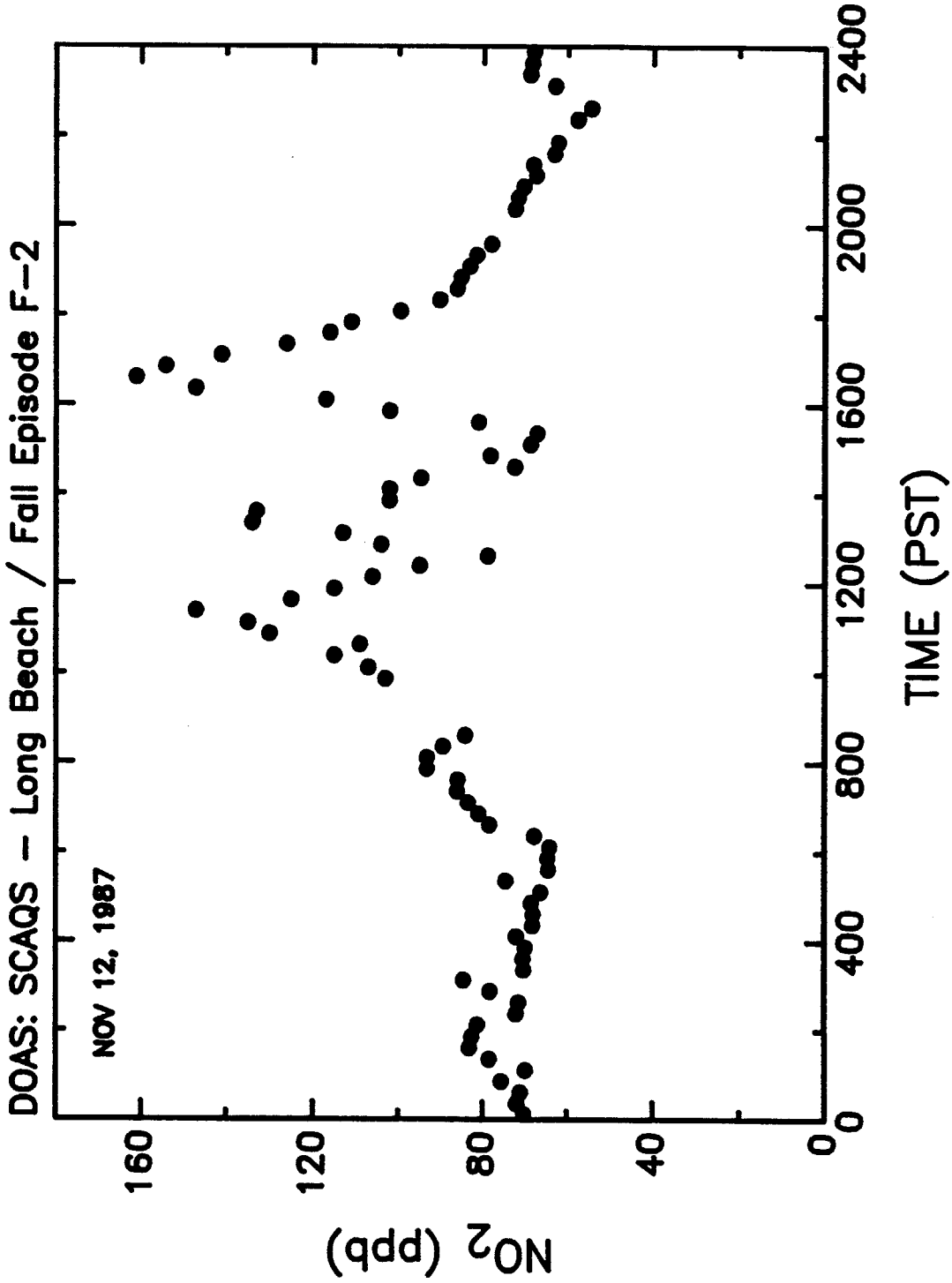

Figure V-37. DOAS 15-min NO_2 concentrations observed at Long Beach during fall episode F-2.

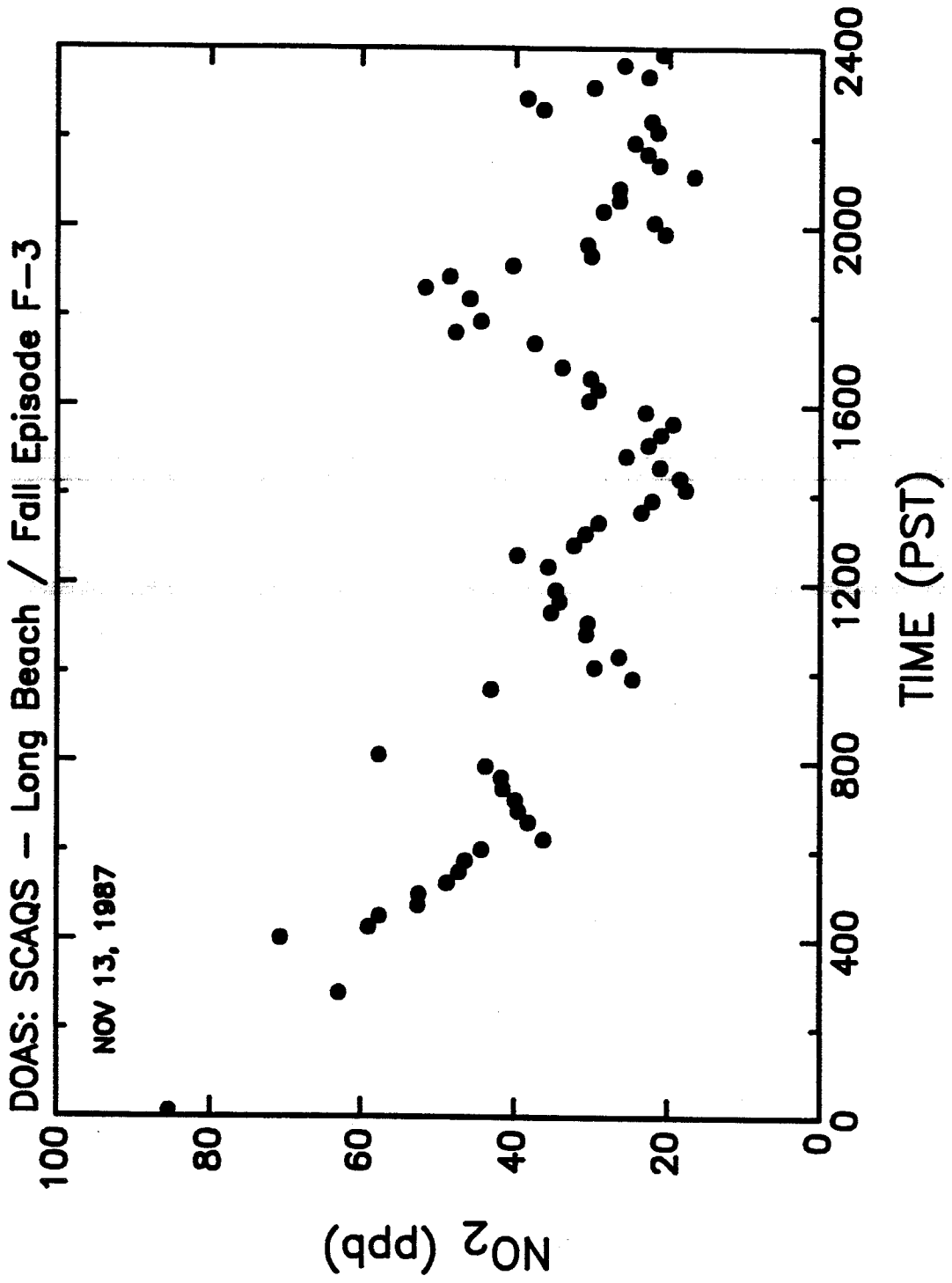

Figure V-38. DOAS 15-min NO_2 concentrations observed at Long Beach during fall episode F-3.

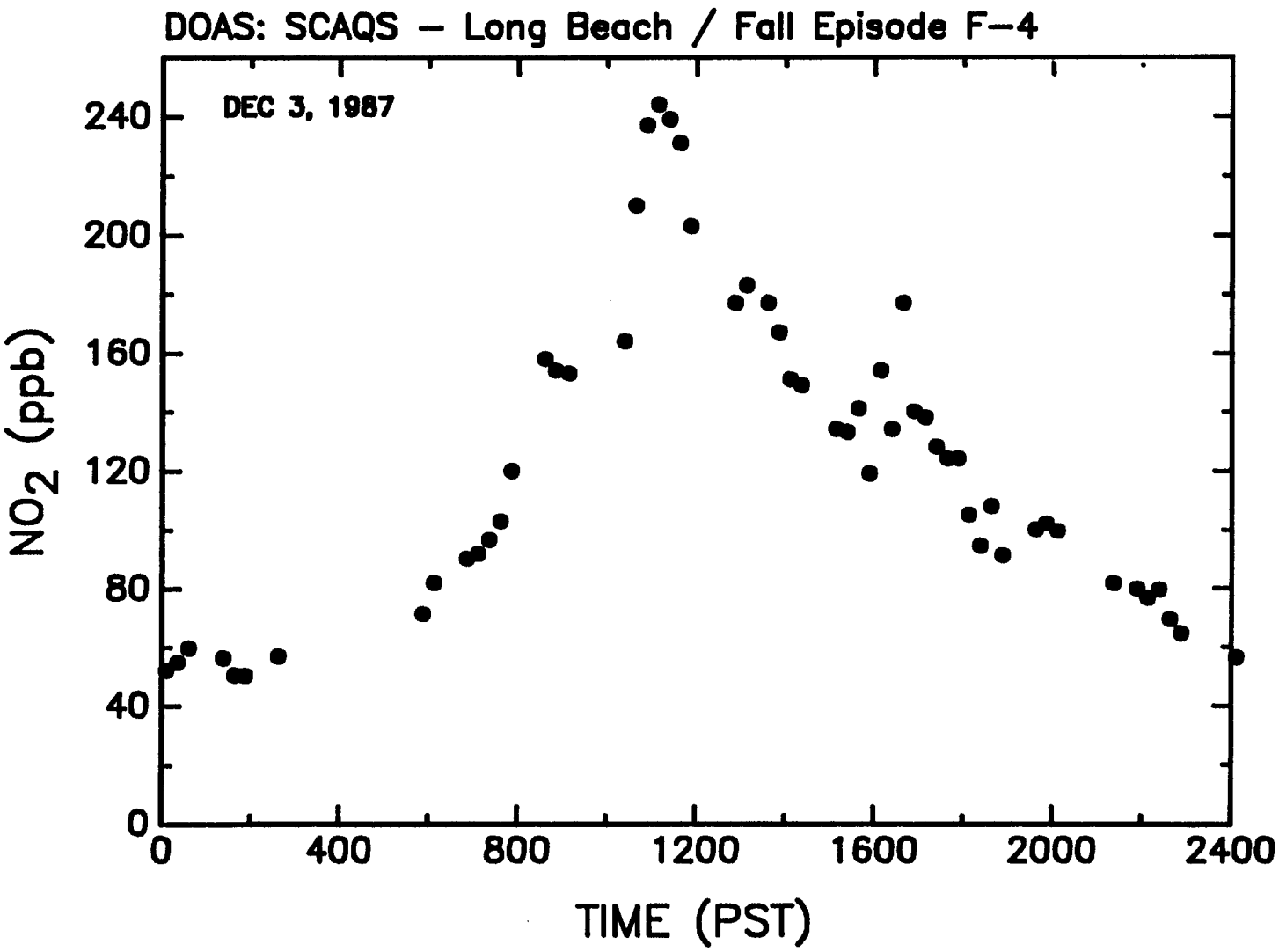

Figure V-39. DOAS 15-min NO_2 concentrations observed at Long Beach during fall episode F-4.

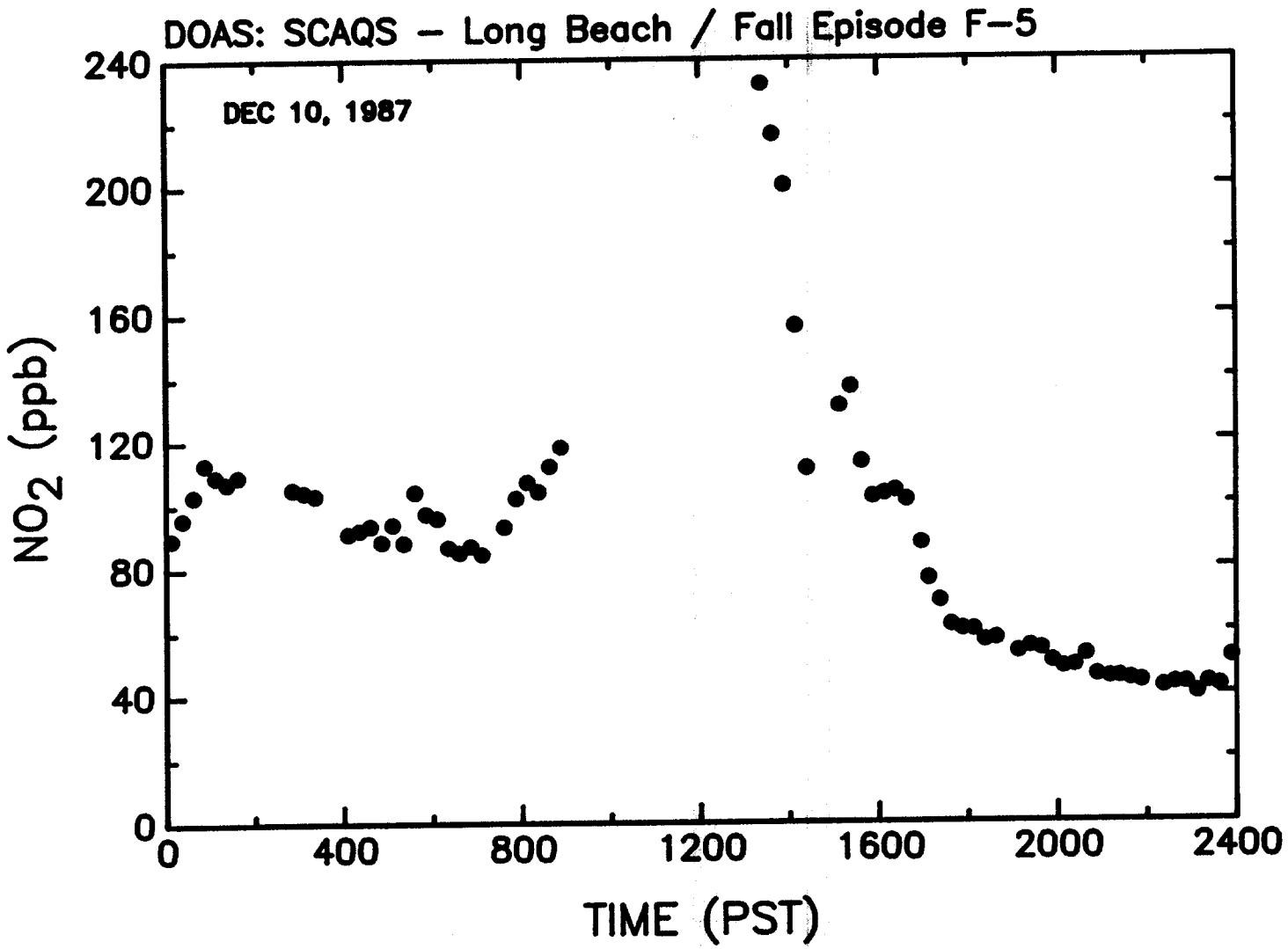

Figure V-40. DOAS 15-min NO_2 concentrations observed at Long Beach during fall episode F-5.

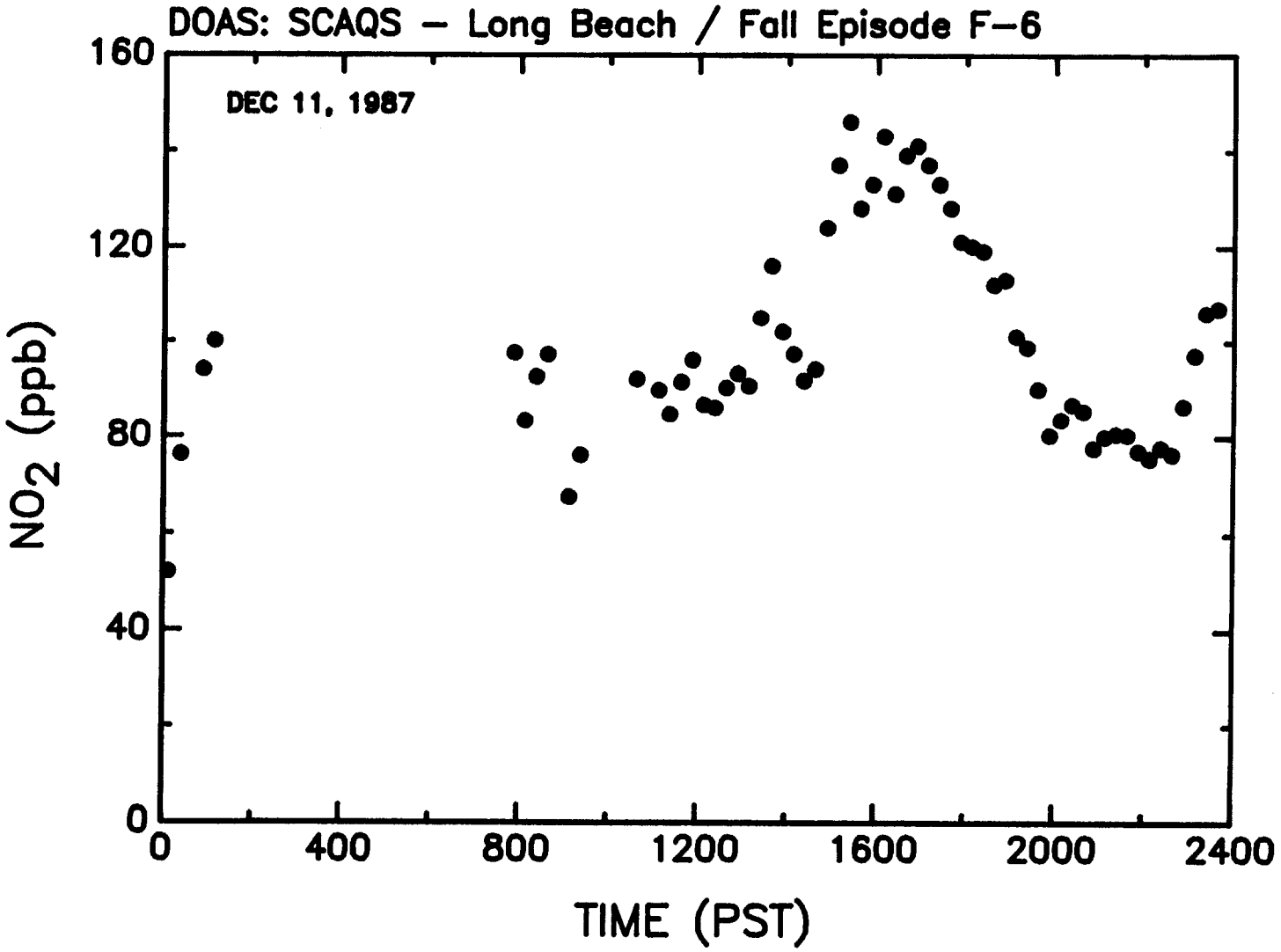

Figure V-41. DOAS 15-min NO_2 concentrations observed at Long Beach during fall episode F-6.

Note that gaps in the NO_2 (and other pollutant) data for these episodes are due primarily to acquisition of reference spectra and periods of fog, particularly during the early morning hours, which prevented transmission of the white light source through the open multiple reflection cell interfaced to the DOAS spectrometer. There were no known problems with stray light interferences during the fall episodes.

These data, when coupled with ARB and GM chemiluminescence measurements of maximum NO concentrations between 500 and 700 ppb, serve to indicate the degree to which NO_x (=NO + NO_2) concentrations can be elevated during periods with low, strong temperature inversions along the coastal region of the SoCAB in the fall and winter.

2. Nitrous Acid

The 15-min DOAS measurements of HONO during the Long Beach fall episodes are shown in Figures V-42 through V-47. As discussed in more detail in Section VI, these represent among the most interesting and important DOAS data obtained during the SCAQS project. From Figures V-45 and V-46, it can be seen that maximum HONO concentrations in the early morning hours of episodes F-4 and F-5 exceeded 15 ppb, and that during the early morning or late evening periods of episodes F-1, F-2 and F-6 maximum HONO levels reached or exceeded 10 ppb.

These are the highest HONO concentrations observed to date by the DOAS technique. The highest ambient HONO concentration reported previously was the 11 ppb value we measured for one 15-min period on January 28, 1986 at Torrance, California, during the study at El Camino College (Winer et al. 1987; Biermann et al. 1988b). However, in the Torrance study, for all other measurement periods (a total of eight nights) maximum HONO concentrations were in the range 4-8 ppb. In contrast, as seen in Figures V-42 to V-47, during five of the six fall SCAQS episodes maximum HONO concentrations were in the range 8-16 ppb, and these levels persisted in most cases over a period of many hours.

Particularly striking in the 15-min fall Long Beach HONO data, are both the rapid formation of HONO following sunset for a number of episodes, reaching plateau levels at around midnight, and the rapid loss of HONO after sunrise due to photolysis. The latter is particularly well characterized for the mornings of November 12 and December 10 and 11. On December 3, arguably the most heavily polluted day of the SCAQS program,

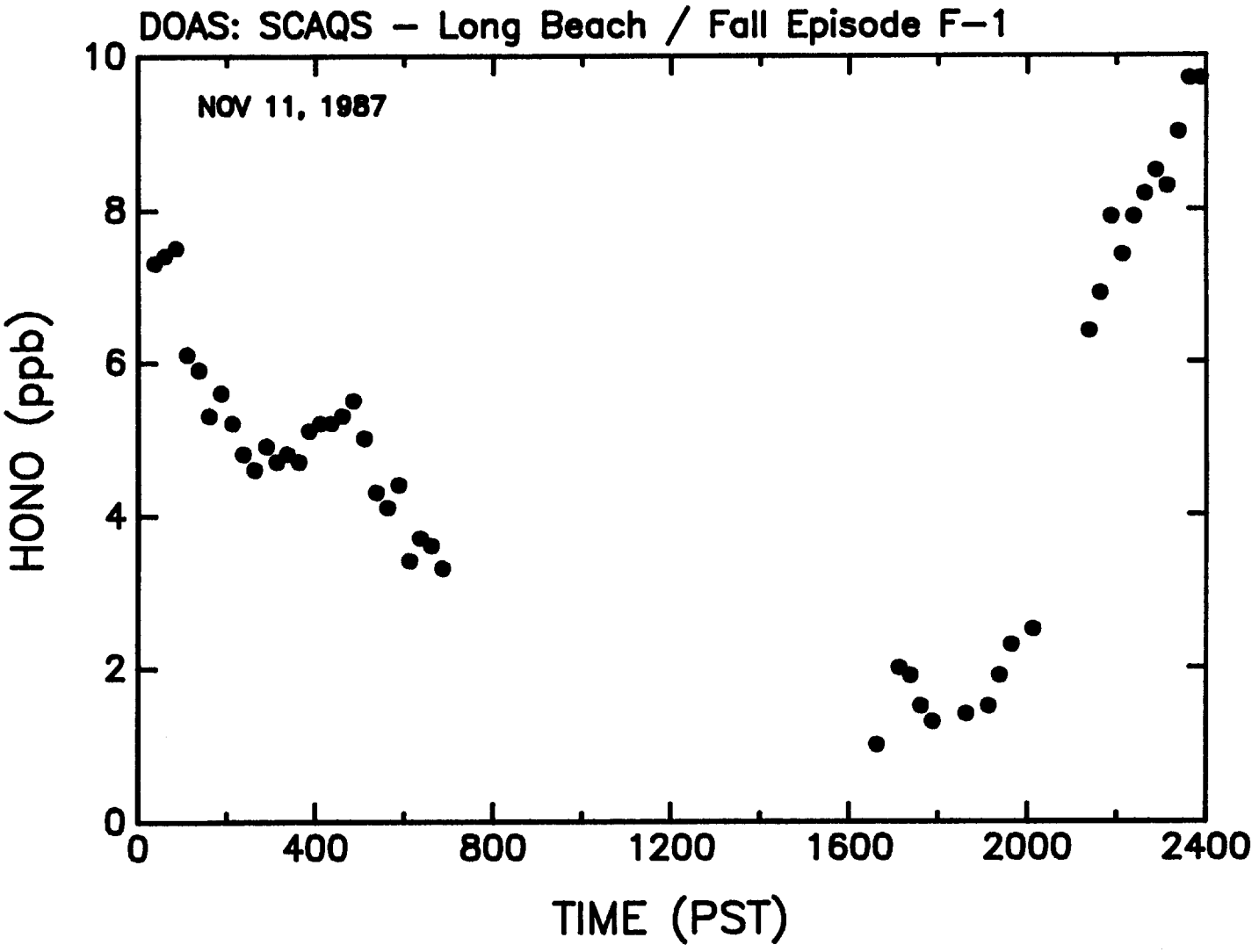

Figure V-42. DOAS 15-min HONO concentrations observed at Long Beach during fall episode F-1.

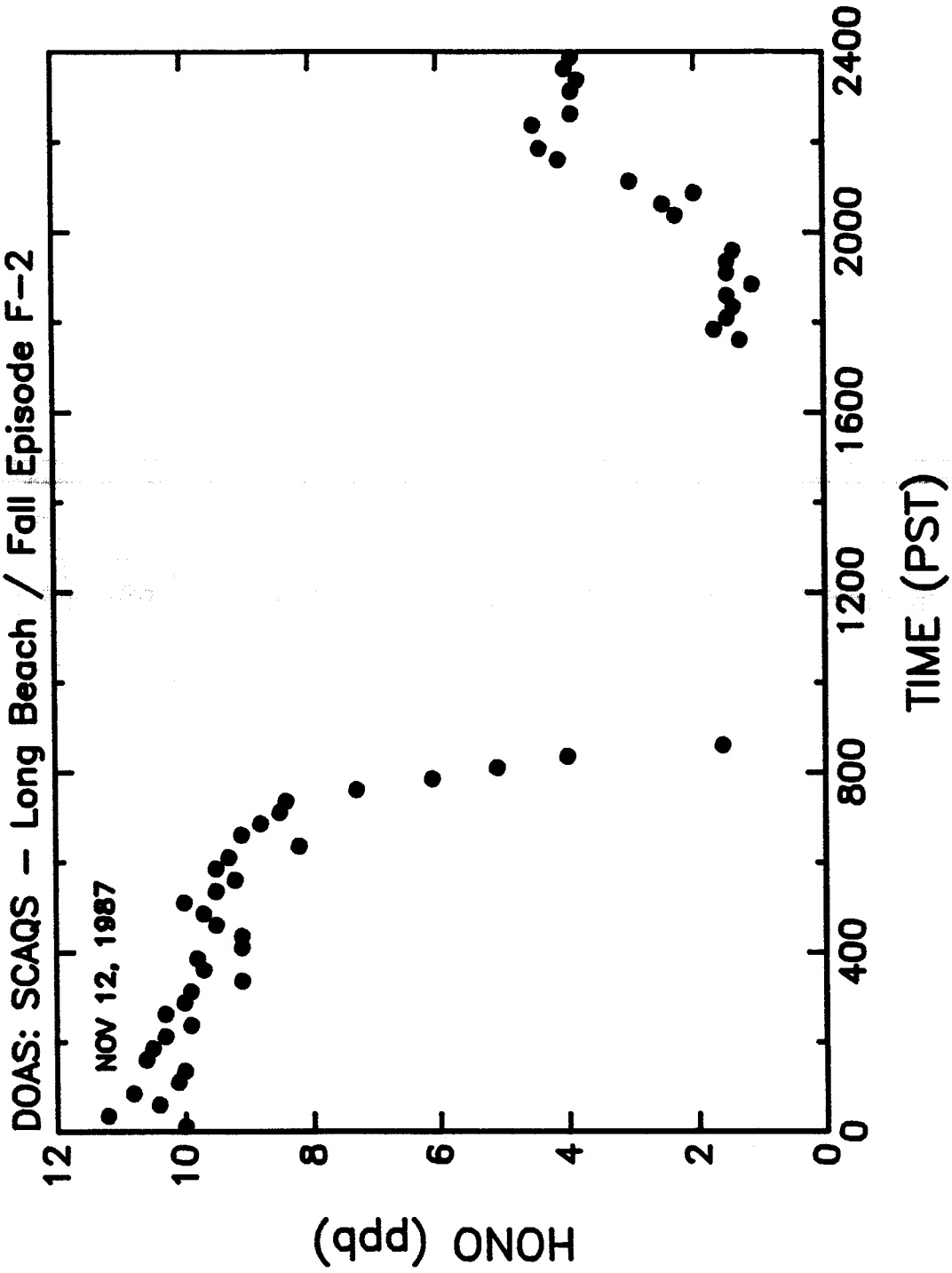

Figure V-43. DOAS 15-min HONO concentrations observed at Long Beach during fall episode F-2.

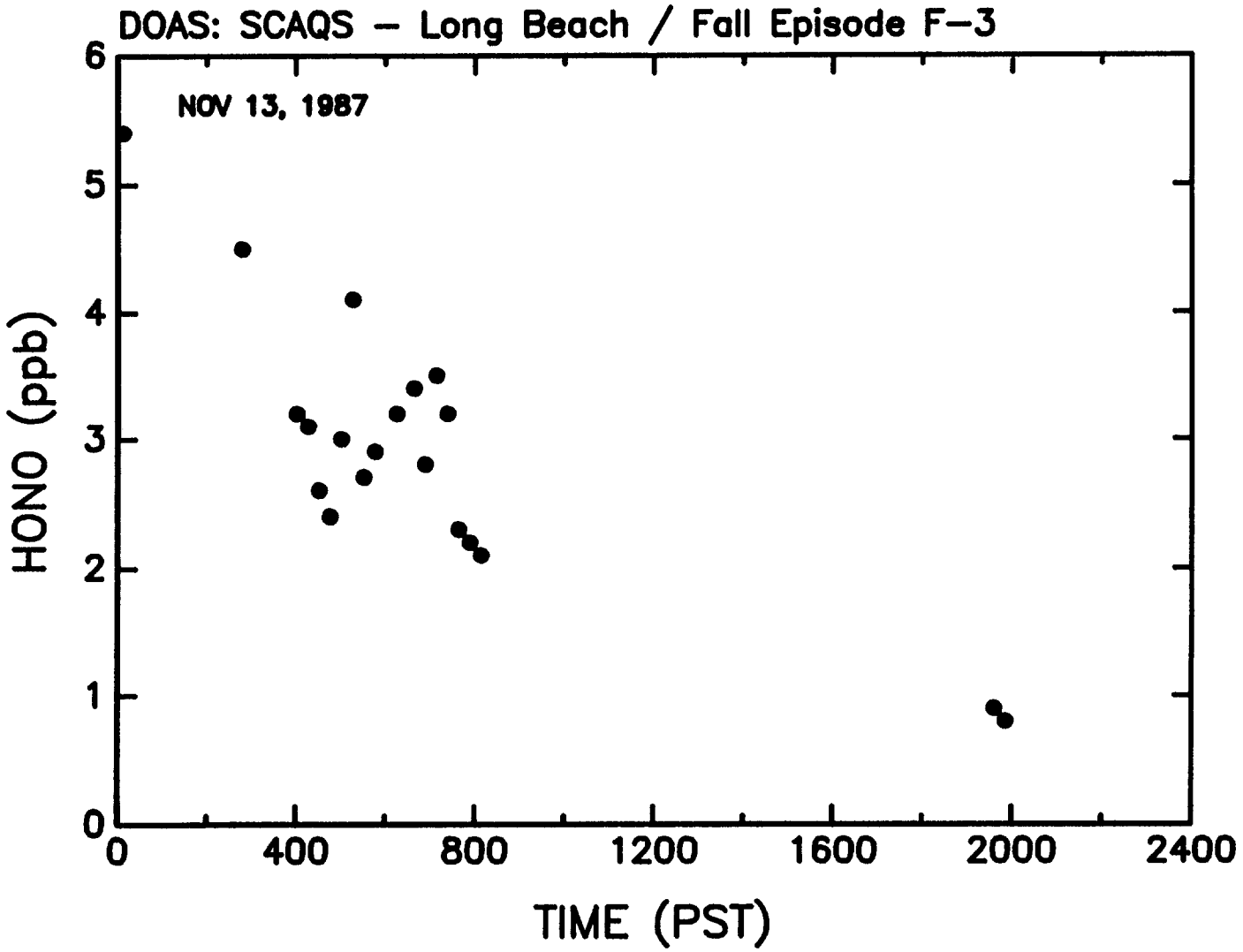

Figure V-44. DOAS 15-min HONO concentrations observed at Long Beach during fall episode F-3.

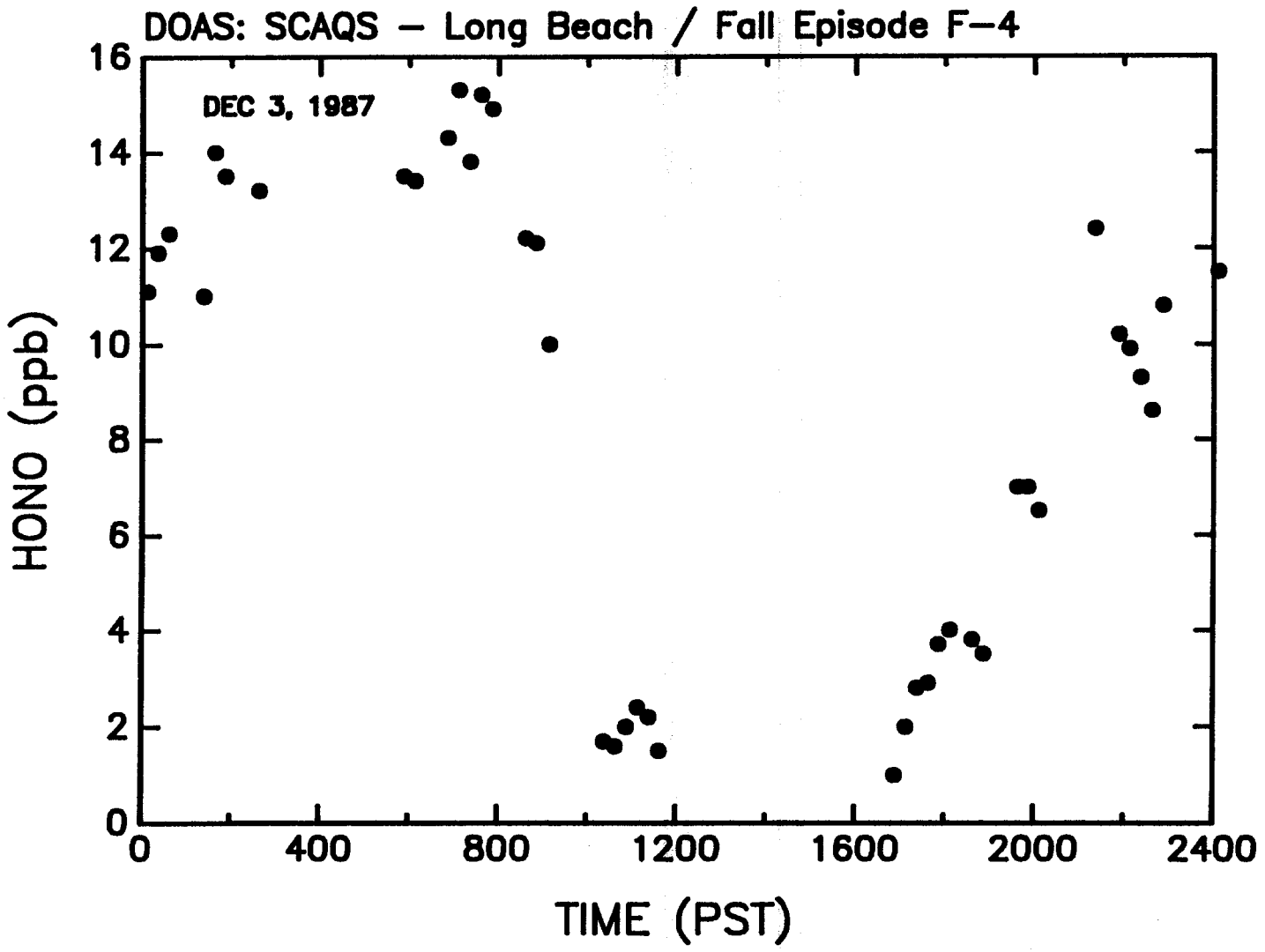

Figure V-45. DOAS 15-min HONO concentrations observed at Long Beach during fall episode F-4.

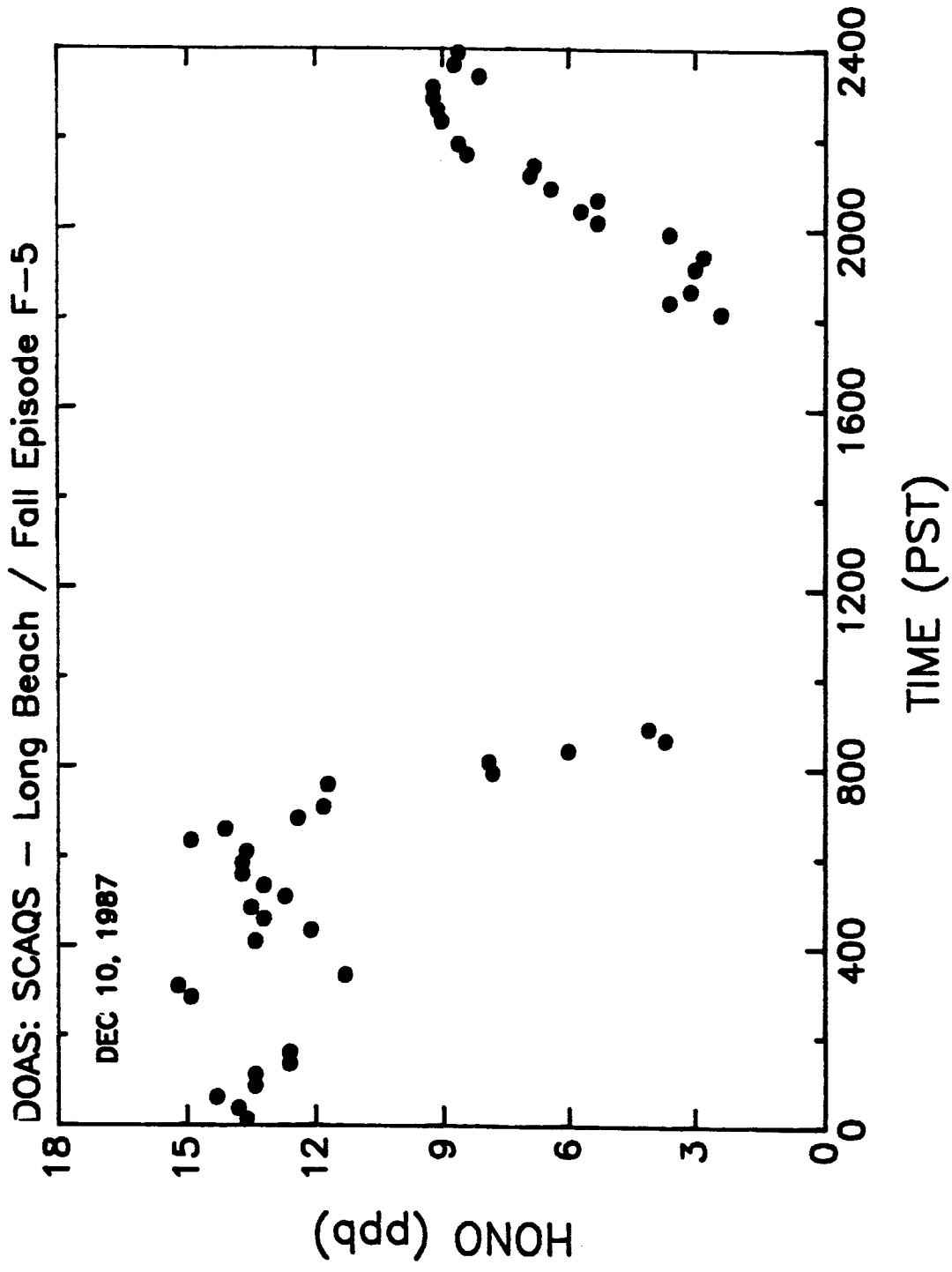

Figure V-46. DOAS 15-min HONO concentrations observed at Long Beach during fall episode F-5.

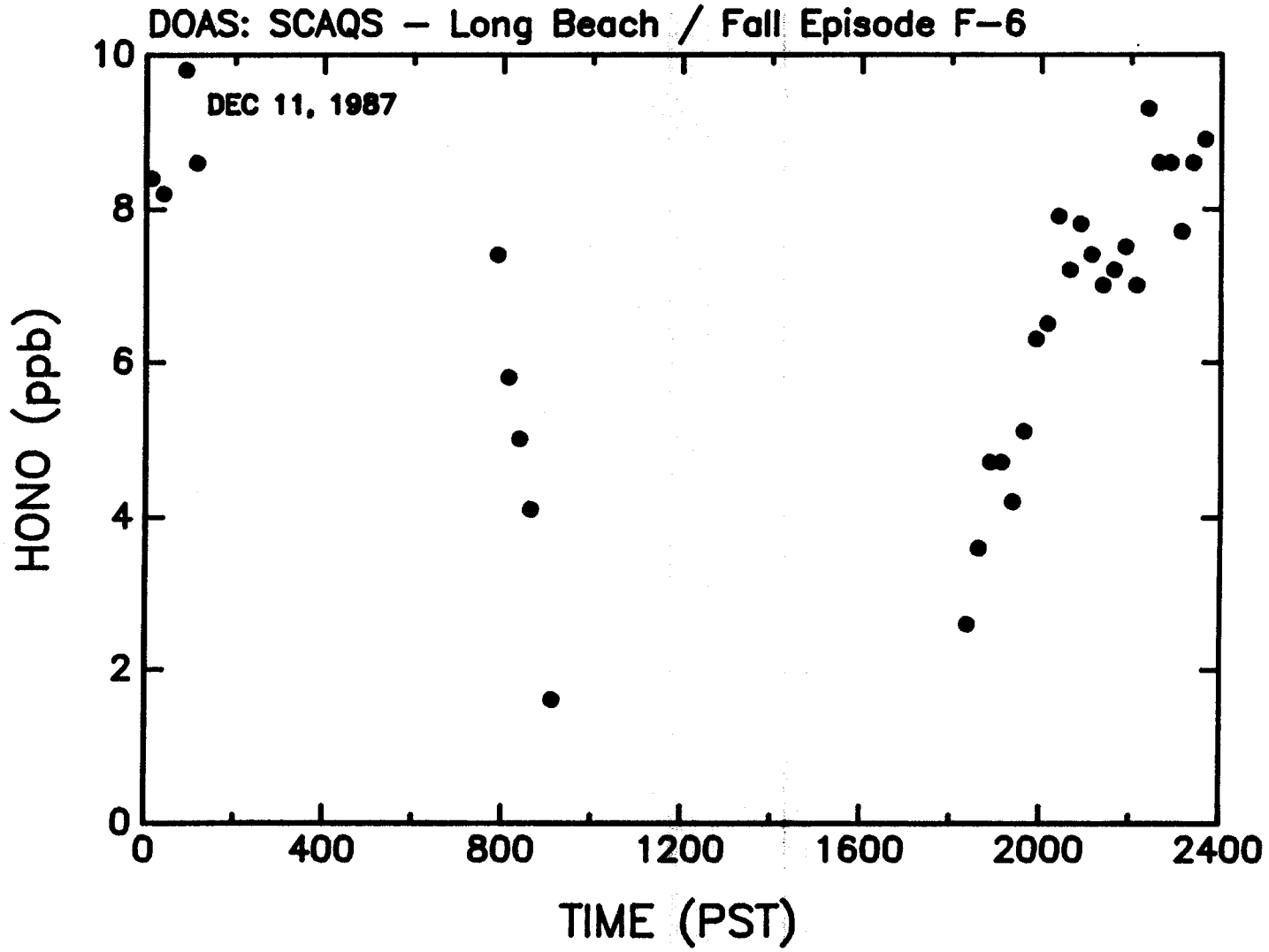

Figure V-47. DOAS 15-min HONO concentrations observed at Long Beach during fall episode F-6.

HONO persisted long after sunrise, with measurable levels continuing almost until noon. (Missing data during mid-morning was due to the acquisition of reference spectra, taken during a period when normally HONO concentrations would have decreased to below the 0.8 ppb detection limit.) The observation of HONO above the detection limit during daylight hours was presumably due to the combination of low light intensities near the time of the winter solstice and the large source strength for HONO from emission sources or significant formation of HONO from secondary reactions (including reaction of NO with OH radicals), or both.

Discussion of the atmospheric chemistry and regulatory implications of these HONO data is given in Section VI.A, and comparison of the DOAS HONO measurements with time-averaged HONO concentrations obtained with a denuder difference technique (Appel et al. 1989, 1990) is given in Section IV.C.2.

3. Formaldehyde

DOAS 15-min data for HCHO at Long Beach are shown in Figures V-48 through V-53. Again, the maximum concentrations observed by DOAS for HCHO during these episodes were the highest of the SCAQS project, reaching 40 ppb shortly before noon on December 3, 1987 and approaching 30 ppb on December 10. Maximum HCHO concentrations reached or exceeded 20 ppb on three of the remaining four episodes. These elevated levels usually, although not always, occurred during the daytime, but with no consistent pattern discernable in the DOAS 15-min data.

A comparison of these data with corresponding measurements using a TDLAS system is presented in Section IV.C.3.

4. 1-Hr Average Data

Figures V-54 through V-59 show the 1-hr average DOAS data for the Long Beach fall episodes. For all three pollutants, the result has been to "smooth" the 15-min data, enhancing the diurnal patterns. As seen from Figure V-57, the 1-hr average NO_2 concentration approached 250 ppb at mid-day on December 3.

The 1-hr average HONO data reinforce that these are the highest HONO concentrations observed to date by the DOAS technique. For example, as shown in Figure V-57, HONO levels had already reached 12 ppb at midnight when DOAS monitoring began, and continued to rise to a 1-hr average of 15 ppb near sunrise.

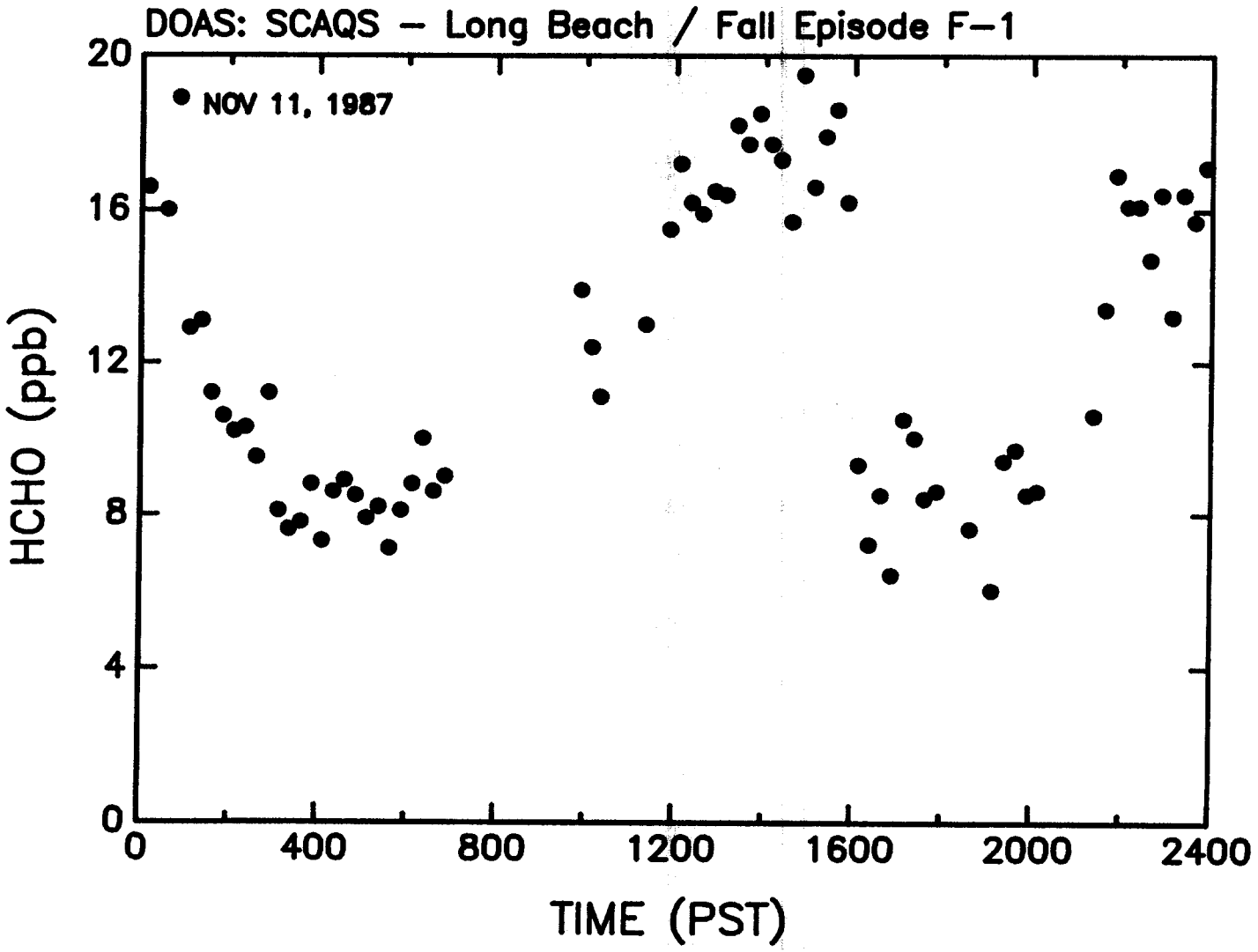

Figure V-48. DOAS 15-min HCHO concentrations observed at Long Beach during fall episode F-1.

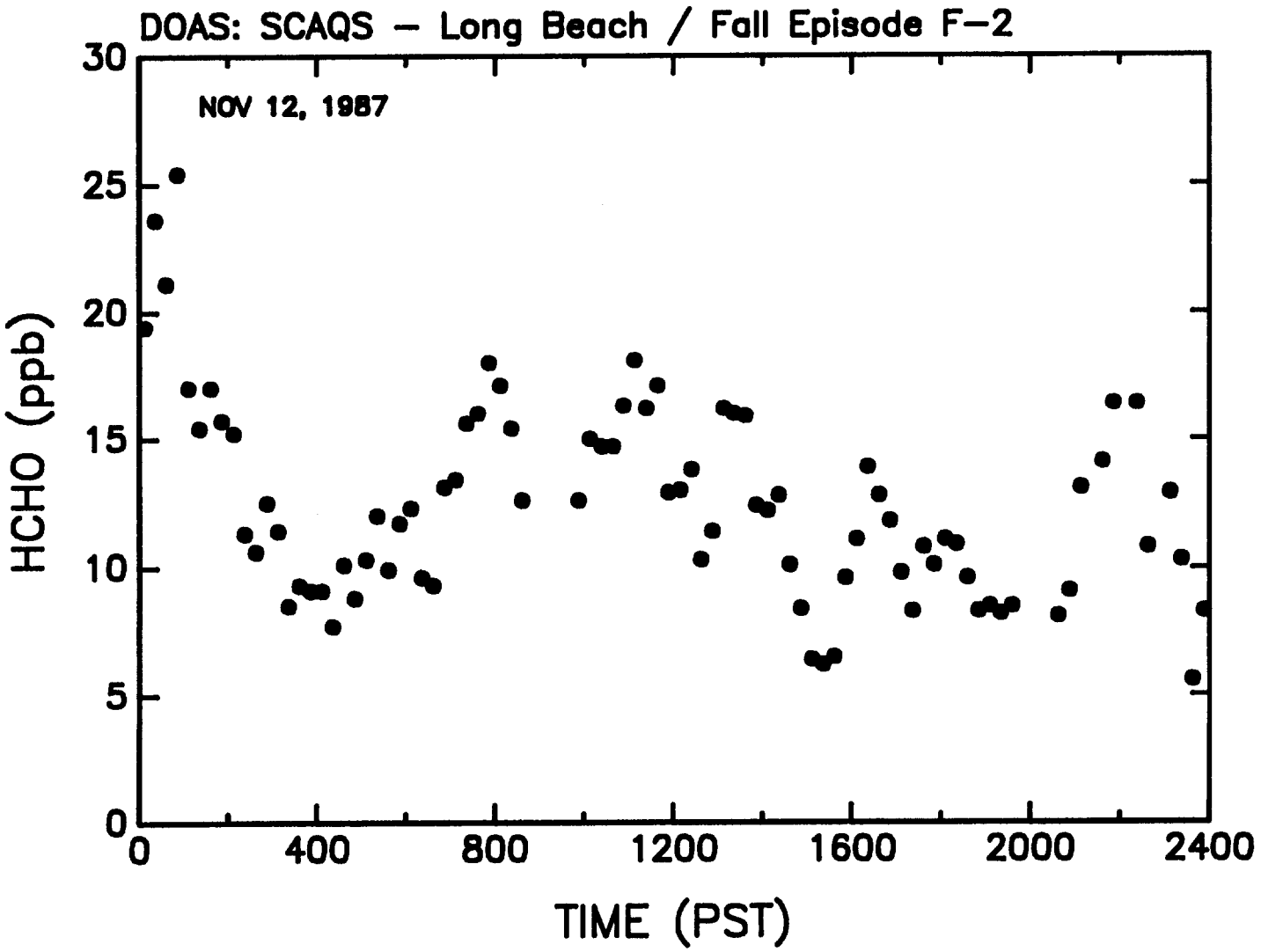

Figure V-49. DOAS 15-min HCHO concentrations observed at Long Beach during fall episode F-2.

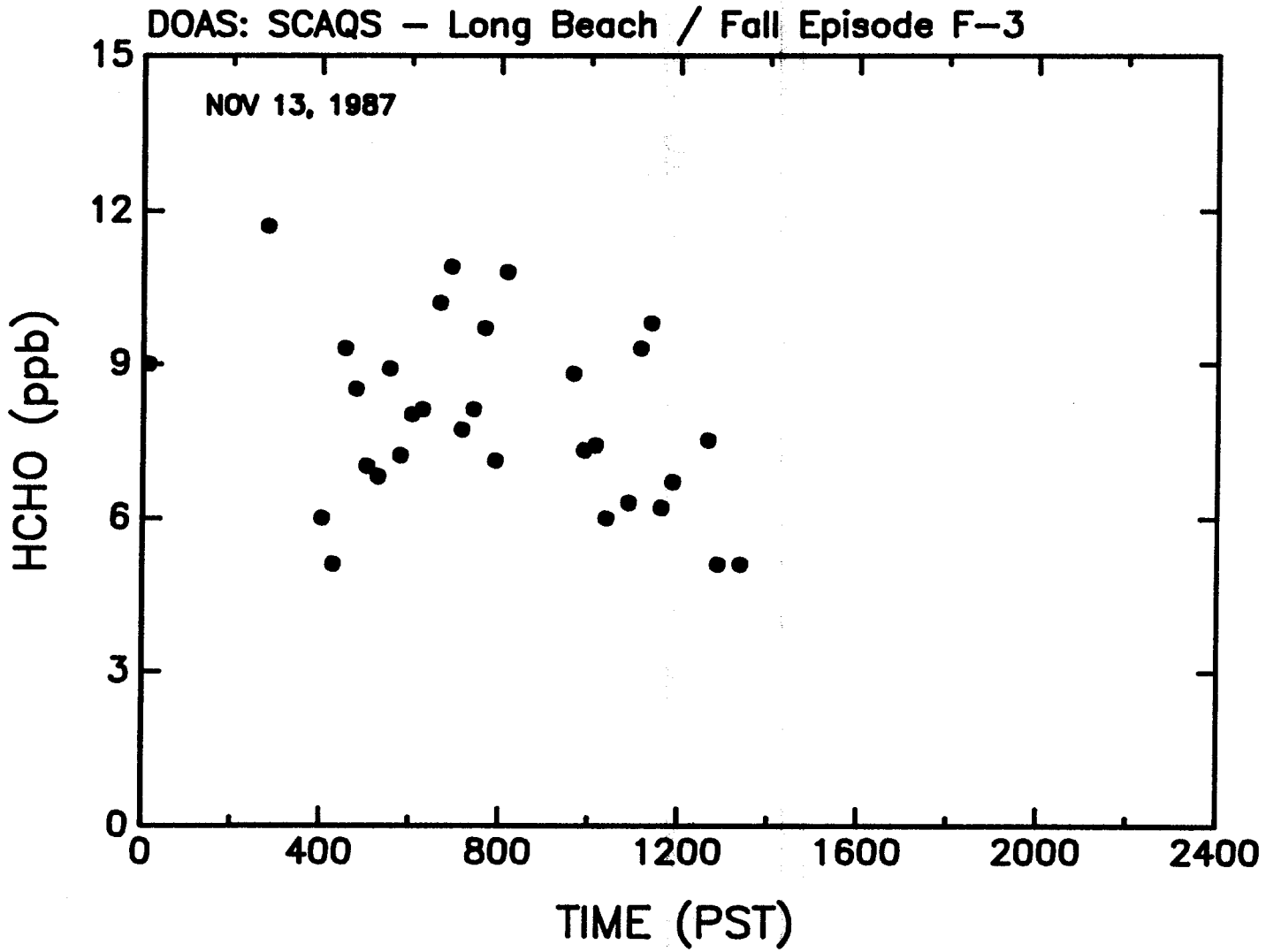

Figure V-50. DOAS 15-min HCHO concentrations observed at Long Beach during fall episode F-3.

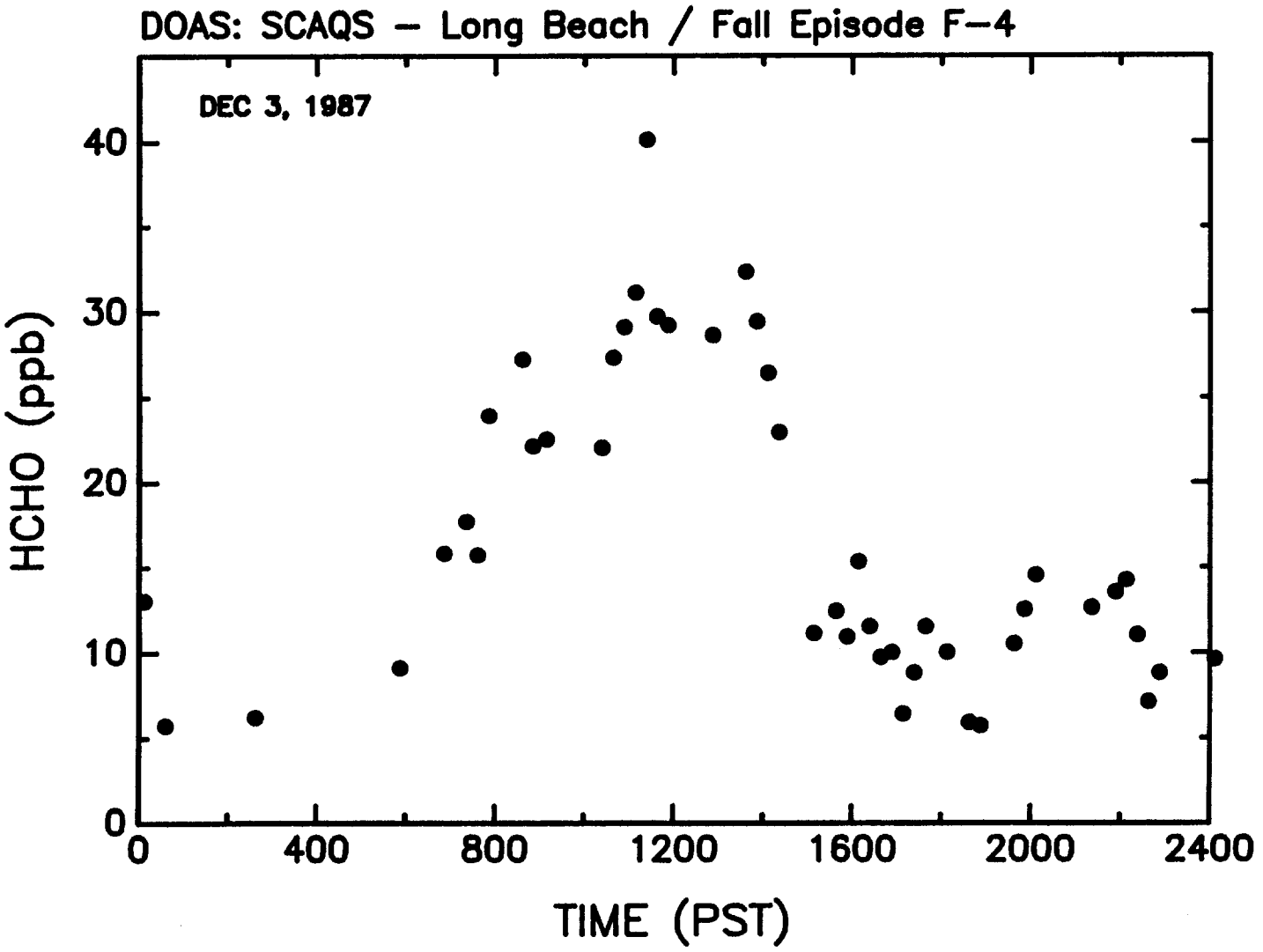

Figure V-51. DOAS 15-min HCHO concentrations observed at Long Beach during fall episode F-4.

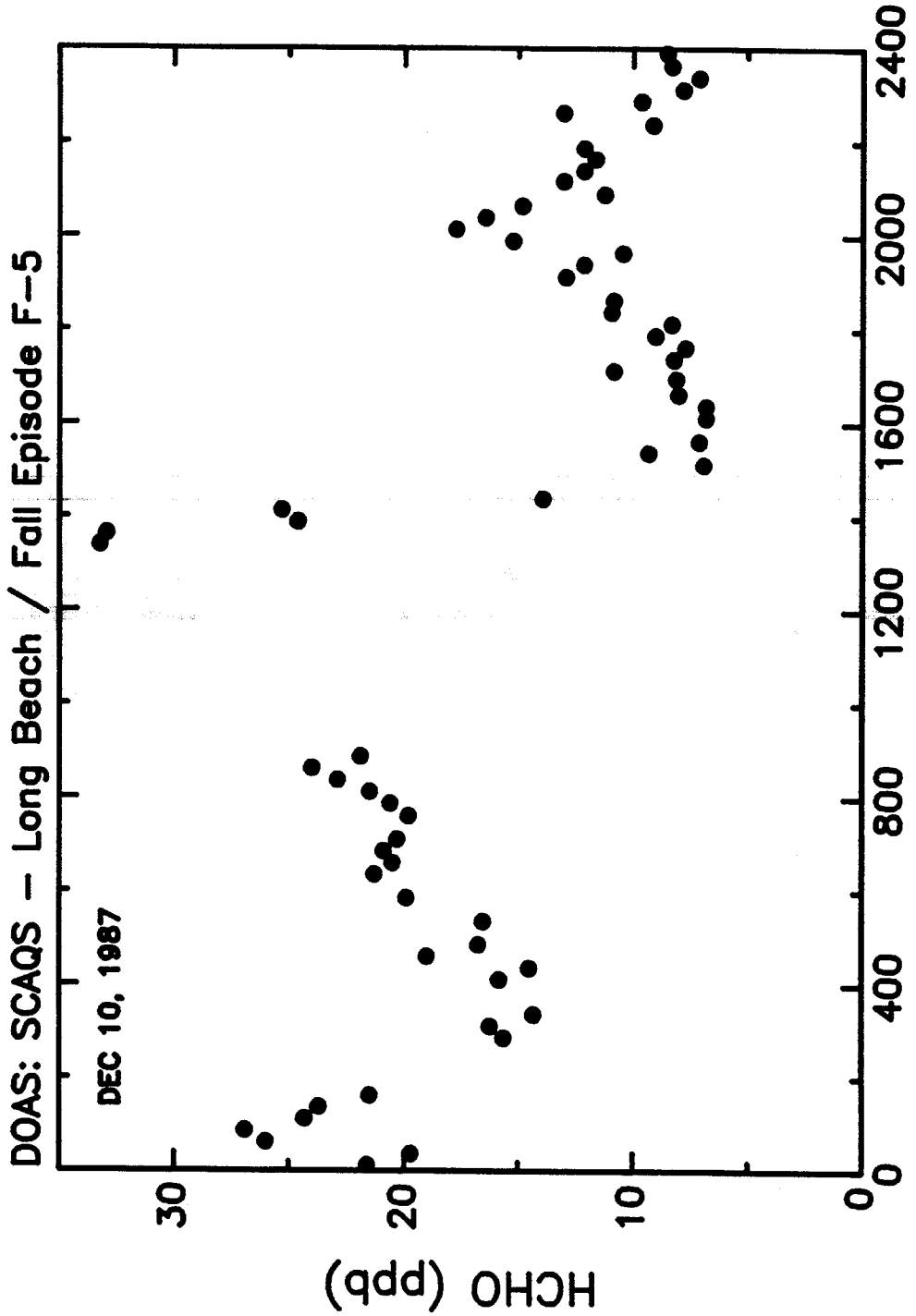

Figure V-52. DOAS 15-min HCHO concentrations observed at Long Beach during fall episode F-5.

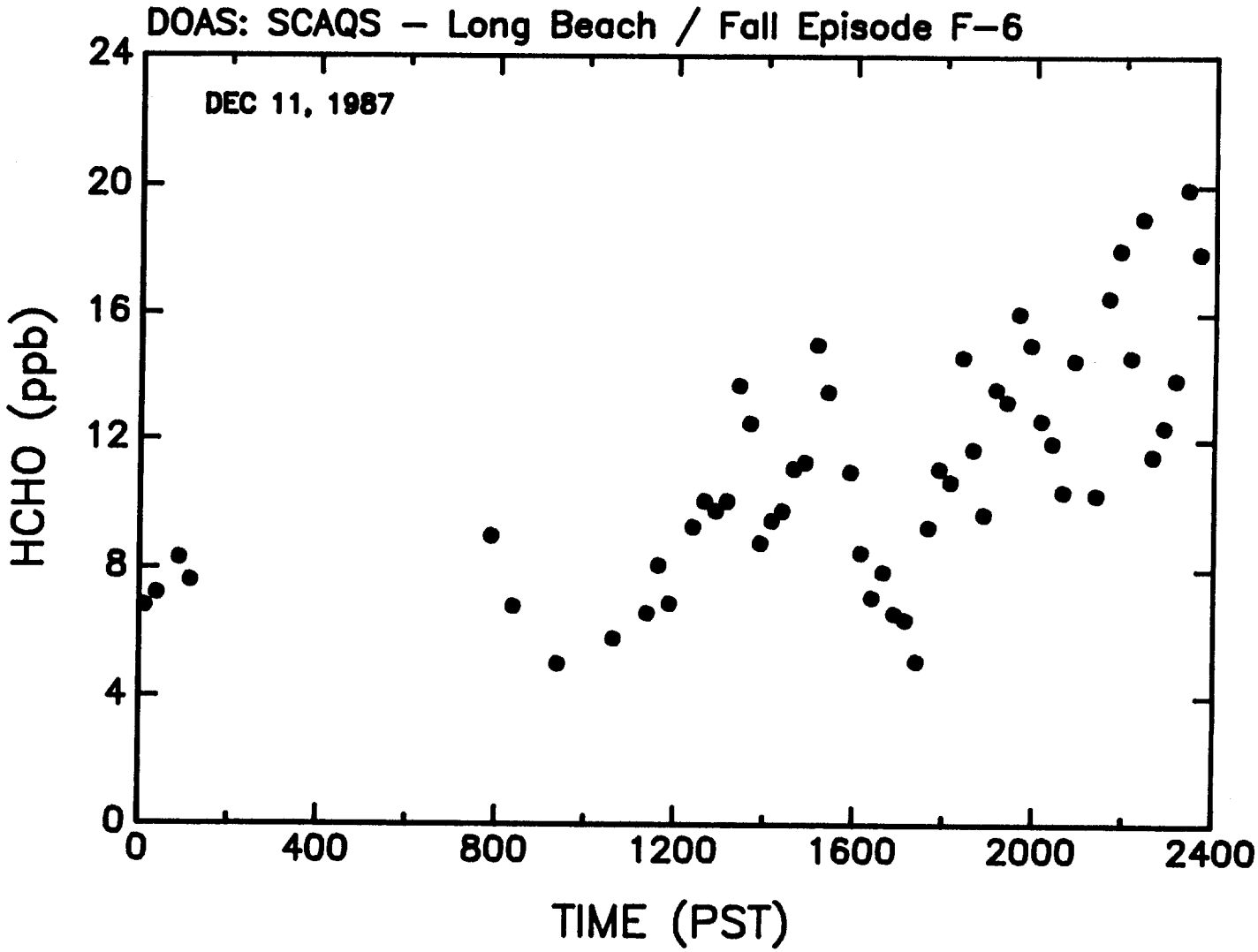

Figure V-53. DOAS 15-min HCHO concentrations observed at Long Beach during fall episode F-6.

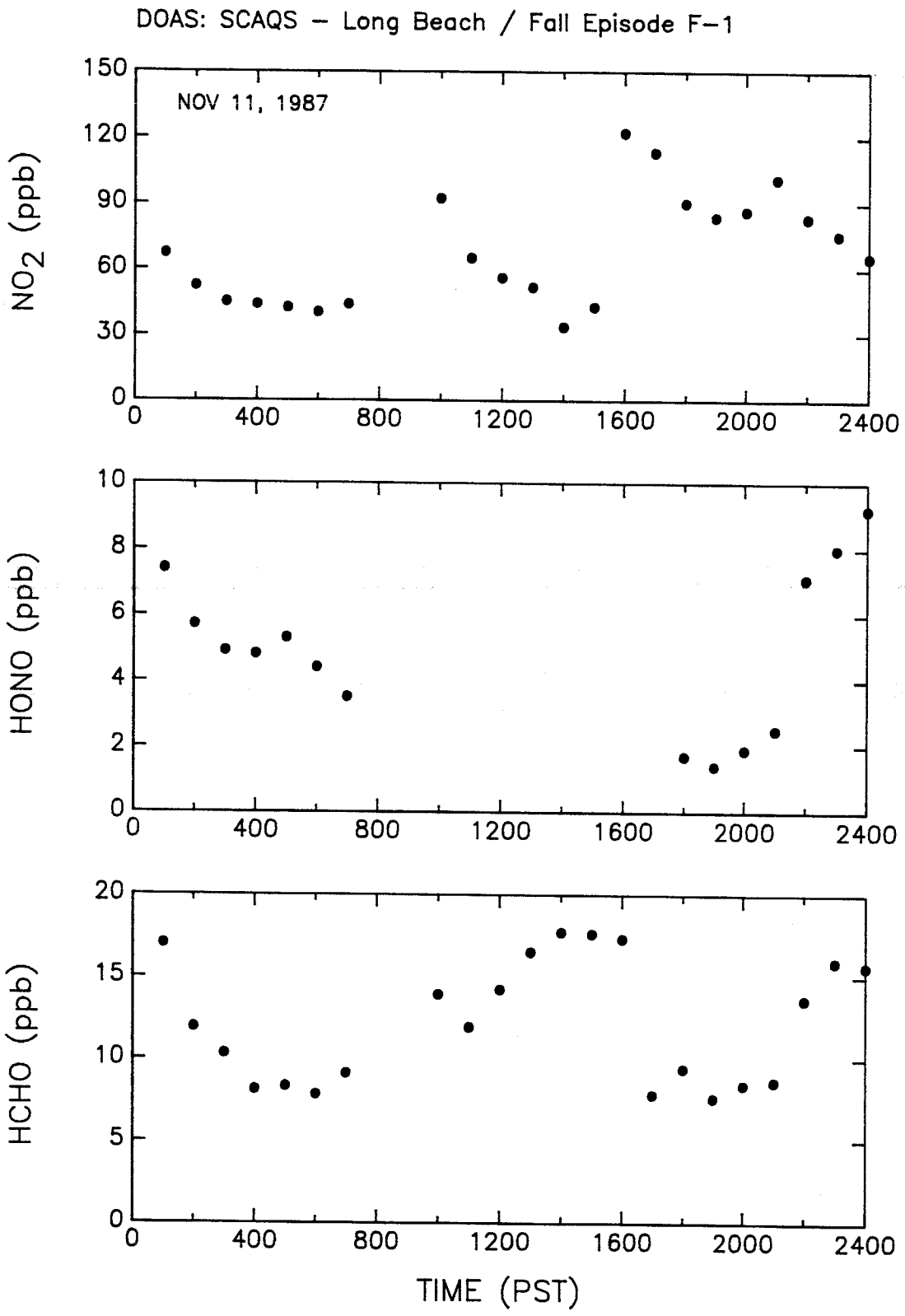

Figure V-54. DOAS 1-hr average concentrations observed at Long Beach during fall episode F-1.

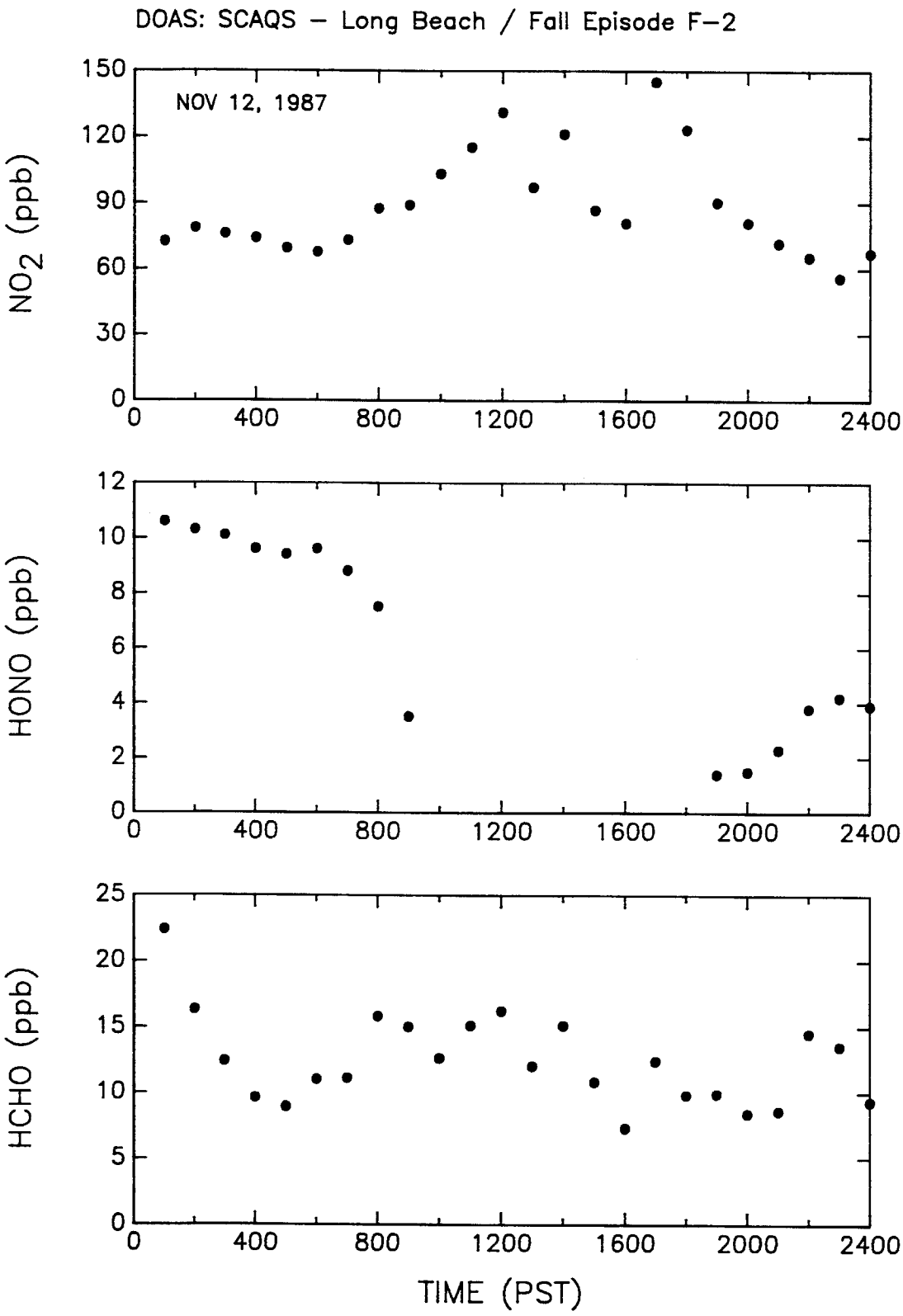

Figure V-55. DOAS 1-hr average concentrations observed at Long Beach during fall episode F-2.

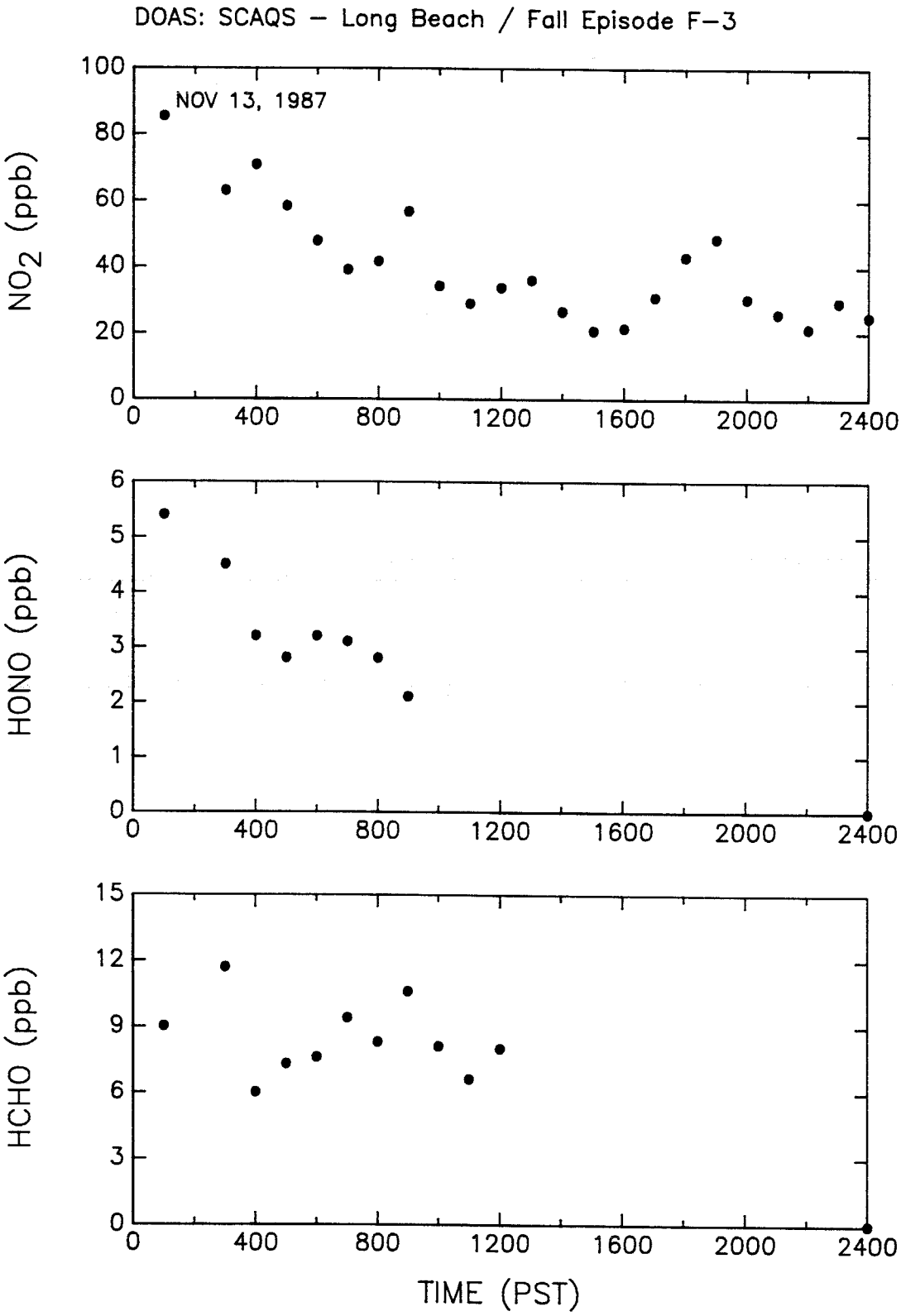

Figure V-56. DOAS 1-hr average concentrations observed at Long Beach during fall episode F-3.

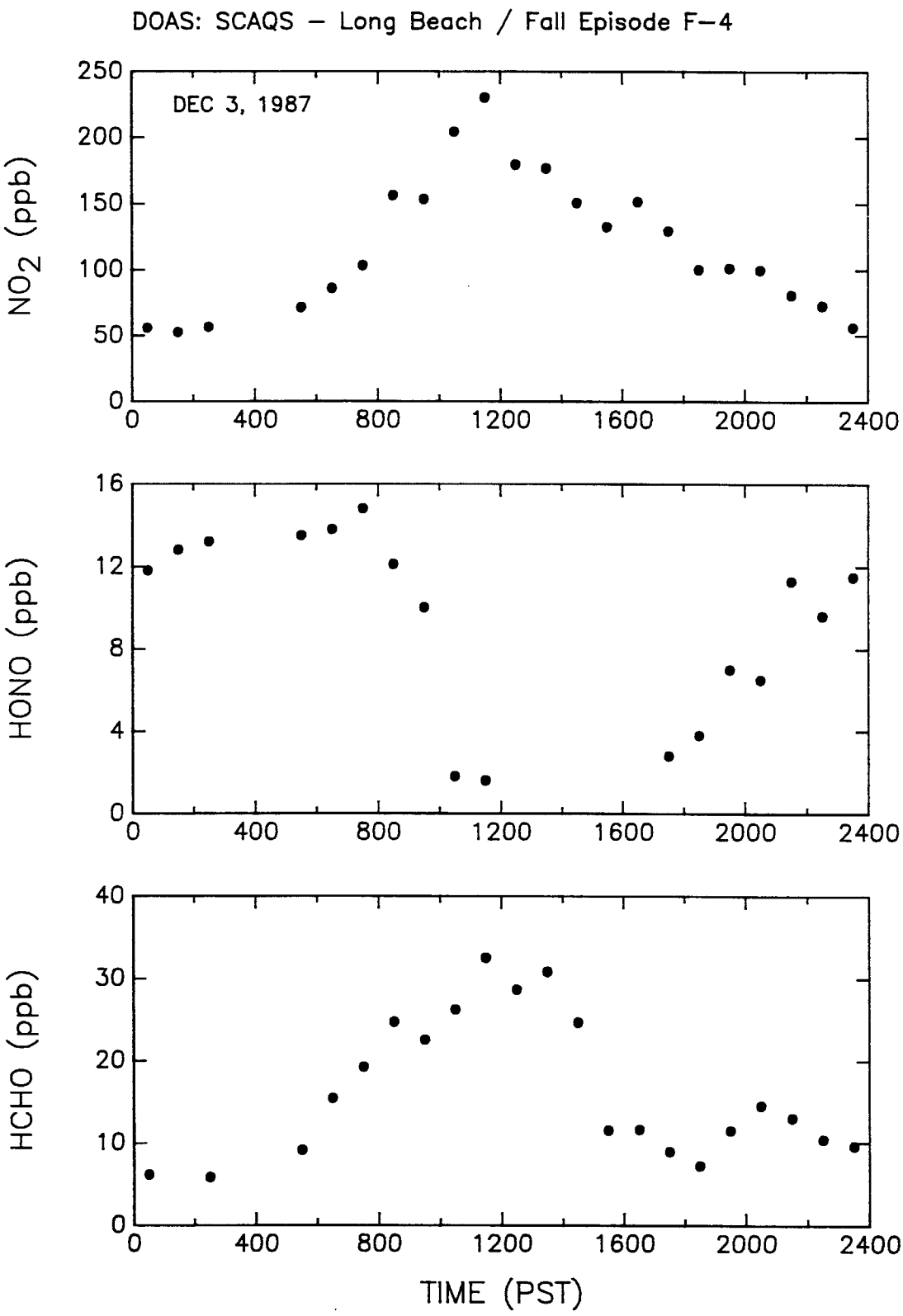

Figure V-57. DOAS 1-hr average concentrations observed at Long Beach during fall episode F-4.

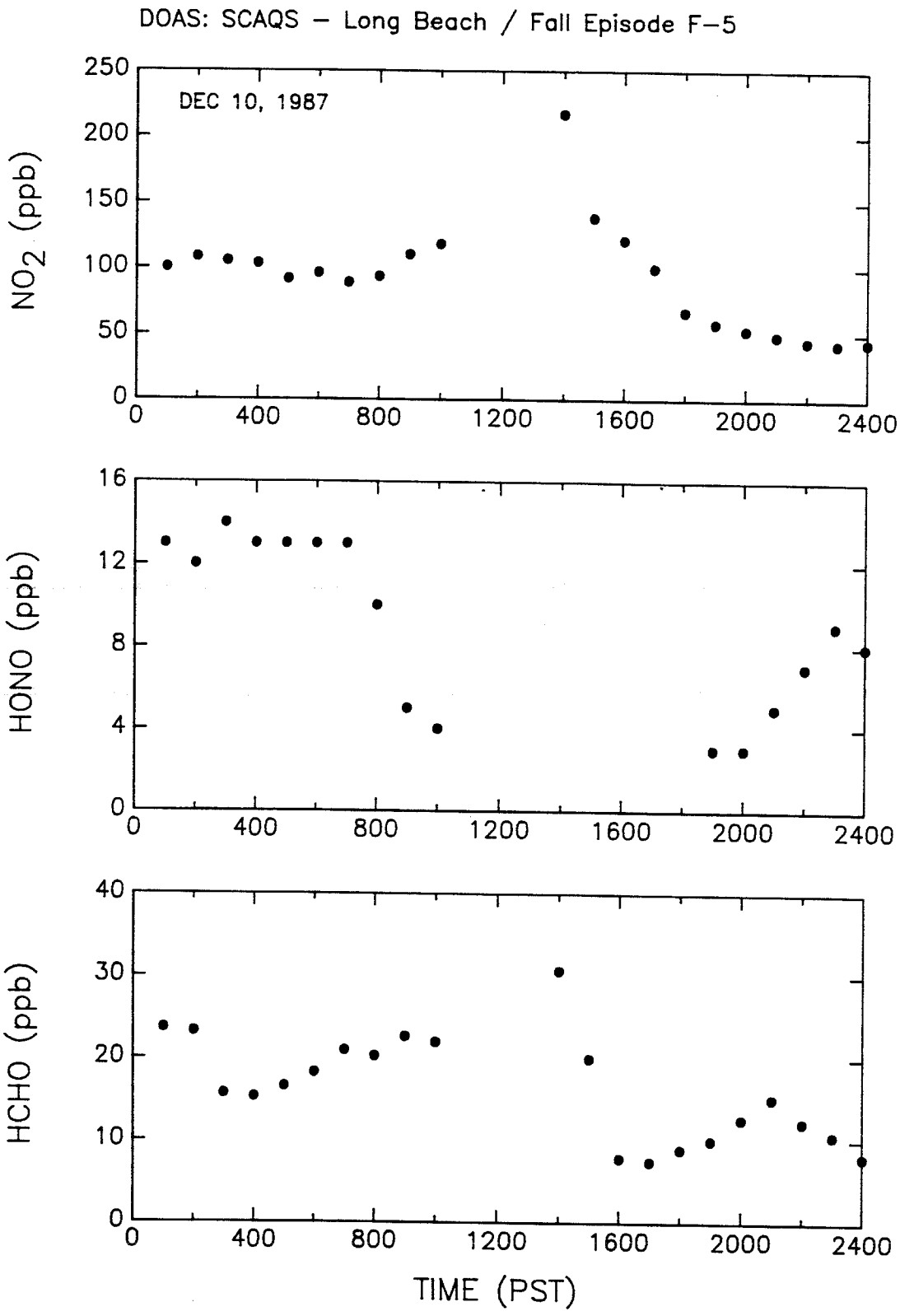

Figure V-58. DOAS 1-hr average concentrations observed at Long Beach during fall episode F-5.

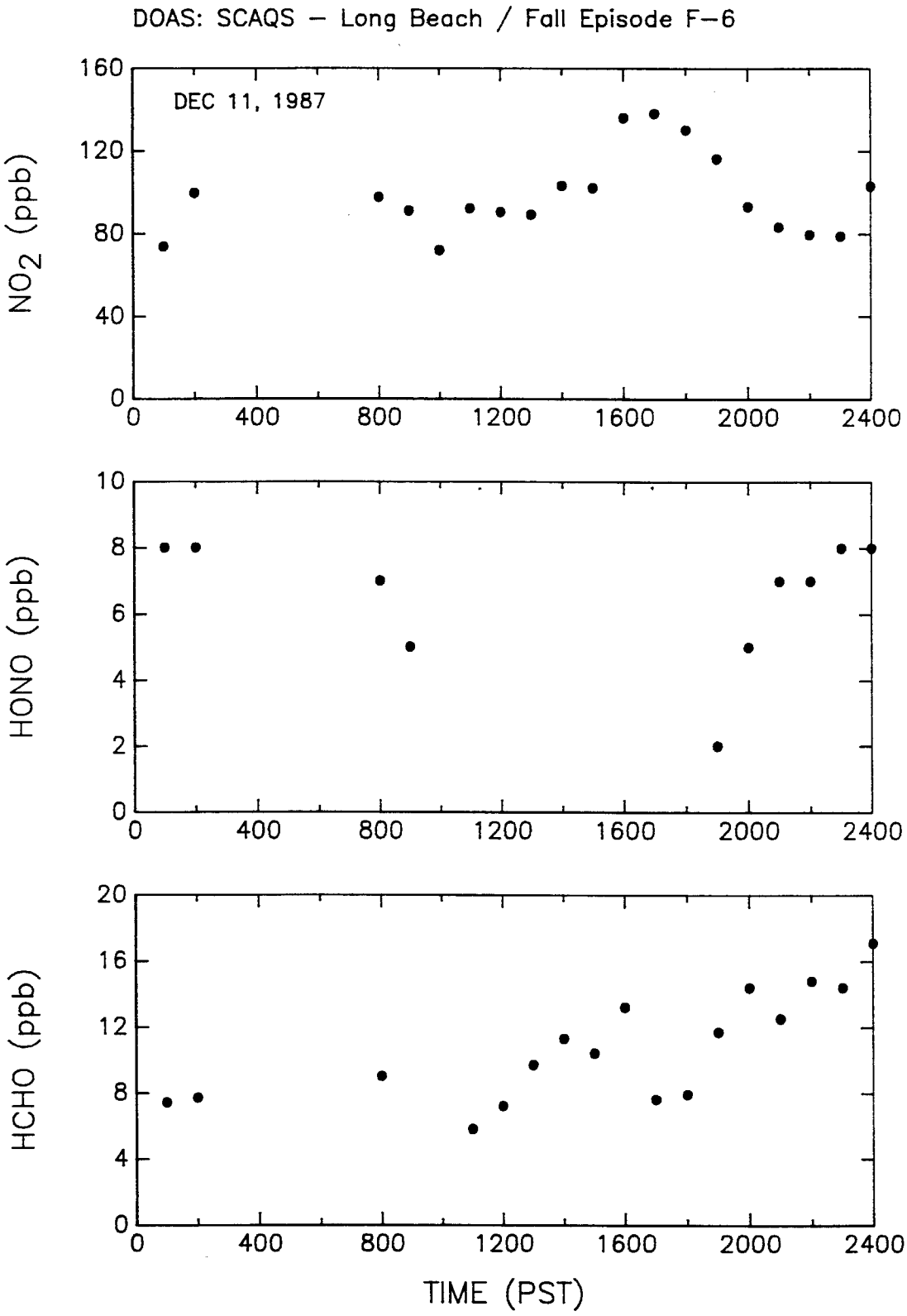

Figure V-59. DOAS 1-hr average concentrations observed at Long Beach during fall episode F-6.

For most of the six fall episodes, the time-concentration profiles for 1-hr HCHO concentrations roughly parallel those for NO_2 concentrations, suggesting the importance of primary emissions in determining the atmospheric concentrations of both of these pollutants.

Due to the importance of the HONO measurements obtained at Long Beach in the fall episodes, the 1-hr average numerical concentrations for HONO are provided in Table V-9, along with the corresponding 1-hr average NO_2 and HCHO concentrations measured by the DOAS technique. For purposes of intercomparison with results from the denuder difference method (Appel et al. 1989, 1990), four- and six-hour average (depending on time of day) HONO (and NO_2 and HCHO) concentrations were calculated and these are presented in Table V-10.

Table V-9. One-Hour Average DOAS Data for SCAQS Fall Episodes at Long Beach

Date (1987)	Episode	Period (PST)	Average Concentrations (ppb)		
			NO_2	HONO	HCHO
Nov. 11	F-1	0000-0100	67.0	7.4	17.0
		0100-0200	52.2	5.7	11.9
		0200-0300	44.8	4.9	10.3
		0300-0400	43.7	4.8	8.1
		0400-0500	42.2	5.3	8.3
		0500-0600	40.2	4.4	7.8
		0600-0700	43.8	3.5	9.1
		0700-0800			
		0800-0900			
		0900-1000	92.1	< .8	13.9
		1000-1100	64.9	< .8	11.9
		1100-1200	55.9	< .8	14.2
		1200-1300	51.6	< .8	16.5
		1300-1400	33.6	< .8	17.7
		1400-1500	42.8	< .8	17.6
		1500-1600	122	< .8	17.3
		1600-1700	113	< .8	7.8
		1700-1800	90.0	1.7	9.4
		1800-1900	83.6	1.4	7.6
		1900-2000	86.3	1.9	8.4
		2000-2100	101	2.5	8.6
		2100-2200	83.0	7.1	13.6
		2200-2300	75.3	8.0	15.9
		2300-2400	65.3	9.2	15.6
Nov. 12	F-2	0000-0100	72.2	10.6	22.4
		0100-0200	78.4	10.3	16.3
		0200-0300	75.8	10.1	12.4
		0300-0400	73.8	9.6	9.6
		0400-0500	69.2	9.4	8.9
		0500-0600	67.4	9.6	11.0
		0600-0700	72.8	8.8	11.1
		0700-0800	87.3	7.5	15.8
		0800-0900	88.8	3.5	15.0
		0900-1000	103	< .8	12.6
		1000-1100	115	< .8	15.1
		1100-1200	131	< .8	16.2
		1200-1300	96.8	< .8	12.0
		1300-1400	121	< .8	15.1
		1400-1500	86.4	< .8	10.8
		1500-1600	80.5	< .8	7.3
		1600-1700	145	< .8	12.4
		1700-1800	123	< .8	9.8
		1800-1900	90.0	1.4	9.9
		1900-2000	80.8	1.5	8.4
		2000-2100	71.5	2.3	8.6

Table V-9 (continued) - 2

Date (1987)	Episode	Period (PST)	Average Concentrations (ppb) NO_2	HONO	HCHO
		2100-2200	65.2	3.8	14.5
		2200-2300	55.8	4.2	13.5
		2300-2400	67.1	3.9	9.3
Nov. 13	F-3	0000-0100	85.4	5.4	9.0
		0100-0200			
		0200-0300	62.9	4.5	11.7
		0300-0400	70.7	3.2	6.0
		0400-0500	58.2	2.8	7.3
		0500-0600	47.7	3.2	7.6
		0600-0700	39.0	3.1	9.4
		0700-0800	41.6	2.8	8.3
		0800-0900	56.7	2.1	10.6
		0900-1000	34.1	< .8	8.1
		1000-1100	28.9	< .8	6.6
		1100-1200	33.7	< .8	8.0
		1200-1300	36.0	< .8	<5.0
		1300-1400	26.5	< .8	<5.0
		1400-1500	20.7	< .8	<5.0
		1500-1600	21.5	< .8	<5.0
		1600-1700	30.9	< .8	<5.0
		1700-1800	43.1	< .8	<5.0
		1800-1900	48.6	< .8	<5.0
		1900-2000	30.4	< .8	<5.0
		2000-2100	25.9	< .8	<5.0
		2100-2200	21.4	< .8	<5.0
		2200-2300	29.4	< .8	<5.0
		2300-2400	25.0		
Dec. 3	F-4	0000-0100	55.6	11.8	6.1
		0100-0200	52.3	12.8	<5.0
		0200-0300	56.4	13.2	5.8
		0300-0400			
		0400-0500			
		0500-0600	71.2	13.5	9.1
		0600-0700	85.6	13.8	15.4
		0700-0800	103	14.8	19.2
		0800-0900	156	12.1	24.7
		0900-1000	153	10.0	22.5
		1000-1100	204	1.8	26.2
		1100-1200	230	1.6	32.5
		1200-1300	179	< .8	28.6
		1300-1400	176	< .8	30.8
		1400-1500	150	< .8	24.6
		1500-1600	132	< .8	11.5
		1600-1700	151	< .8	11.6
		1700-1800	129	2.8	8.9

Table V-9 (continued) - 3

Date (1987)	Episode	Period (PST)	Average Concentrations (ppb) NO_2	HONO	HCHO
		1800-1900	99.9	3.8	7.2
		1900-2000	101	7.0	11.5
		2000-2100	99.5	6.5	14.5
		2100-2200	80.6	11.3	13.0
		2200-2300	72.6	9.6	10.4
		2300-2400	56.2	11.5	9.6
Dec. 10	F-5	0000-0100	100	13.8	23.6
		0100-0200	108	12.9	23.2
		0200-0300	105	14.9	15.6
		0300-0400	103	13.2	15.2
		0400-0500	91.3	13.1	16.5
		0500-0600	95.8	13.3	18.2
		0600-0700	88.6	13.8	20.9
		0700-0800	93.2	10.4	20.2
		0800-0900	110	5.4	22.6
		0900-1000	118	4.1	21.9
		1000-1100			
		1100-1200		< .8	
		1200-1300			
		1300-1400	217	< .8	30.6
		1400-1500	138	< .8	19.9
		1500-1600	121	< .8	7.8
		1600-1700	99.9	< .8	7.4
		1700-1800	67.0	< .8	8.9
		1800-1900	58.2	3.0	10.0
		1900-2000	53.1	3.1	12.6
		2000-2100	48.8	5.6	15.1
		2100-2200	44.5	7.6	12.2
		2200-2300	42.6	9.1	10.6
		2300-2400	44.1	8.7	8.0
Dec. 11	F-6	0000-0100	73.6	8.8	7.4
		0100-0200	99.5	8.7	7.7
		0200-0300			
		0300-0400			
		0400-0500			
		0500-0600			
		0600-0700			
		0700-0800	97.5	7.4	9.0
		0800-0900	91.0	5.0	<5.0
		0900-1000	71.8	.8	<5.0
		1000-1100	92.1	< .8	5.8
		1100-1200	90.4	< .8	7.2
		1200-1300	89.1	< .8	9.7
		1300-1400	103	< .8	11.3

Table V-9 (continued) - 4

Date (1987)	Episode	Period (PST)	Average Concentrations (ppb) NO_2	HONO	HCHO
		1400-1500	102	< .8	10.4
		1500-1600	136	< .8	13.2
		1600-1700	138	< .8	7.6
		1700-1800	130	< .8	7.9
		1800-1900	116	2.7	11.7
		1900-2000	93.0	5.0	14.4
		2000-2100	83.2	7.3	12.5
		2100-2200	79.5	7.3	14.8
		2200-2300	78.8	8.3	14.4
		2300-2400	103	8.4	17.1

Table V-10. Four- and Six-Hour Averaged DOAS Data for SCAQS Fall Episodes at Long Beach

Date (1987)	Episode	Period (PST)	Average Concentrations (ppb)		
			NO_2	HONO	HCHO
Nov. 11	F-1	0000-0600	48.4	5.4	10.6
		0600-1000	67.9	1.7	11.5
		1000-1400	51.5	<0.8	15.1
		1400-1800	91.9	<0.8	13.0
		1800-2400	82.4	5.0	11.6
Nov. 12	F-2	0000-0600	72.8	9.9	13.4
		0600-1000	88.0	5.0	13.6
		1000-1400	116	<0.8	14.6
		1400-1800	109	<0.8	10.0
		1800-2400	71.7	2.8	10.7
Nov. 13	F-3	0000-0600	65.0	3.8	8.3
		0600-1000	42.9	2.0	9.1
		1000-1400	31.3	<0.8	5.0
		1400-1800	29.1	<0.8	<5.0
		1800-2400	30.1	<0.8	<5.0
Dec. 3	F-4	0000-0600	58.9	12.8	5.2
		0600-1000	124	12.7	20.4
		1000-1400	197	.8	29.5
		1400-1800	140	.8	14.2
		1800-2400	85.0	8.3	11.0
Dec. 10	F-5	0000-0600	101	13.5	18.7
		0600-1000	102	8.4	21.4
		1000-1400	217	<0.8	30.6
		1400-1800	106	<0.8	11.0
		1800-2400	48.5	6.2	11.4
Dec. 11	F-6	0000-0600	86.6	8.7	7.5
		0600-1000	86.8	4.4	4.6
		1000-1400	93.7	<0.8	8.5
		1400-1800	127	<0.8	9.8
		1800-2400	92.3	6.5	14.1

VI. DISCUSSION AND CONCLUSIONS

A. SCAQS-DOAS Data Summaries

The entire DOAS data set, not including the NO_3 radical measurements, for the 1987 SCAQS program is summarized in graphical form in this section. These figures present the 15-min concentrations of NO_2, HONO and HCHO, each plotted on a single page for either the eleven summer episodes at Claremont and Long Beach, or the six fall episodes at Long Beach. From these figures, ranges of concentrations observed during all summer or fall measurement periods, and the diurnal patterns of the respective pollutants, can be readily identified. Summary tables of the numerical 1-hr average concentrations for all episodes were provided in the preceding chapter.

1. Claremont Summer Episodes

From Figure VI-1 it can be seen that the NO_2 concentration during the summer episodes at Claremont ranged from a low of ~10 ppb on September 2, to a maximum concentration approaching 125 ppb on the morning of September 3. The dominant diurnal feature in these data was the prominent traffic-associated peak usually centered around 0800. Maximum NO_2 concentrations for these peaks fell in the range from about 70 ppb to ~120 ppb. A secondary NO_2 peak generally occurred in the early evening hours, with maxima in the range from ~50 to ~80 ppb.

As seen in Figure VI-2, HONO concentrations ranged from below the 0.8 detection limit, during daytime periods and some evenings until approximately midnight, to a maximum concentration of 7 ppb just before sunrise on August 29. Both the range of HONO maximum concentrations, and the observation of peaks or plateaus in the early morning hours, followed by rapid loss due to photolysis shortly after sunrise, are consistent with earlier DOAS studies at SoCAB receptor sites such as Claremont and Glendora (Winer et al. 1987; Biermann et al. 1988a).

Figure VI-3 shows that HCHO measured by DOAS at Claremont ranged from below the detection limit of 5 ppb, primarily during evening hours, to a maximum of nearly 25 ppb on the afternoon of June 25.

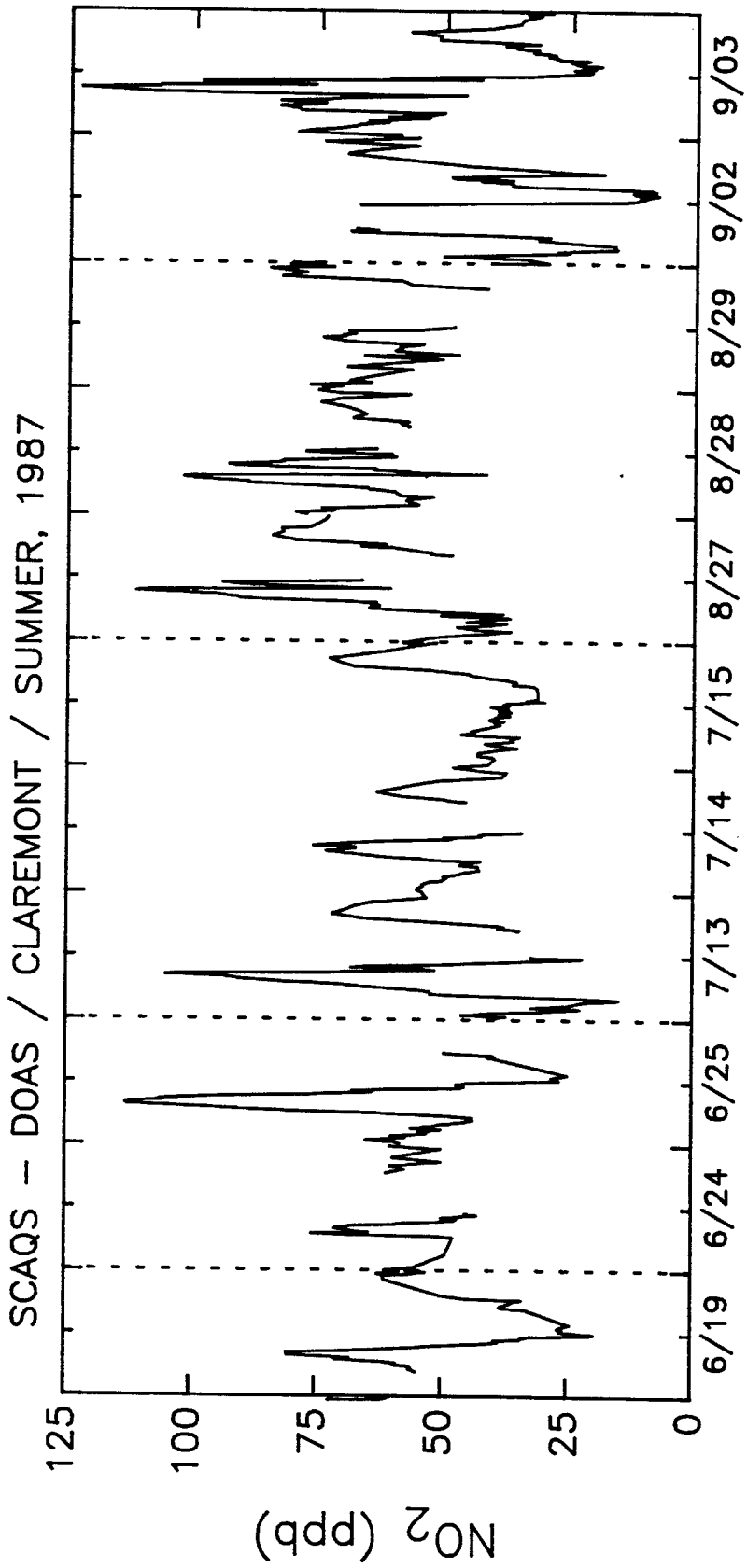

Figure VI-1. Time-concentration profiles for NO_2 measured by DOAS during eleven summer (1987) episodes at Claremont, CA.

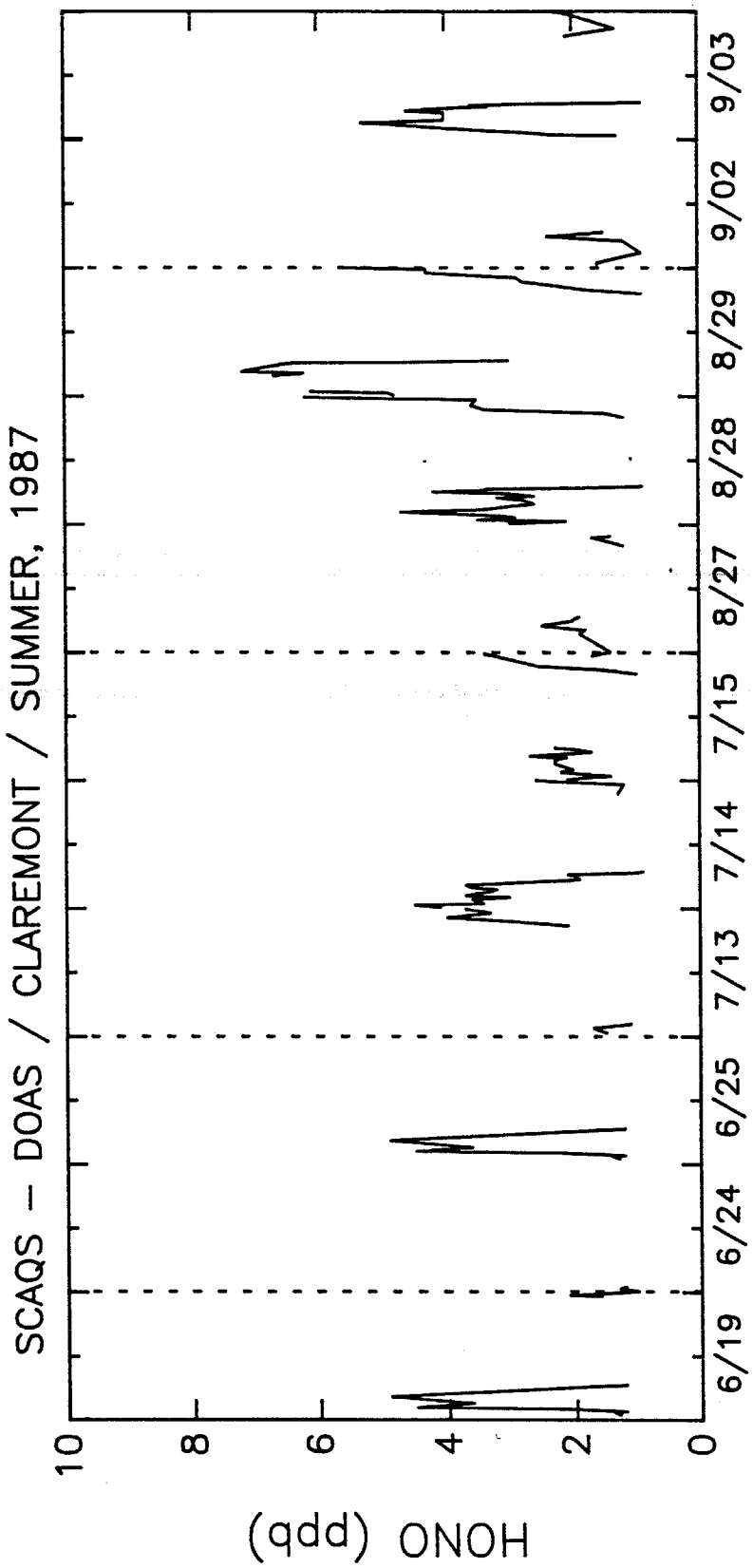

Figure VI-2. Time-concentration profiles for HONO measured by DOAS during eleven summer (1987) episodes at Claremont, CA.

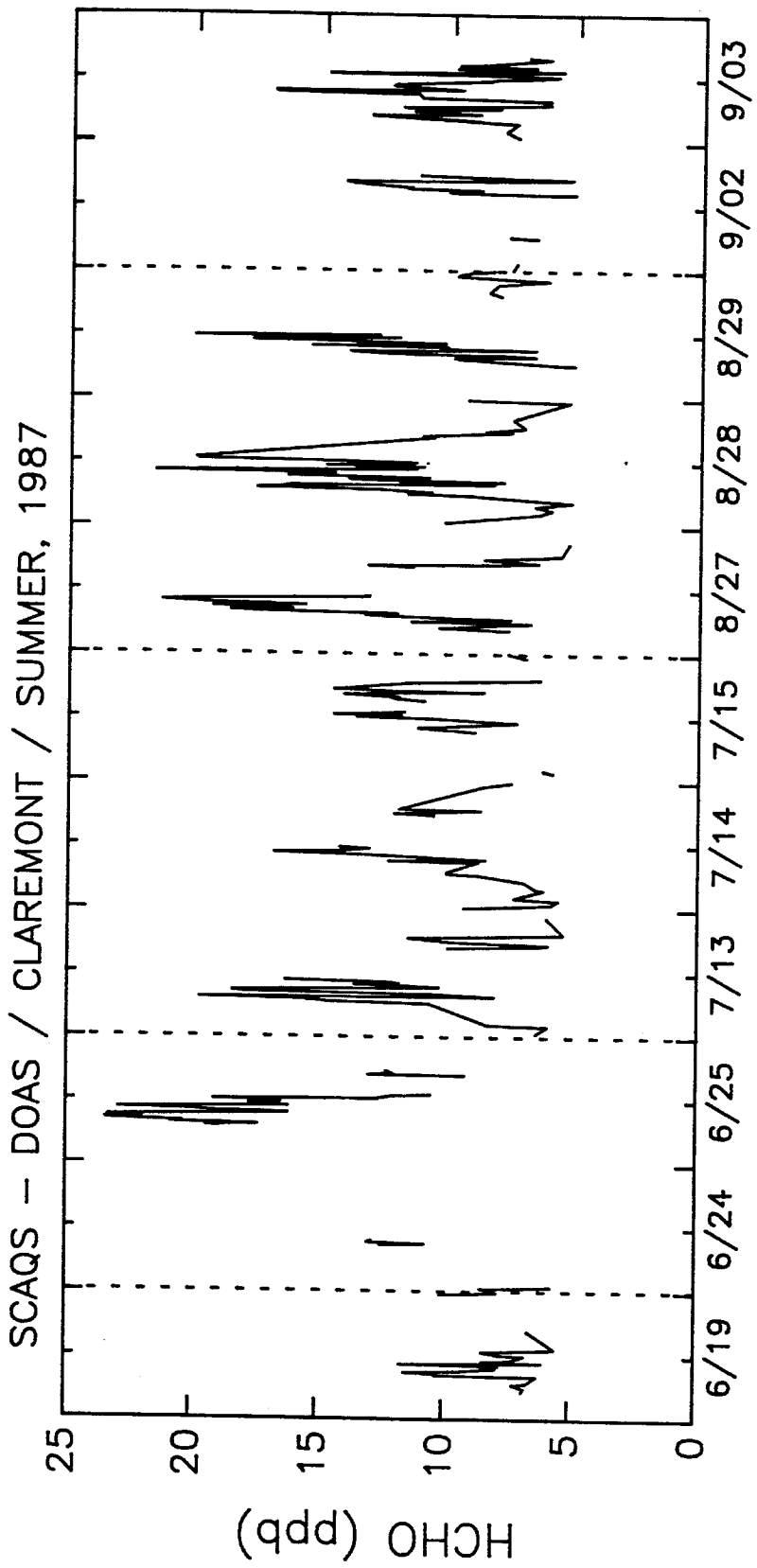

Figure VI-3. Time-concentration profiles for HCHO measured by DOAS during eleven summer (1987) episodes at Claremont, CA.